University of Nottingham
UK | CHINA | MALAYSIA

Design, synthesis, and evaluation of inhibitors of InhA to prevent cell wall biosynthesis in *Mycobacterium bovis*

Thesis submitted to the University of Nottingham for the degree of Doctor of Philosophy

Matthew Stevenson

stxmast@nottingham.ac.uk

Supervisor: Prof Neil R. Thomas

Secondary Supervisor: Cristina de Matteis

Abstract

Tuberculosis is a disease primarily affecting the lungs caused by *Mycobacterium bovis (Mycobacterium tuberculosis* in humans*)* which is transmitted via airborne droplets through mucosal fluids. It is classified as both a major health threat and cattle farming threat as well as a leading cause of death worldwide ranked alongside HIV and in 2016, 1.6 million people died as a result of the disease. It is a particular problem in the farming industry where culling of livestock is generally utilised rather than expensive and lengthy treatment. Most recent statistics from the UK indicated 4,395 new contaminated herds with over 44,000 animals slaughtered due to the disease.[1] The nature of treatment (long-term combination therapy) as well as unwillingness to vaccinate cattle breeds resistance, the subject of which is a growing issue with both multidrug (MDR-TB) and extensively drug resistant (XDR-TB) tuberculosis strains becoming increasingly prevalent worldwide.

Isoniazid (INH) is a prodrug activated by KatG, the active form then inhibits InhA. INH is one of the most potent antitubercular drugs which acts to prevent the production and replenishment of mycolic acids, which form the outer coat of the *Mycobacterium,* by inhibiting the FASII section of the fatty acid biosynthetic pathway. Mutation in KatG renders the prodrug inert but by targeting InhA directly we can still inhibit production of mycolic acids, and as InhA has an identical structure in *bovis* as in *tuberculosis* there is the potential for treating both humans and cattle.

Work has been carried out on the synthesis of a new class of potential inhibitors based on L-ascorbic acid, which as a readily available starting material that shows little to no toxicity in the body provides an interesting route for drug development. These compounds are considered a second generation of inhibitors compared to the work of Manjunatha *et al* who screened the Novartis compound library and found 4-hydroxy-2-pyridones had potent antitubercular activity against InhA.[1]

A series of compounds have been synthesised incorporating phenyl and benzyl ethers attached to the L-ascorbic acid scaffold. These have been tested in an isolated enzyme assay, with *trans*-2-octenoyl CoA as substrate, to determine their percentage inhibition of InhA at 50 μM. None of the compounds tested exhibited an inhibitory effect on InhA at this concentration.

Acknowledgements

I would like to thank Prof Neil. R. Thomas and Cristina de Matteis firstly for a thoroughly engaging project as well as for their continued guidance and support throughout my studies. It is also important to thank all of the support staff in the School of Chemistry, School of Pharmacy, Centre for Biomolecular Sciences, and all involved at the BBSRC for funding me and this project.

All members of the NRT group past and present deserve recognition for their help and guidance in this project and for keeping me partway sane, in particular James Reekes, Malcolm Lamont, Tom Armstrong, and Dr Francesco Zamberlan. My friends and family have continued to show their support and kindness when times have been tough and giving me the focus I need to carry on.

I would also like to thank all involved at Nottingham Forest football club, for providing me with both highs and lows throughout the seasons but mainly for a stress release of allowing me to shout at a referee for two hours every weekend.

Declaration

I declare that the content of this thesis has not been submitted, nor is currently being submitted for any other degree. I also declare that any work reported in this thesis is the result of my own investigation. Any work conducted by other investigators has been fully acknowledged and referenced in the text.

Matthew Stevenson

Table of Contents

List of Figures

List of Schemes

List of Tables

Abbreviations

Ac	Acetone
ACP	Acyl carrier protein
ADME	Absorption, distribution, metabolism, and excretion
Ar	Aromatic group
BCG	Bacillus Calmette-Guerin
CSA	Camphorsulfonic acid
DBU	1,8-Diazabicyclo[5.4.0]undec-7-ene
DCM	Dichloromethane

DIPEA	*N,N*-Diisopropylethylamine
DMAP	Dimethylaminopyridine
DMS	Dimethylsulfate
DMSO	Dimethylsulfoxide
E. coli	Escherichia coli
ESI	Electrospray ionisation
FAS I	Fatty acid synthesis pathway one
FAS II	Fatty acid synthesis pathway two
HIV	Human immunodeficiency virus
HRMS	High resolution mass spectrometry
IC_{50}	Inhibitory concentration for 50% reduction
InhA	Enoyl-acyl carrier protein reductase
IPTG	Isopropyl β-D-1-thiogalactopyranoside
LB	Luria-Bertani medium
M. bovis	Mycobacterium bovis
M. tuberculosis/M.tB	Mycobacterium tuberculosis
M. smegmatis	Mycobacterium smegmatis
MDR-TB	Multidrug resistant tuberculosis
MHz	Megahertz
MIC	Minimum inhibitory concentration
MMP	Matched molecular pair
MOM	Methoxymethyl
MOMCl	Methoxymethyl chloride
NAD^+	Oxidised nicotinamide adenine dinucleotide
NADH	Nicotinamide adenine dinucleotide
nd	Not determined

NMR	Nuclear magnetic resonance
OcCoA	*trans*-2-Octenoyl-CoA
OD_{600}	Optical density measured at 600 nm
PIPES	Piperazine-N,N'-bis(2-ethanesulfonic acid)
PMB	Para-methoxybenzyl
PLIF	Protein-ligand interaction fingerprint
ppm	Parts per million
PyBOP	Benzotriazol-1-yl-oxytripyrrolidinophosphonium hexafluorophosphate
QSAR	Quantitative structure–activity relationship
r.t	Room temperature
rRNA	Ribsomal ribonucleic acid
S. typhimum	Staphylococcus typhimum
SAR	Structure-activity relationship
SDS-PAGE	Sodium dodecyl sulfate-polyacrylamide gel electrophoresis
SLI	Second-line injectables
TB	Tuberculosis
TBAB	Tetra-*n*-butylammonium bromide
TBDMS	*tert*-Butyldimethylsilyl
TBDPS	*tert*-Butyldiphenylsilyl
TDR-TB	Totally drug resistant tuberculosis
TES	Triethylsilyl
THF	Tetrahydrofuran
TMS	Trimethylsilyl
TRC	Triclosan

tRNA	Transfer ribonucleic acid
Tyr	Tyrosine
UK	United Kingdom
WHO	World Health Organisation
XDR-TB	Extensively drug resistant tuberculosis

1.0 Introduction

1.1 Tuberculosis Background

Tuberculosis (TB) is a disease primarily affecting the lungs caused by *Mycobacterium tuberculosis (MTB) (Mycobacterium bovis* in cattle*)* which is transmitted via airborne droplets through mucosal fluids. A stained image of the bacterium is shown in **Figure 1**.

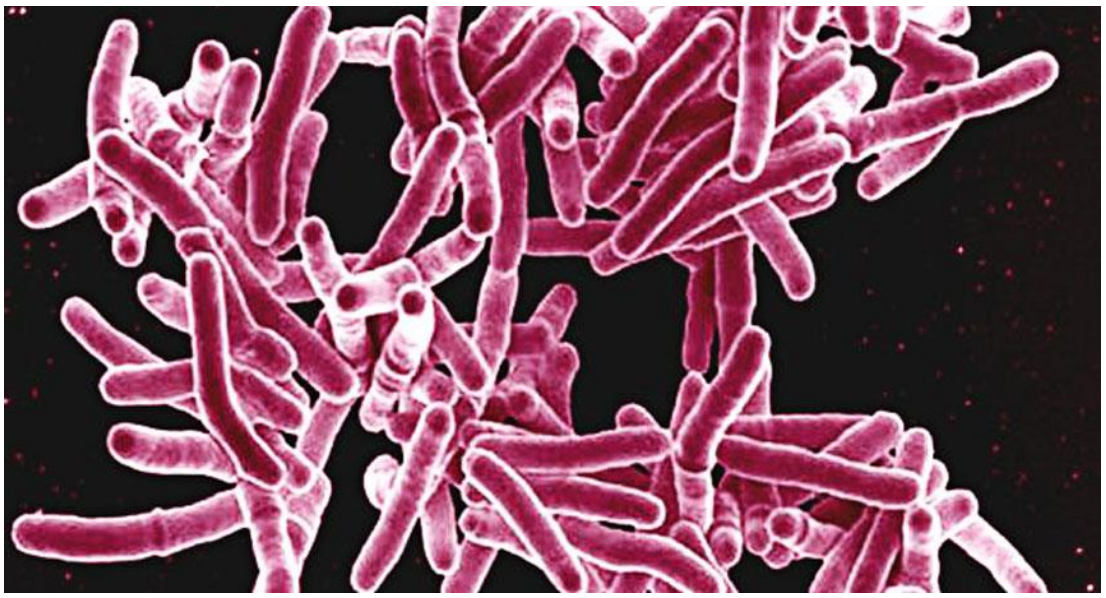

Figure 1. Image of MTB taken with a scanning electron micrograph.[2]

Tuberculosis is classified as a major health threat and is a leading cause of death worldwide considered alongside conditions such as HIV and malaria. In 2017, 1.3 million people died as a result of the disease (HIV negative) with over ten million new cases diagnosed in total.[3, 4] Up to one third of the world's population is estimated to be infected with either the latent or the active form of the bacterium and so it is imperative we develop new effective forms of treatment to counteract the spread of resistant strains.[5]

The bovine strain of the bacterium causes a drain on the economics of countries ill-equipped to deal with treatment of infected livestock, and in 2017 the global economic losses were estimated to be more than US $3 billion as a direct result of *M. bovis*.[6, 7] The disease may cross the species barrier to infect humans and indeed the most recent data shows 142,000 cases worldwide with 12,500 deaths, regions at higher risk are Africa and South-East Asia.[4]

MTB is a highly opportunistic bacterium, which is especially dangerous to those suffering from HIV who have a reduced immune response and struggle to fight off the infection (in addition to reported incompatibility with Rifamycin).[8] Indeed an additional 300,000 deaths resulted from those co-infected worldwide.[3, 9-11] Incidence worldwide with and without HIV is shown in **Figure 2** and **Figure 3**.

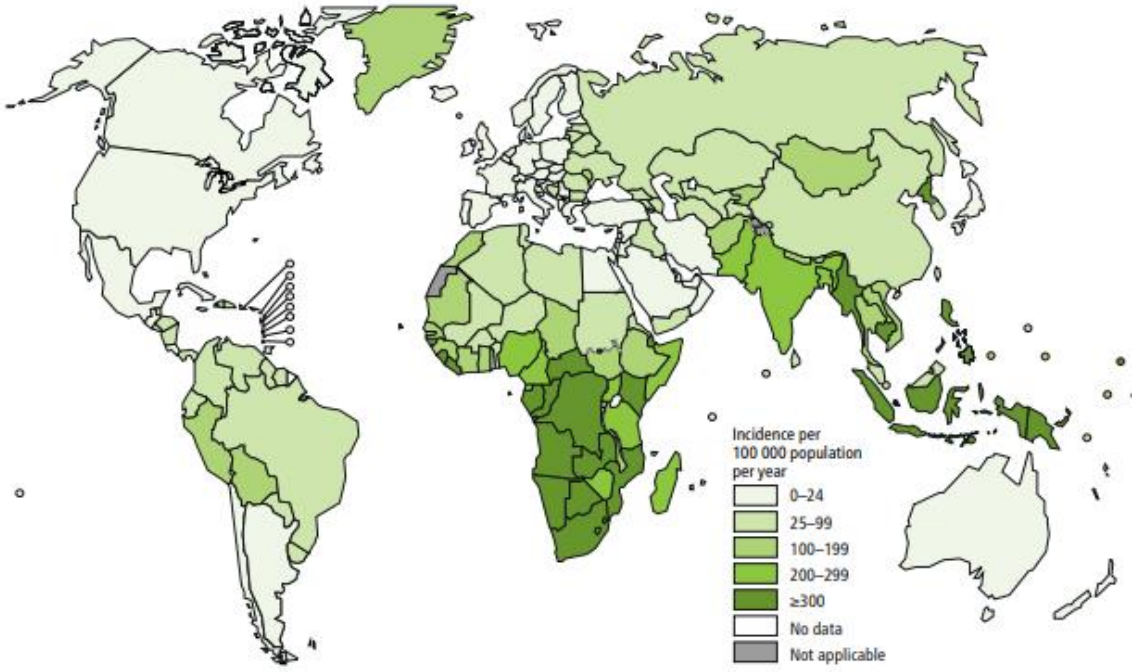

Figure 2. Estimated TB incidence worldwide in 2016.[4]

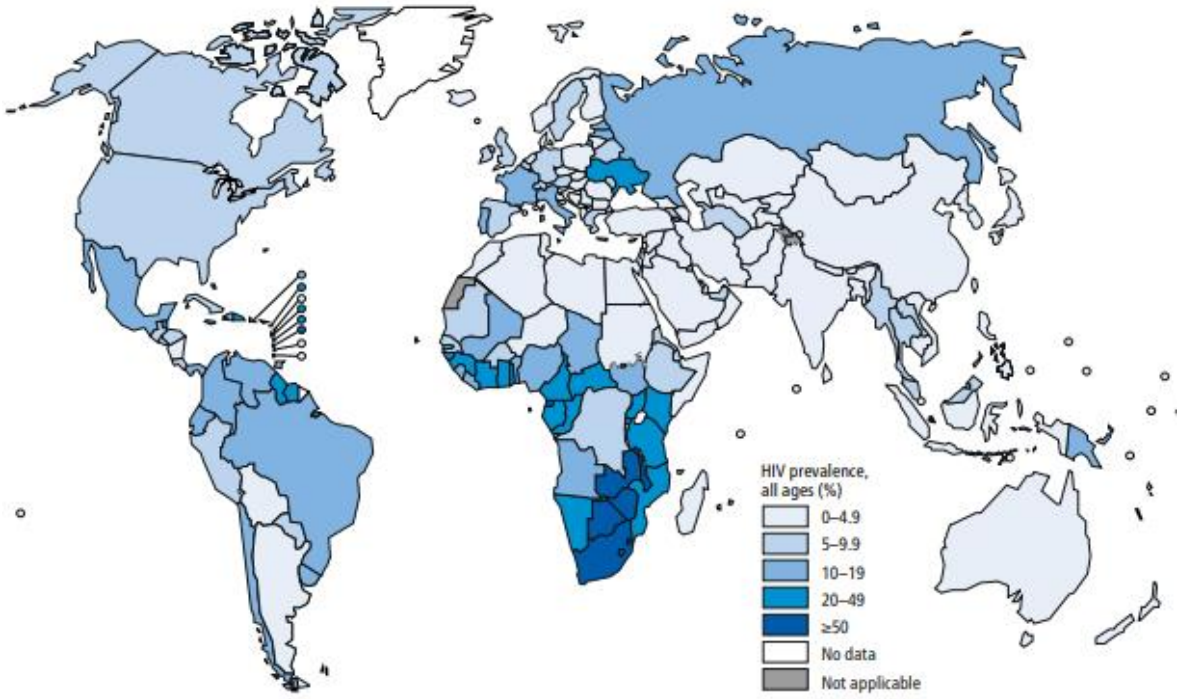

Figure 3. Estimated HIV prevalence in new and relapsed TB cases for 2016.[4]

Estimates by the World Health Organisation (WHO) may not be as accurate as they seem given that predictions of prevalence and incidence are based upon registered cases then factored into population size to give an overall sense of spread, as well as "expert" opinion about the accuracy of reporting.[12]

It is this last point that proves particularly troublesome for data acquisition and subsequent distribution of global resources to combat the spread and provide treatment for those regions who need it most. Inaccuracy of data lead to surveillance to establish a more accurate read, and indeed the first of its kind in Nigeria in 2012 resulted in a vast increase in cases than were predicted prior to this survey (200% increase in incidence, 100% increase in prevalence, 400% increase in mortality).[12]

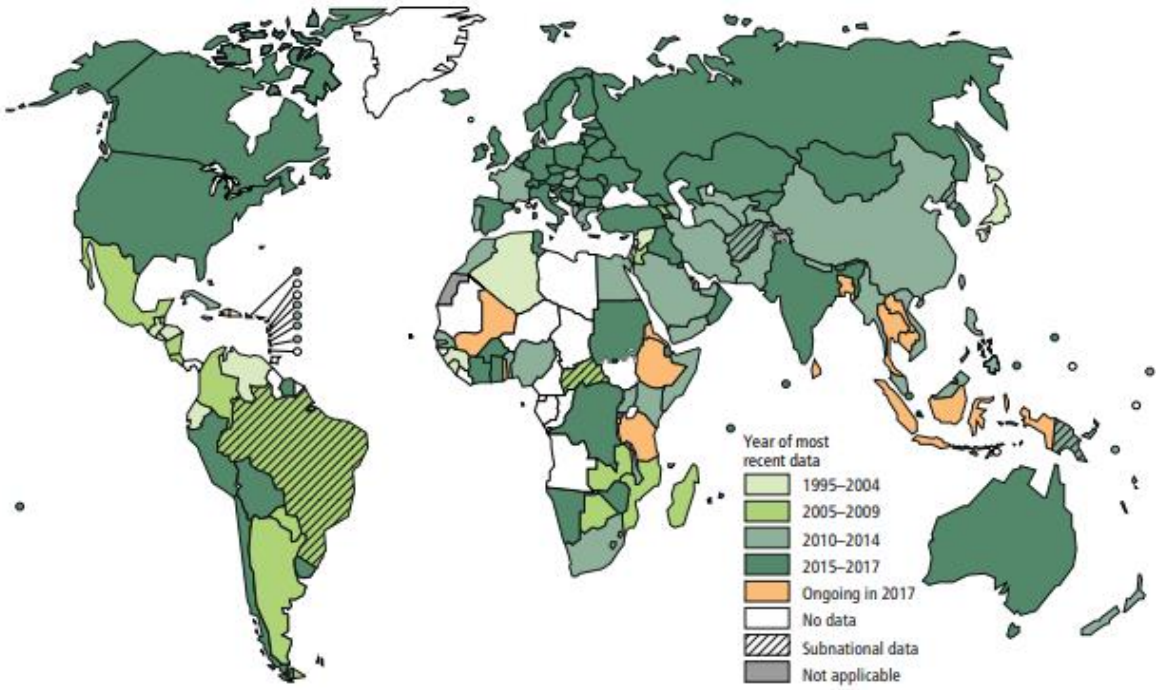

Figure 4. Figure showing data collection for tuberculosis.[4]

The current coverage of surveillance is shown in **Figure 4**, further reiterating that it is only recently that researchers have been able to grasp just how destructive the disease has been in South East Asia and Africa. **Figure 5** and **Figure 6** show the drastic change in TB prevalence figures upon recent surveillance as compared to reports prior to 2007.

Ensuring all countries comply with disease reporting regulations as well as appointing better trained healthcare professionals to medical institutions will allow a more accurate understanding of the spread of tuberculosis, as the current reported number of cases (7 million worldwide) of TB is far below estimates (10 million). The WHO attribute a large portion of this to underreporting of disease cases as well as underdiagnosis (i.e. people with TB not accessing healthcare or being misdiagnosed).[13]

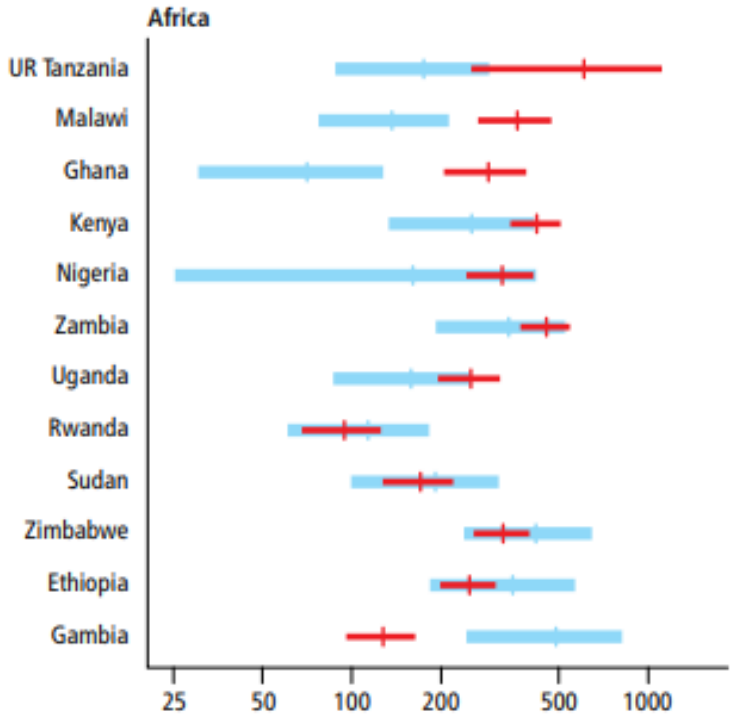

Figure 5. Prevalence (per 100,000 population) of TB before (blue) and after (red) national surveys carried out post 2007.[4]

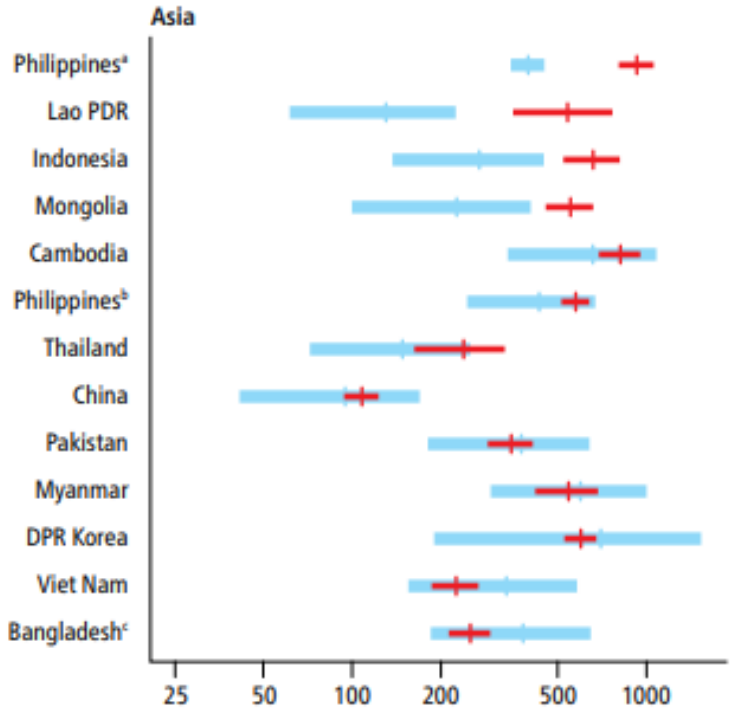

Figure 6. Prevalence (per 100,000 population) of TB before (blue) and after (red) national surveys carried out post 2007.[4]

The ever-growing increase in collaboration between African scientists and research councils such as The European & Developing countries Clinical Trials Partnership (EDCTP) is aiding the development of existing and emerging methods for the control and treatment of tuberculosis. There is also significant investment in facilities associated with disease control and healthcare development. This level of connectivity is encouraging that not only will estimates of the global spread of TB be more accurate but also that sequential utilisation of this will be more beneficial to patients in terms of understanding the countries needs as well as delivering appropriate healthcare.[14]

As can be seen in **Figure 2**, the vast majority of estimated new cases were in the South East Asian region and African region with 45% and 25% respectively of the global level of incidence.[4] These regions unsurprisingly exhibit higher incidence rates than more developed areas of the world as there is perhaps a lower level of accessibility to medicine. This is due to both the cost involved and the often vast distance to travel to receive treatment, in addition to general hygiene in rural areas being lower than more developed regions of the nations surveyed. As European mortality levels were merely a tenth of those recorded in Asia and Africa we can see that correct application of the relevant treatment (dependant on identification of bacterial strain) will greatly enhance survival rates in high risk areas, with the collaboration described above a vital component of such desires.

Around 25% of carriers are asymptomatic and carry the bacterium without developing the symptoms associated with active TB, known as latent TB. Symptoms include a chronic cough (commonly coupled with blood containing sputum), fever, night sweats and weight loss.[15] The danger of latent TB is that approximately 10% of patients will develop the active form during their lifetime Recommendations on the course of action once latent TB is unveiled tend to be cautionary observance of any developing symptoms rather than immediate therapy dependant on individual circumstances.

Generic treatment regimens are in place to cure the patient commonly using a combination of isoniazid, rifampicin, ethambutol, streptomycin, and pyrazinamide for nine months (illustrated in **Figure 7**), the respective mechanisms of action will be discussed in more detail later in the report.[16]

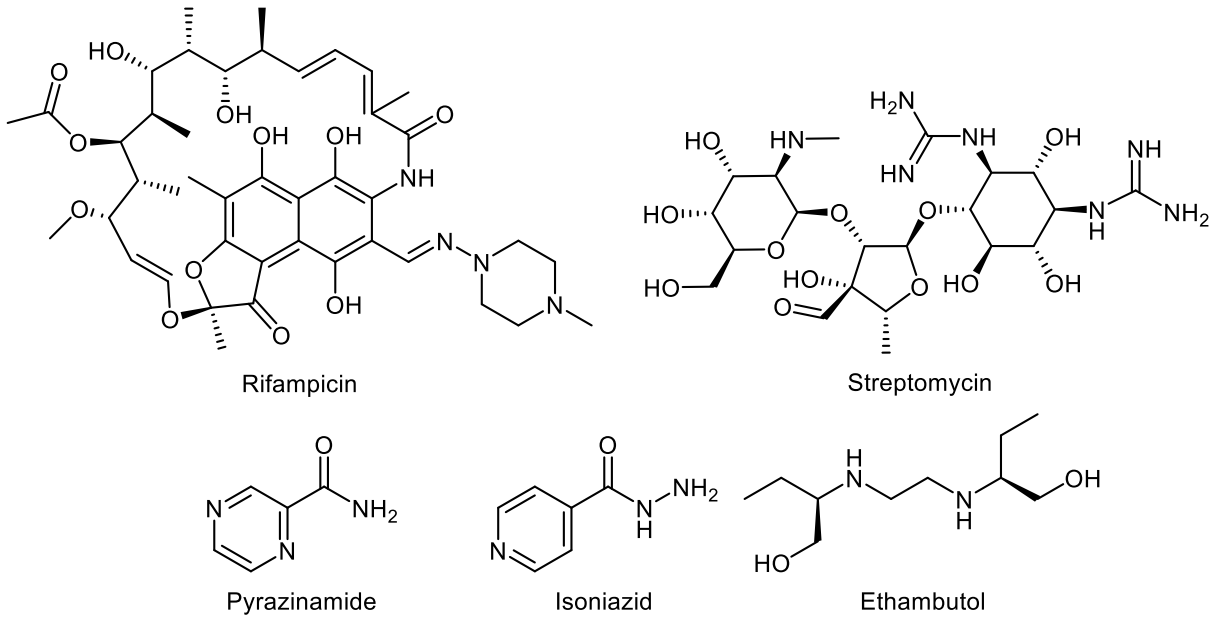

Figure 7. Structures of first-line treatments for tuberculosis

It is important to note that there are separate regimens for latent and active tuberculosis as resistant strains may not respond to the first line combinations used for non-resistant strains and need more specialised levels of treatment. Those deemed most at risk may be advised to begin chemotherapy, consisting of those with specific immunocompromised conditions such as HIV/diabetes as well as those from particular geographic locations.[3]

The most common outcome of this early treatment is not necessarily a lifetime cure, merely a higher chance (up to 90%) that the patient won't develop the active form of the disease in their lifetime. Hepatotoxicity concerns and patient unwillingness to complete the regimen (nine months minimum) leads to inefficacy of prevention in certain regions.[17]

1.1.1 *Mycobacterium bovis* in the farming industry and other areas of work

The spread of TB has led to problems in the farming industry where cattle are culled if tested positive for the disease, due to the ability of *M. bovis* to cross the species barrier and infect humans. The slow growing nature of the disease means that discovery of an infected animal may only take place once symptoms appear, when the whole herd may have been already infected. Infected humans may then unknowingly transmit the disease from farm to farm as well as developing symptoms themselves, due to poor hygiene regimens and lack of disinfection procedures.[18-20]

The BCG vaccine may be incorporated into cattle feedstock to provide immunity toward *M. bovis* but this method interferes with the commonly used skin test (single intradermal cervical comparative test) to diagnose cattle with TB, and in 2016 there developed a worldwide shortage of BCG vaccine so stocks were conserved for human use.[21]

The cattle – human cross species infection occurs in a similar way to *M. tuberculosis* as the bacterium traverses through airborne droplets, blood and faeces.[18] Furthermore, infection may be transmitted through drinking infected cow's milk as well as a small proportion via contaminated meat.[22] The prevention of bacterial spread through consumption of milk is controlled by milk pasteurisation which kills the bacteria, and in the developed world this method has halted this route of infection. For example, a recent study conducted in the UK indicated the percentage of tuberculosis cases as a direct product of *M. bovis* infection was 0.9%.[23] **Figure 8** shows the density of *Mycobacterium bovis* cases in the UK from 2002-2014, further reinforcing the notion that in developed countries which utilise pasteurisation methods that *M. bovis* is fairly well controlled.

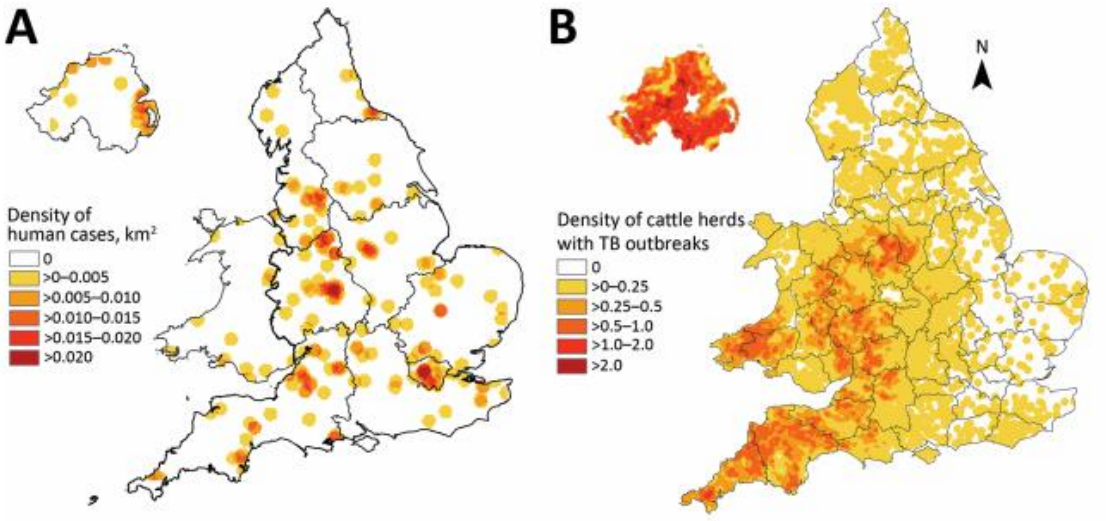

Figure 8. Mycobacterium bovis density for human and cattle cases in the UK from 2002-2014[23]

In less developed countries, where pasteurisation isn't used primarily due to the cost involved, the threat of infection through contaminated milk still exists. It is therefore important to develop potent low-cost vaccines which may be (more) available for third world countries to ensure minimal loss of livestock and damage to human life. There is a particular concern over the prevalence of *M. bovis* amongst rural regions due to the lack of routine surveillance carried out, so the spread of the strain may be worse than predicted.[24] It is important to note that in many regions there is not a mandatory differential test performed to distinguish between *M. tb* and *M. bov*, and given the bovine strain is resistant to pyrazinamide, this may lengthen treatment times.[22]

Additional concerns arise for those not working directly in the farming industry but who still have contact with infected animals. A systematic review was carried out by Flora Vayr *et al* in 2018 to determine various aspects of occupational hazards to *M. bovis* in which numerous studies were scrutinised and results combined to determine the level and differing risks associated with directly working with or indirect exposure to a contaminated source.[22]

Livestock farmers or those who live in close contact with bovine animals are understandably extensively represented in these studies, their direct contact with infected herds/individuals affords a larger risk of cross contamination than other areas of work.

Another common pathway for disease to infect humans is via veterinary study of an infected animal, either by inhaling airborne droplets when applying treatment to the animal or if any cuts/wounds are left uncovered. This is similar to abattoir workers who may become infected in the same manner.[22]

A common pathway for farm to farm transmission between livestock has been attributed to carriers of the disease, for example the common brushtail possum in New Zealand.[25] Pest control strategies were put in place to control the levels of possum in order to restrict *M. bovis* transmission across farms, with widespread success.[25] Similar strategies have been proposed in Great Britain with regards to badger culling, but there is widespread debate over the legitimacy of the badger as a vector for *M. bovis* transmission.[26]

1.1.2 End TB Strategy

The WHO initiated the End TB Strategy in 2014 which is a global effort to both reduce the number of incidences of tuberculosis as well as the number of deaths.[3] This is based around three principles which are to be adopted worldwide for: accurate data collection, strong governmental participance in funding and disease prevention, and enabling and encouraging rapidly developing research for the projected decreases in incidence/death to take place in the desired timeframe. This is shown in **Figure 9**.

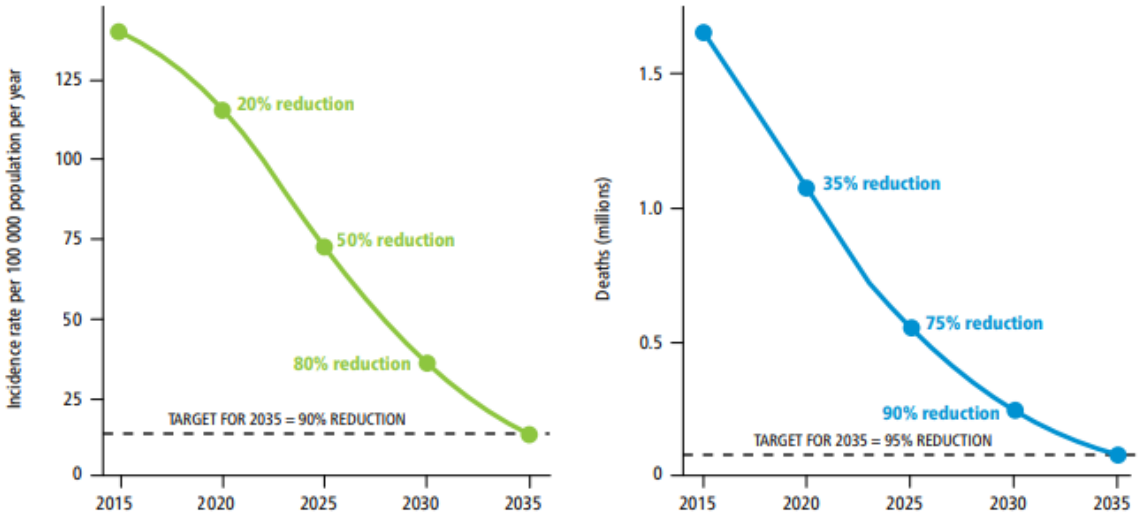

Figure 9. Projected incidence and mortality curves to reach tuberculosis targets by 2035.[4]

The current global reduction in mortality is at a level of 3% per annum and the incidence rate 2% which is required to reach 4-5% by 2020 to achieve desired WHO targets.[4] It is also positive that while incidence/prevalence cases are not falling as quickly as desired, the reduction in mortality rate is promising. **Figure 10** shows the death rate amongst both those with and without HIV is decreasing so it is encouraging that current treatment regimens are being implemented effectively, which further reinforces the need for continued partnership with healthcare and research councils, even though the threat of drug resistant strains looms.

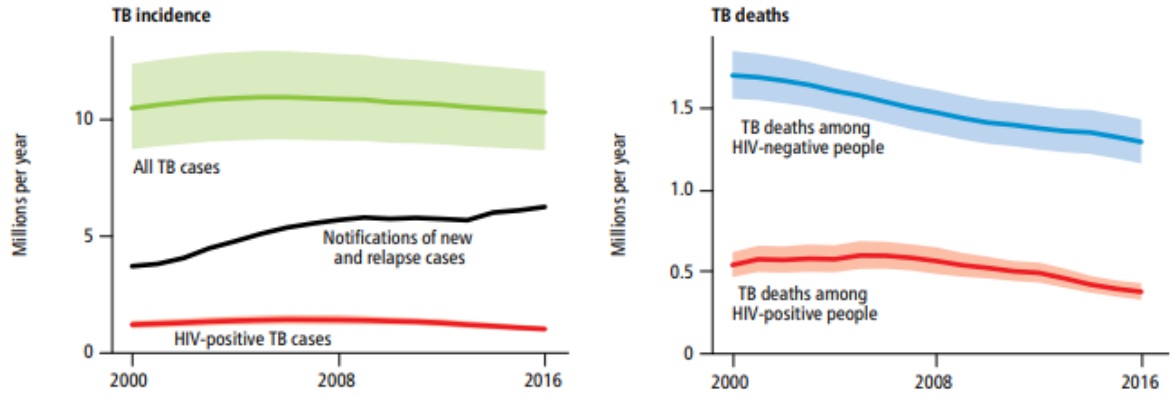

Figure 10. Global trends in the estimated number of incident TB cases and the number of TB deaths (in millions), 2000–2016. Shaded areas represent uncertainty intervals.[4]

1.2 Bacterial Cell Wall Composition

M. bovis and *M. tuberculosis* are acid fast bacteria (occasionally termed Gram positive acid fast) with outer cell walls primarily consisting of branched, long chain (C_{60}-C_{90}), fatty acids termed mycolic acids. This differs from the typical Gram positive bacterial cell wall which mainly comprises of a thick layer of peptidoglycan (> 50%) and is bridged by teichoic acids for rigidity and support. Gram negative bacteria contain a smaller portion of peptidoglycan (10%) in the cell wall as well as a thin coating of lipopolysaccharides to aid integrity and resist attack by harmful species. Mycolic acids comprise up to 60% of the whole cell dry weight.[27] These are functionalised at regular intervals by cyclopropyl, ketyl, or methyl ethers; an illustration of the differing types of mycolic acid is shown in **Figure 11**.[27-32] An illustration of the acid-fast cell wall is shown in **Figure 12**.

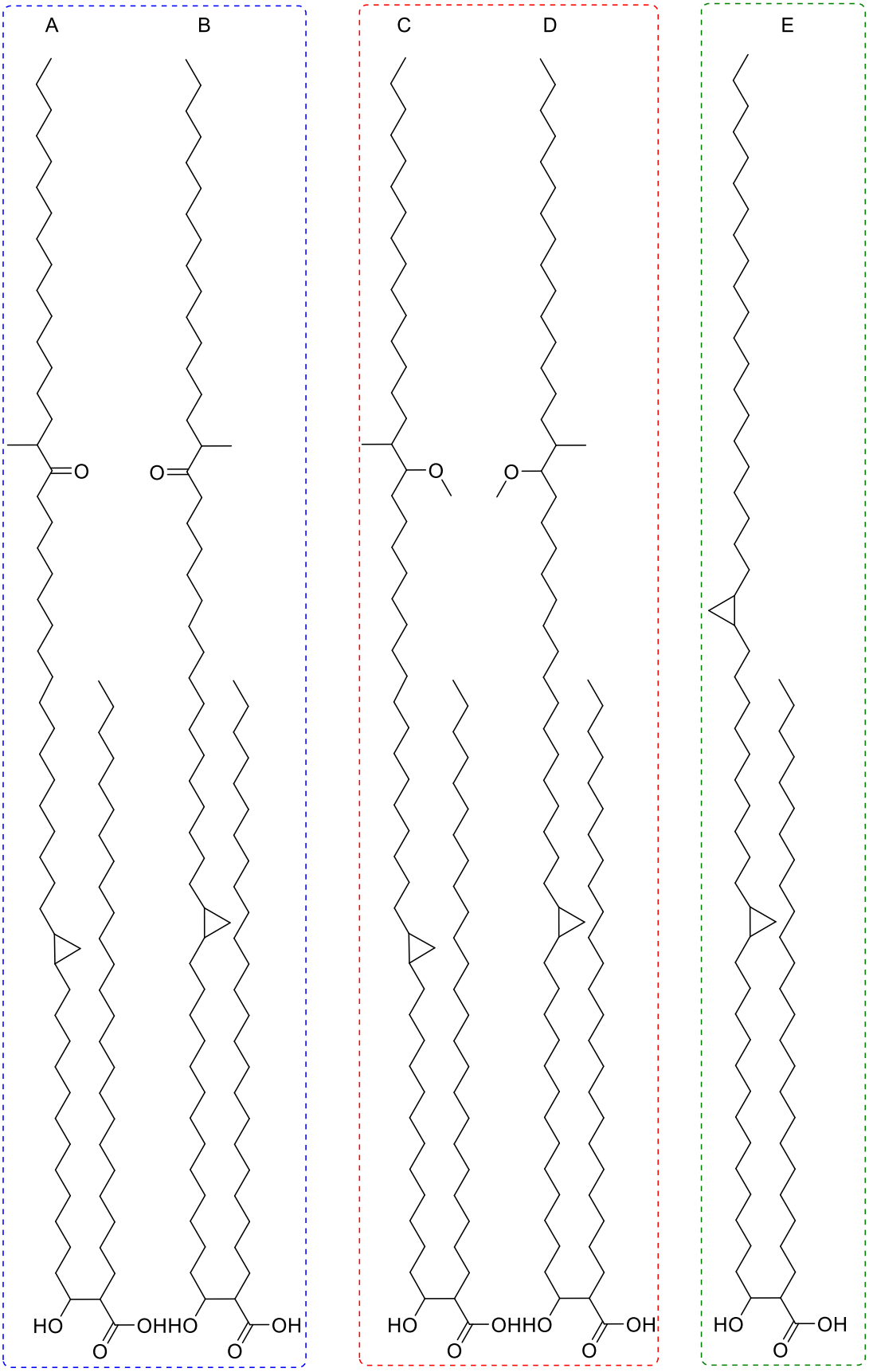

Figure 11. A = trans keto-mycolic acid, B = cis keto-mycolic acid, C = trans methoxy-mycolic acid, D = cis methoxy-mycolic acid, E = α-mycolic acid

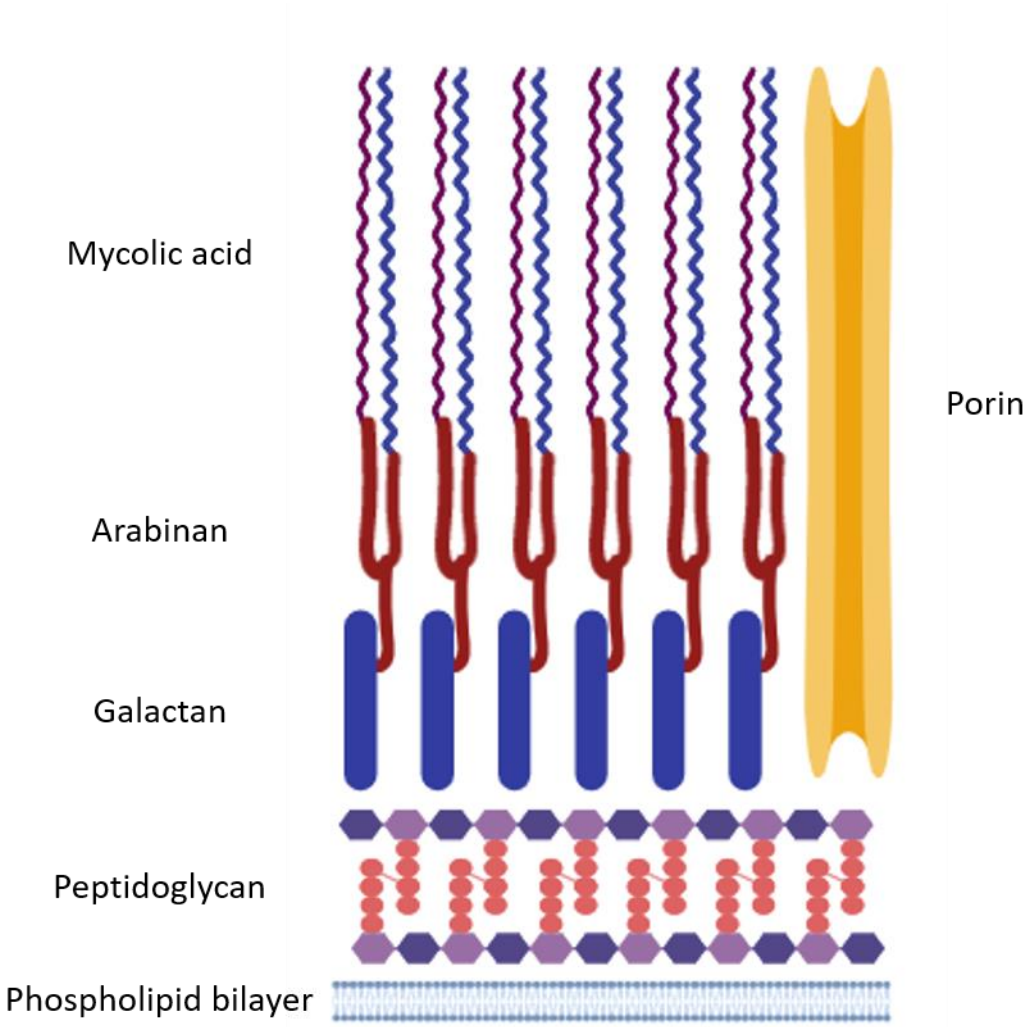

Figure 12. Illustration of the acid-fast cell wall.

Mycolic acids are produced by the mycobacterial fatty acid synthase type I (FASI) and type II (FASII) biosynthetic pathways. FAS I catalyses the synthesis of smaller fragments of hydrocarbon chains ($C_{20\text{-}24}$) (FASI) before extension in the chain length is carried out by FASII to produce fatty acyl-CoA (C_{50}+).[33]

Mycolic acids create a hydrophobic environment which envelops the cell thus giving the cell wall a reduced permeability to hydrophilic species such as some nutrients and antibiotics. As such the bacterium is slow growing, dividing once every ~18 hours. In

comparison, *E. coli* divides once every 20 - 60 minutes. However, hydrophobic species may permeate via passive diffusion through the lipid bilayer – a route utilised by macrolides and fluoroquinolones.[34-37] Some low molecular weight hydrophilic species and certain drugs may enter the cell passively via membrane bound porins, the deletion of which has been shown to drastically decrease drug uptake therefore the effectiveness of the drug, thus proving their importance for targeted cell death.[35, 37-39] Other methods used include active transport by cellular wall proteins or diffusion when the drug is hydrophobic in nature. The waxy mycolic coating is able to resist dehydration and chemical damage from radical species, and is involved with invasion of macrophages as it contains several compounds relating to pathogenesis such as adhesins.[28,40]

1.3 Pathogenesis

To facilitate host infection the bacterium travels to the pulmonary alveoli and invades endosomes of alveolar macrophages. The macrophages recognise the bacterium as foreign which activates the immune response. Phagocytosis is attempted and the phagosome combines with a lysosome where the immune system utilises oxidative species to try and kill the encapsulated cell. The mycolic acid capsule is able to resist this; the bacterium is then able to replicate within the phagosomes and eventually kill the immune cell.[41] A brief graphic of this is shown in **Figure 13**.

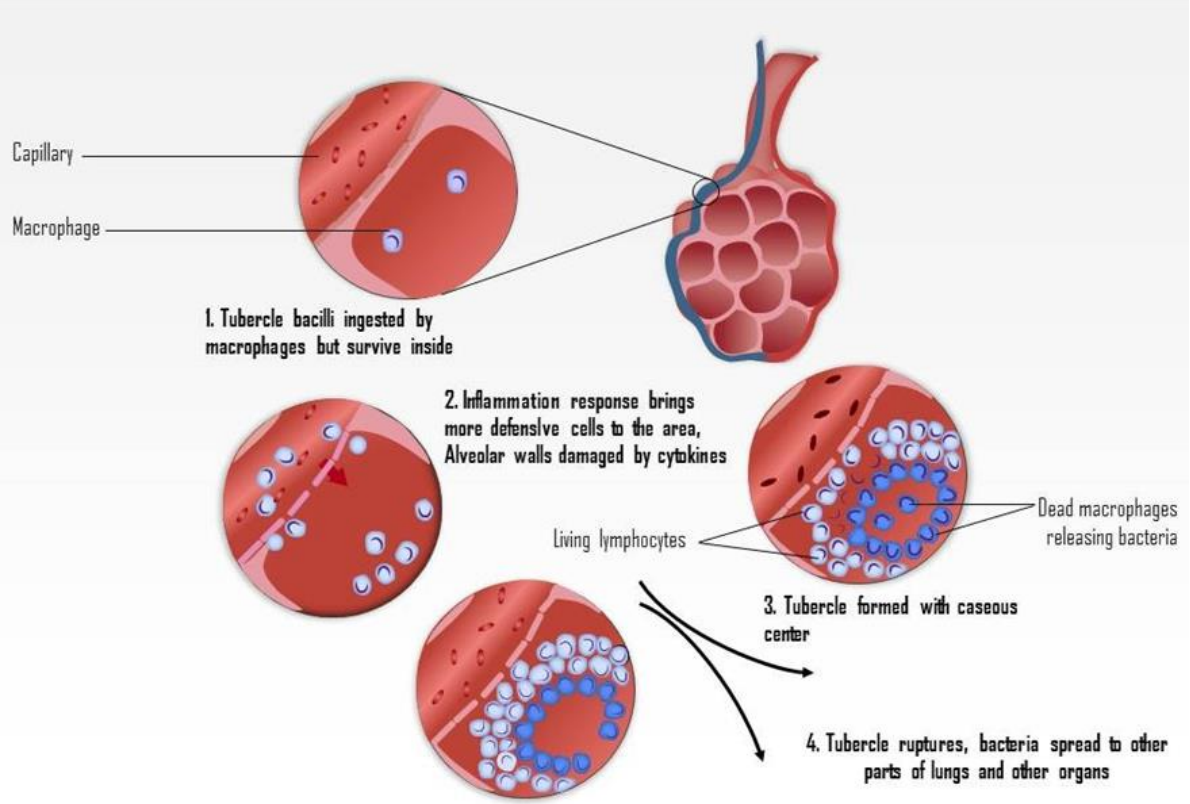

Figure 13. Graphic describing pulmonary tuberculosis spread.[42]

Upon bursting of the macrophages there is further spread of the bacilli both locally and by expulsion via aerosol to facilitate new host infection. Locally this leads to granuloma forming providing a region for the bacteria to grow which ultimately leads to necrosis and the lung damage tuberculosis is renowned for.[43] If the host immune system cannot rid itself of the bacteria then nodules of necrotic tissue may form and potentially liquify which are known as "tubercles", of which the disease gets its name. [44] They may break off from the lining of the lung inadvertently during the host immune response and traverse the bloodstream causing extrapulmonary tuberculosis. This form is where the bacteria spreads to various regions around the body including lymph nodes, central nervous system and bones.[45]

1.4 Diagnosis

Figure 14. Chest X-Ray showing lesions caused by tuberculosis.[46]

Diagnosis of pulmonary tuberculosis is achieved by a number of methods, the first being a chest x-ray (example in **Figure 14**) which will show any abnormalities caused by lesions, as well as a sputum test to look for bacteria.[47]

In humans, a discussion of recent health and a physical examination is often performed. A skin test (commonly Mantoux test) is performed where a small sample of tubercular proteins is injected intradermally and any inflammation observed hereafter is due to the body exhibiting an immune response, thus indicating prior/current bacterial exposure.[48] The size of the skin irritation as a direct consequence of the test is measured in diameter, with results indicated by various factors including recent contact with infected individuals, immune status, and general personal circumstances such as job/area of residence.

Use of this method when the patient has taken the BCG vaccine may provide false positive results.[48] A nucleic acid amplification test can also be performed to indicate mycobacterial nucleic acid in the blood.[49]

Extrapulmonary tuberculosis is diagnosed in the same way, with additional CT scans being taken of the affected areas of the body. An endoscopy may also be needed as well as a biopsy to assess infected areas.[47] If there is concern that the brain and spinal cord are infected then a lumbar puncture is performed.

A more recent test uses an interferon gamma release assay to assess antigen activity in the blood of the patient, these antigens are not present in the BCG vaccine or non-tubercular bacteria and so give a more specific result than skin tests.[50]

1.5 Treatment

1.5.1 Cattle

Due to the cost of treatment for farmers to inoculate herds of cattle, as well as antibacterial therapy upon discovery of the active disease, the cheaper option is to simply cull rather than treat the specimen. Therapy for humans infected with tuberculosis is detailed below in section **2.5.2**. The scale of this spread is unclear due to communication between farms and government officials/surveillance teams being poor, and indeed in many countries this is non-existent although plans are afoot to avert this lack of data.[4] There are new and engaging strategies being employed or planned to ascertain the accuracy and validity of current statistics to further the control of this strain.[4]

Methods of culling to control *M. bovis* spread, with reference to Great Britain, had great success in the period of the 1960's to the 1980's with results shown below in **Figure 15**. Nationwide skin tests were applied and any herds containing bacterial incidence were slaughtered in an attempt to eradicate the disease.[51] Complete eradication was not achieved, although the spread of the disease was kept under relatively good control. The spike in cases in 2002 is as a result of the "foot and mouth" epidemic. A review on bovine

TB elimination in New Zealand showed similar results, in that broadspread culling helped prevent wider disease progression as well as an implemented strategy involving pest management for present and future control of tuberculosis in wildlife.[52]

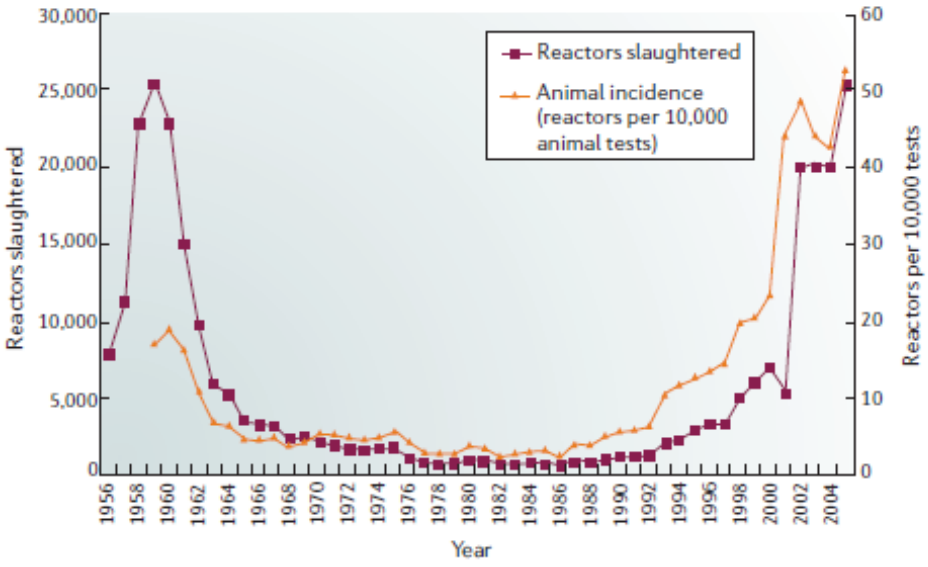

Figure 15. Incidence of *M. bovis* in cattle compared to reactors slaughtered in Great Britain from 1956 to 2004.[51]

Problems associated with the eradication of bovine tuberculosis arise from the resilience of the bacterium as well as the methodology used in such trials.[53] Factors affecting prevention of disease elimination may include a lack of understanding relating to vectors of transmission as well as bacillus resistance to changes in environmental conditions.[53] Past attempts at badger culling have proven ineffective at controlling the spread of bovine TB, and indeed this topic remains under discussion.[54]

1.5.2 Human

As a result of the slow uptake of drugs and the complex nature of the disease, treatment of TB requires long term therapy with a combination of antibiotics which is an issue due to testing for any resistant strains taking place whilst the patient is receiving a general set

of first line anti-TB drugs.[32] This may delay the discovery of drug resistant tuberculosis in the patient and therefore risks wasting drugs which will not work on the particular strain. Another issue is patient non-compliance with prescribed treatment plans: this occurs by refusal or patient complacency to take antibiotics for the prescribed treatment time because of cultural beliefs or the patient feeling better so not finishing the treatment plan. This breeds resistance to first line treatments of TB which in addition to random mutation, leads to multidrug (MDR-TB) and extensively (XDR-TB) drug resistant strains that are becoming increasingly prevalent worldwide.[3, 55, 56] General methods of drug resistance include: random mutation in the binding site of the drug target, overexpression of efflux proteins, deletion of porins to reduce drug uptake, and upregulation of enzymes which inactivate the drug such as peptidases and β-lactamases.[57]

Prior efforts to vaccinate against tuberculosis have given mixed results with debate over efficacy and cost effectiveness at the forefront of such arguments.[58, 59] The Bacillus Calmette-Guérin (BCG) vaccine was given to schoolchildren aged thirteen between 1993 and 2005 but was pulled from UK-wide use due to lower levels of the disease prevalence and it is currently only used for those in high risk areas such as some areas of inner London or any children with a family history of tuberculosis.[60]

The efficacy of this vaccine is also dependent upon genetic variations of not only the patient, but also the bacterial strain in the vaccine, as well as prior patient interaction with mycobacterial species as the patient will have already developed an immune response to them.[61] Current worldwide policy on BCG vaccination is shown in **Figure 16**. Nationwide coverage is shown in **Figure 17**.

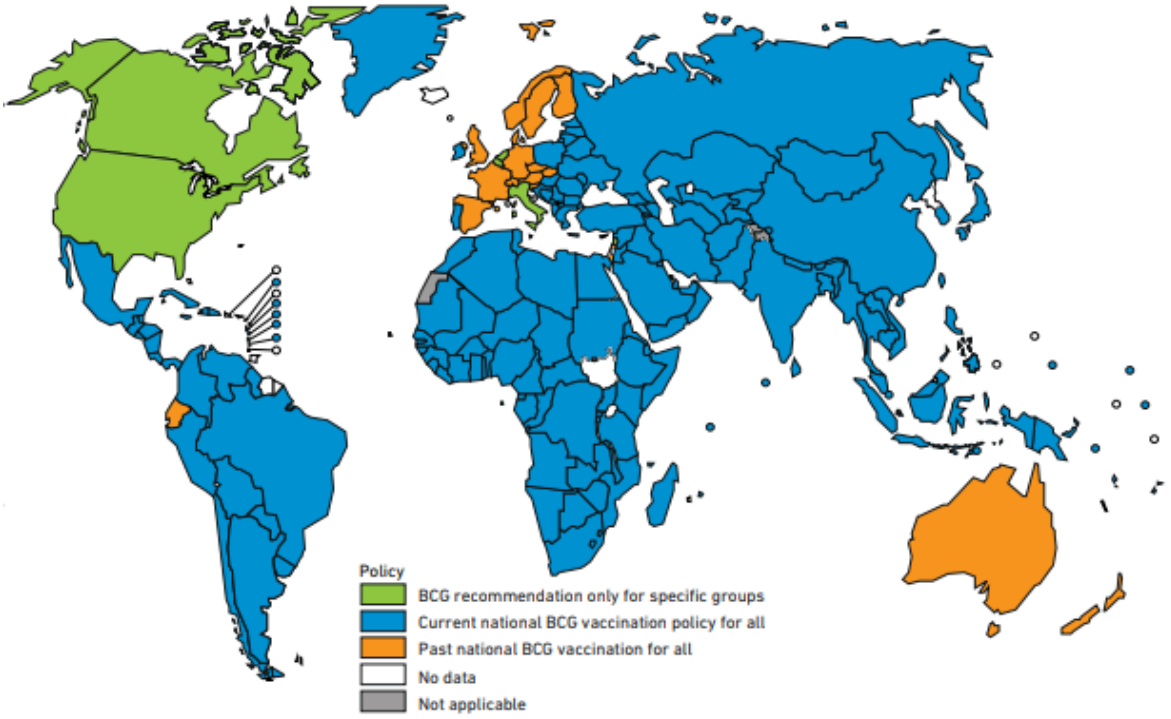

Figure 16. BCG Vaccine policy.[4]

Figure 17. Percentage coverage of BCG vaccine in relevant areas.[4]

A new branch of the bacterium is developing, colloquially described as "totally drug resistant" (TDR-TB), where the strains are resistant to all first and second line treatments, although this has yet to be officially termed by the WHO and has only been seen in a small number of countries.[62, 63] More recent overviews of this bacterial problem indicate that around 2% of MDR-TB turns out to be TDR-TB, although many laboratories in endemic countries lack the required equipment/funding to ascertain which strain of tuberculosis the patient has and so estimates of TDR-TB may be inaccurate.[64]

It is important to note the striking similarity between the genomes of *M. bovis* and *M. tuberculosis*, with only a difference of 0.05% in the average sequence divergence.[51] This closeness in genomic structure indicates that a drug which may be designed for the eradication of tuberculosis ought to have the same effect in both bacteria, providing the targets are the same in both cellular environments.

1.5.3 First-line Treatments

Five key antibiotics termed first-line (isoniazid, rifampicin, pyrazinamide, streptomycin and ethambutol) are delivered as part of a long-term combination therapy with many more drugs developed since to increase efficacy, reduce dosage amounts, and to combat resistant strains, the subject of which is a growing issue with both multidrug and extensively drug resistant tuberculosis strains mutating; upon diagnosis these forms of tuberculosis are still treatable with the appropriate medication.[55]

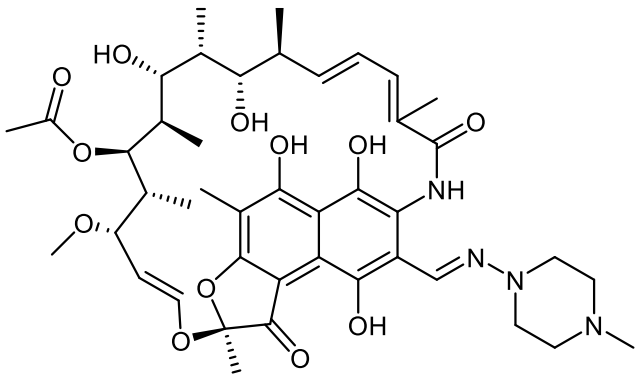

Figure 18. Structure of rifampicin.

Rifampicin (may also be termed as Rifampin) (**Figure 18**) was discovered in 1965 and approved as an antitubercular agent in 1971. It is a natural product belonging to the class ansamycin, made by the gram positive bacterium *Amycolatopsis rifamycinica.* Rifampicin is used as a general antibiotic but more specifically acts upon bacterial DNA dependant RNA polymerase.[65] It has been shown by crystallographic and biochemical data to act via a "steric occlusion" mechanism, whereby the molecule binds to a site away from the active site of the protein.[66] Many drugs act to prevent the natural substrate from entering the active site in perhaps a more conventional manner, but rifampicin blocks the elongation of the growing RNA chain by physically blocking its pathway to exit the protein.[66] This leads to the phosphodiester bond not being formed upon the chain reaching two or three nucleotides in length due to its mislocation compared to the usual mechanism.[67]

Resistance occurs in a number of ways, most commonly a single point mutation in the rifampicin binding site leading to a vastly reduced drug affinity.[68] Another mode of resistance is by overexpression of the Arr family of proteins, as seen in *M. smegmatis,* which aid in ADP ribosylation of rifampicin thereby inactivating the drug.[69]

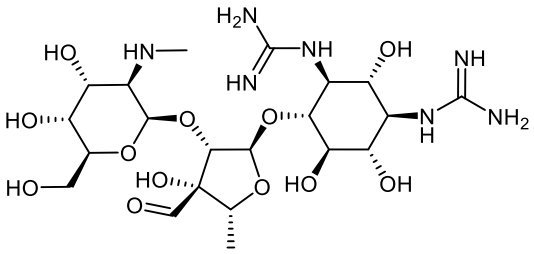

Figure 19. Streptomycin structure.

Streptomycin is used as a broad spectrum antibiotic which was initially isolated from *Streptomyces griseus,* and was the first compound applied to the treatment of TB in 1942, but due to this being the only form of therapy resistance quickly arose.[70] It acts by irreversibly binding to the 16S rRNA of the 30S subunit of the ribosomal protein, which in turn interferes with the proteins interaction upon the incoming tRNA. This interferes with the initiation and elongation steps of protein synthesis, affording codon misreading thereby leading to lack of protein synthesis resulting in death of the cell.[71] Resistance to streptomycin mainly arises from mutations in the 16S region.[72] As with most aminoglycosides, common side effects involve kidney toxicity as well as various problems within the ear – tinnitus, vertigo and deafness.[73]

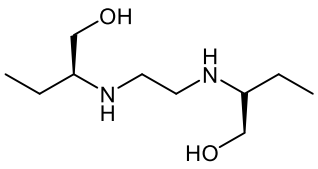

Figure 20. Ethambutol structure.

Ethambutol (**Figure 20**) was discovered in 1961 and approved in 1968 as an antitubercular treatment.[74] It is delivered in combination with rifampicin, isoniazid and pyrazinamide over a long period (commonly six months plus). The precise mechanism of action is debated but commonly perceived as inhibiting the cell wall synthesis (in particular arabinogalactan) thereby increasing cellular permeability.[75] It is thought to directly inhibit

the arabinosyl transferase EmbB which promotes polymerisation of arabinogalactan, but recent studies indicate that this may not be the only target, with certain *M. smegmatis* strains containing EmbB knockouts still viable for ethambutol targeting.[75, 76] Mutations leading to resistance to ethambutol generally arise from single point base alterations in the binding site thus preventing the drug from binding to its intended target.[77, 78]

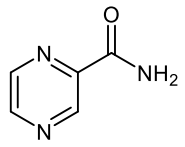

Figure 21. Pyrazinamide structure.

Pyrazinamide (**Figure 21**) was first synthesised in 1936 but wasn't widely used until the 1970's with respect to tuberculosis treatment.[79, 80] A mouse study found that combined use with other regimens of TB treatment shortened treatment times substantially, in particular a combination of isoniazid/rifampicin/ethambutol, which reduced the drug regimen timeframe from 12 months to 6 in combined use cases.[80] Despite its high level of importance to the regimen, Pyrazinamide's mechanism of action is not very well understood and is under continued debate. The compound itself is a prodrug which enters the cell via passive diffusion, and undergoes conversion into the active form by the cytoplasmic enzyme PZase into pyrazinoic acid.[81] This is a strong acid with pKa ~ 2.9 and accumulation in the cell has been proposed to affect various cellular mechanisms as well as disrupting the membrane and interfering with translation, eventually leading to cell death.

Studies to ascertain more specific modes of action of pyrazinoic acid have linked the ribosomal protein RpsA as a potential target, with overexpression of the protein causing a fivefold increase in MIC compared to the experimental control. These studies lead to a

proposed new method of action of the drug as suggested and drawn by the Zhang group in **Figure 22**.

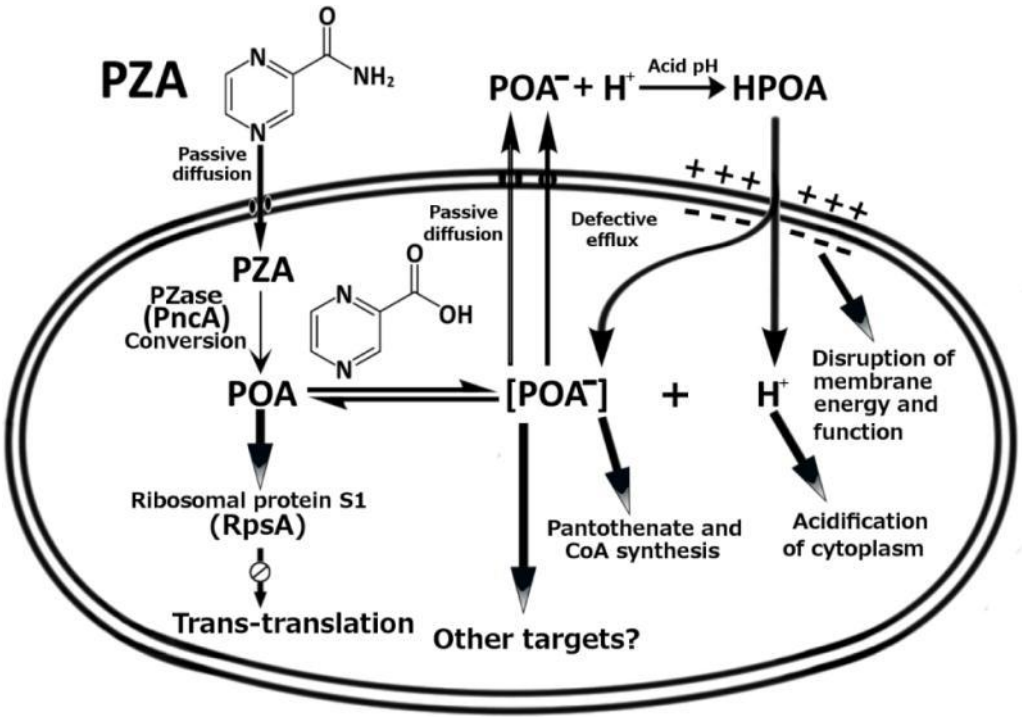

Figure 22. Proposed mode of action of pyrazinamide.[80]

Resistance to pyrazinamide has been shown to arise mainly from mutations in PncA causing amino acid alterations, particularly in the binding site. There are multiple sites at which mutation can arise which may affect: hydrogen bonding capability, active site catalytic triad, or perturbation of the active site shape.[82] New studies have indicated that PanD could be a viable target due to its involvement in the production of β-alanine, which in turn is a precursor for coenzyme-A.[83] Coenzyme-A is vital for cellular metabolism and as such any downregulation in its production would be fatal for the cell.

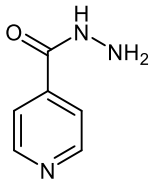

Figure 23. Isoniazid structure.

Isoniazid (**Figure 23**) is one of the most potent antitubercular drugs acting to prevent the production and replenishment of mycolic acids by inhibiting the FASII section of the fatty acid biosynthetic pathway.[84-87] It is a prodrug that is activated by the catalase peroxidase enzyme KatG to form an isonicotinic acyl radical species which is coupled to NADH forming an isonicotinic acyl-NADH complex - as illustrated in **Scheme 1**.[88-90] This complex tightly binds to the enoyl-acyl carrier protein reductase InhA, preventing the natural substrate from entering the active site thereby halting mycolic acid synthesis.[91] The fatty acid biosynthetic pathways are detailed in **Scheme 2**.

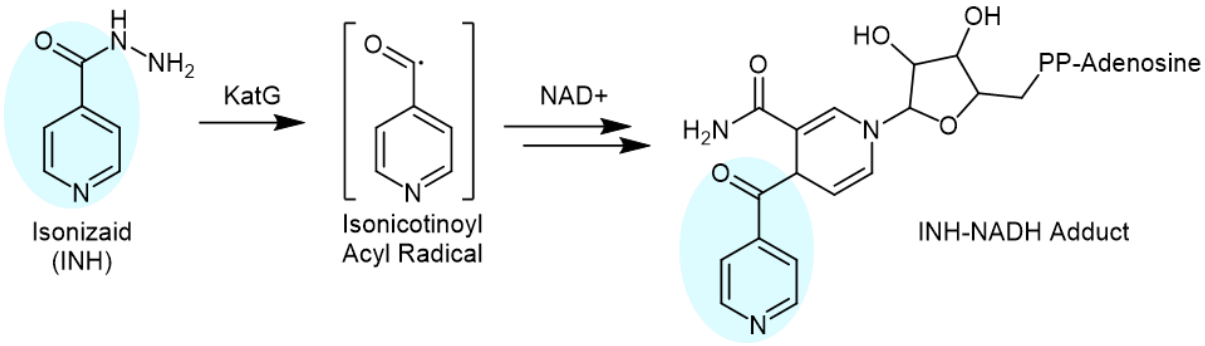

Scheme 1. Scheme to illustrate general activation pathway of isoniazid.[92]

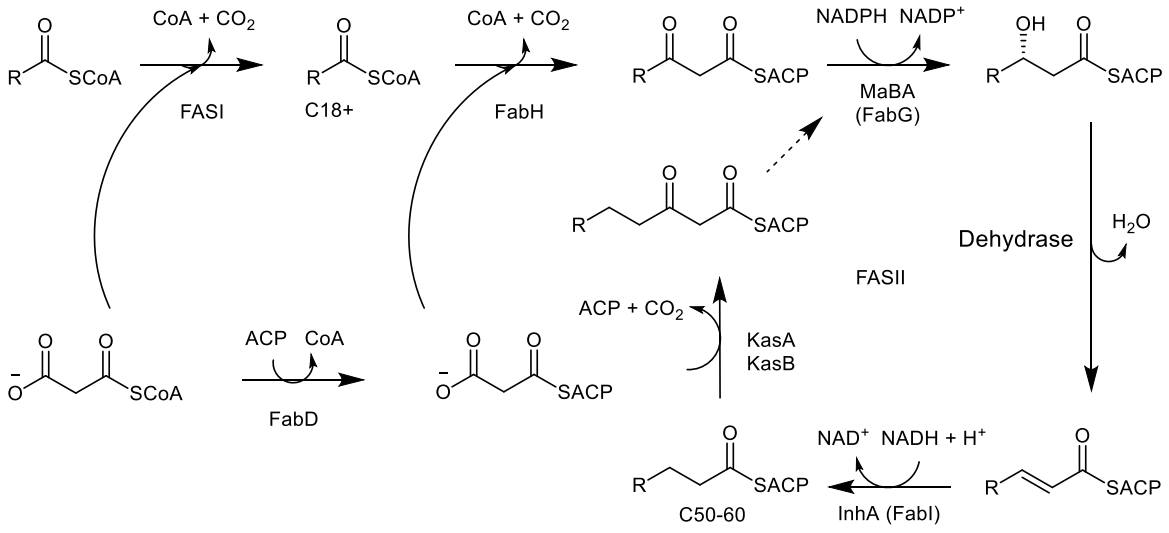

Scheme 2. Fatty acid biosynthesis in *Mycobacterium tuberculosis:* FASI facilitates mycolic acid chain growth up to C18 via a decarboxylation mediated Claisen condensation, FabH operates in a similar way extending the chain by C2 each time as well as altering the thioester from SCoA to SACP, FabG acts to catalyse the reduction of the beta-ketoacyl-ACP substrates to beta-hydroxyacyl-ACP products, Dehydrase acts to form an alkene via the removal of water, FabI then reduces the alkene to an alkane using NADH, and KasA/KasB operate in a similar way to FabH. After one cycle is completed FabD is used to replace SCoA with SACP before KasA/KasB Claisen addition to the growing carbon chain. This cycle of KasA/KasB-FabG-Dehydrase-FabI is repeated until carbon chain length of C50-C60 is achieved.

OxyR is a protein that upon expression activates genes to resist oxidative substances amassing in the cell thus giving resistance to oxidative stress and preventing cell lysis, found in various bacteria such as *E. coli* and *S. typhimum. Mycobacterium tuberculosis* is an oxyR knockout species thus lacking the ability to combat this change in cellular environment; as a consequence of InhA inactivation, a build-up of radicals occurs which it is unable to quench, damaging cellular components such as lipids, proteins, and nucleic acids ultimately leading to bacterial cell death. [93-95] Any drug which inhibits KatG, thereby preventing radical quenching from InhA, would result in cell death but there is bacterial

resistance to this particular method of attack. Mutation in KatG prevents isoniazid from binding to the active site thus remaining a prodrug, eliminating its activity.[96, 97]

It is therefore clear that treatment regimens that aim to disrupt the cell wall biosynthesis would weaken the cell and leave it vulnerable to osmotic pressure causing lysis and cell death.

One of the first experiments to investigate mutations in KatG and its involvement in the fatty acid biosynthetic pathway showed a single base pair replacement of thymine with guanine caused an amino acid substitution of alanine to serine which gave a reduction in isoniazid efficacy, suggesting KatG's involvement in fatty acid elongation.[32] Detailed studies have been performed to elucidate the exact mechanisms for KatG's activity upon its natural substrate to assist the understanding of isoniazid resistance, with the location of mutated residues and assessment of subsequent protein activity critical for understanding the oxidative process; the subject of which will not be covered herein. The mechanism of interaction of KatG with its substrate has been debated although hydrogen bonding in the active site, difference in heme or active site side chain oxidation potential and stability of the oxidation complex are all important for activity.[98]

Mutation in InhA is less common than KatG, which has been shown in numerous studies. A study in Kyrgyz Republic described the percentage differences of mutations in MDR-TB isolates as 91.2% for KatG, compared to 7% for InhA.[99] A similar survey in China gave resistance conferring mutations in KatG as 86.2% compared to 19.6% for mutations in InhA.[100] A key mutation conferring isoniazid resistance arises from a serine to alanine substitution which reduces the affinity of NADH to InhA seventeen-fold.[101] In addition, mutations in the promoter region lead to overexpression of InhA meaning the efficacy of standard regimens involving isoniazid is lowered.[102]

Inactivation of InhA results in cell death, so an inhibitor that targets InhA and does not require activation by KatG should still retain activity against the FASII pathway and therefore against isoniazid-resistant tubercular strains.[95, 97]

1.5.4 Second-line Treatments

Due to the slow growing nature of *M.tb* and *M.bovis* it takes a number of weeks for culture tests to grow and as such for determination of the correct strain to be achieved. This means that during this time the patient is given a general course of treatment which may inadvertently be ineffective towards the strain due to bacterial resistance. Upon discovery of the specific strain, more targeted treatment may be administered which aims to counteract resistance. These are termed "second-line" treatments, a series of which are briefly described below.

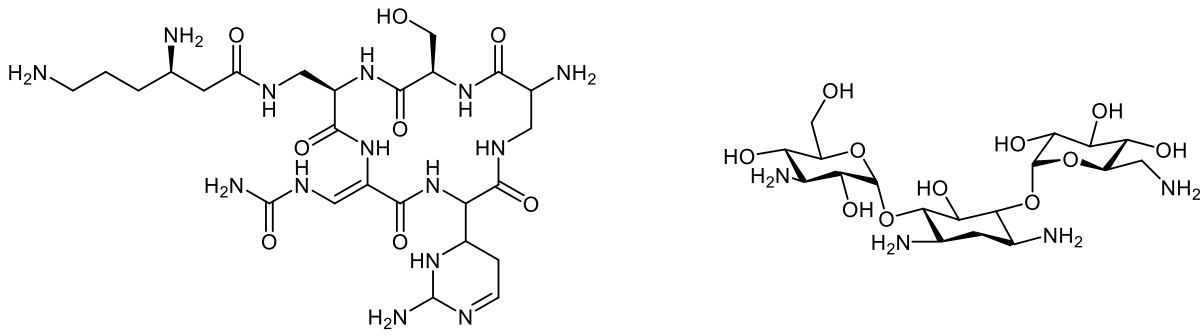

Figure 24. Structures of Capreomycin (Left) and Kanamycin A (Right)

Capreomycin and Kanamycin A are part of a group of compounds termed "SLI drugs" (second line injectable). Although they have vastly different structures (**Figure 24**) they act on the same target, binding to the bacterial ribosome resulting in an alteration of the 16S subunit.[70] This in turn alters the interaction between ribosomal subunits leading to misreading of codons thereby the production of abnormal proteins, affording cell death. Common side effects include hearing impairment including tinnitus, as well as impaired

renal function in some cases.[103] Resistance may comprise of mutations in the *rrs* gene thus inducing changes in the binding region of the large ribosome subunit, preventing the drugs from binding.[70, 104] Alternate studies show mutation in the *tlyA* gene may confer resistance to Capreomycin and the SLI family of antitubercular compounds.[105]

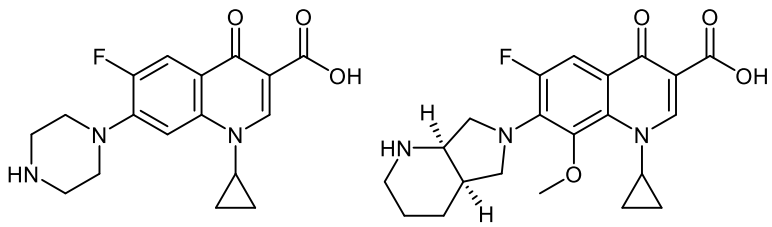

Figure 25. Ciprofloxacin and Moxifloxacin

The class of compounds known as fluoroquinolones have been in use for therapy for a number of years, with ciprofloxacin achieving patent in 1980 followed by introduction into therapy regimens in 1987.[106] Ciprofloxacin and a more recent analogue moxifloxacin are shown above in **Figure 25**. This class of compounds aims to disrupt bacterial DNA division and replication by inhibiting DNA gyrase, as well as topoisomerase IV thus halting cell division. Resistance to these branch of compounds arises chiefly in the *gyrA* gene which encodes for DNA gyrases, the region of which is termed the "quinolone resistance determining region". The primary mode of resistance arises from single as well as double point amino acid mutations, conferring resistance by altering the binding region of quinolones thus reducing drug affinity for the protein.[107] Alternative routes of bacterial resistance act via increasing the activity of efflux pumps in the cell membrane via mutations in a pump activity repressor gene.[107] Common side effects of fluoroquinolones include gastrointestinal discomfort, as well as various CNS issues including but not limited to; insomnia, convulsions and psychosis.[108, 109]

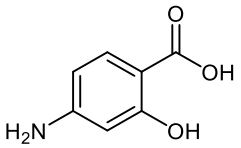

Figure 26. 4-aminosalicylic acid structure

4-Aminosalicylic acid (also termed *para*-aminosalicylic acid) was first synthesised in 1902 and brought into medical use in 1944, primarily as an antitubercular agent (also rarely used as treatment for inflammatory bowel disease).[110] Initial use was in combination therapy with isoniazid and streptomycin, although it was downgraded from first-line to second-line with the discovery of rifampicin/ethambutol/pyrazinamide, and is now only given as part of drug resistant tuberculosis therapy.[70] The mechanism of action is believed to be direct competition with para-aminobenzoic acid for the enzyme dihydropteroate synthase, preventing formation of folic acid.[111] There are various genes associated with resistance to para-aminosalicylic acid, all comprising different steps in folate synthesis.[70, 112] Common side effects include nausea, abdominal pain, and diarrhoea as well as liver damage in some patients.[111]

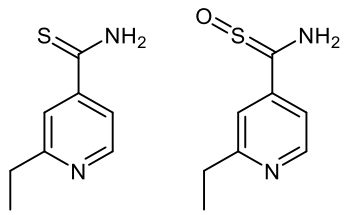

Figure 27. Ethionamide and ethionamide sulfoxide structures

Ethionamide is a compound which can be considered an analogue of isoniazid, acting in a similar way to the first-line drug. It is a prodrug which undergoes activation by the mono-oxygenase enzyme encoded by the gene *ethA* to form ethionamide sulfoxide, with the active form binding to NAD^+ in the same way as isoniazid, subsequently inhibiting InhA to prevent mycolic acid synthesis.[70] Mutations in *ethA* as well as *inhA* confer resistance to the

drug, preventing the activation of the prodrug and binding of the active form respectively.[113] Common side effects include nausea and wide-ranging levels of hepatotoxicity, depending on the treatment regimen in place. [15, 114]

1.5.5 Recently developed drugs

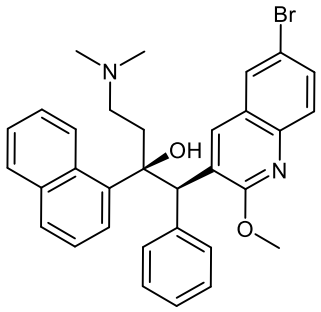

Figure 28. Bedaquiline structure

Bedaquiline (**Figure 28**) is a recently developed compound (approved in 2012) which acts upon bacterial ATP synthase to prevent production of ATP, without this vital energy source the cell dies.[115] Bedaquiline is given with a black box warning of increased risk of death, as it has been shown to interfere with patient cardiac function – causing severe arrhythmia. Controversy over its approval arose from several patient deaths while undergoing clinical trials, although there was no direct proof that treatment with bedaquiline caused these deaths. [116] Significant concerns are still held over its safety and as such its use is only recommended in cases where a more conventional regimen cannot be applied due to resistance, although this recommendation is only compliant with restrictions on other medication being taken which may affect the QT interval.[117] Resistance to bedaquiline has been shown to rely on mutations in the atpE gene which codes for ATP synthase, as well as a separate mutation which upregulates production of efflux pumps in the cell membrane.[70]

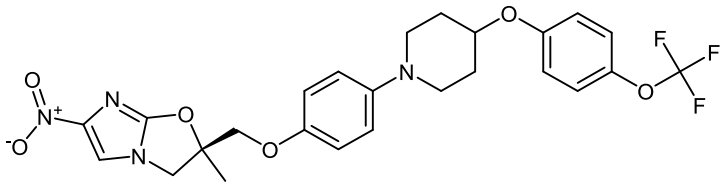

Figure 29. Delamanid structure

Delamanid (**Figure 29**) was approved in 2014 and acts to inhibit synthesis of mycobacterial cell components such as methoxymycolic acid and ketomycolic acid.[118] It is a prodrug, the process of its activation in the cell is unclear but the mycobacterial coenzyme F420 is thought to be utilised.[119] An interesting point to note is the lack of effectiveness against gram negative and gram positive bacteria, thus drastically lowering the potential for resistance arising from mutation in such species.[119] Interference with the QT interval has been observed in some studies and as such co-administration with other agents which may cause arrhythmia is not advised such as bedaquiline. It shares common side effects with almost all anti-tubercular agents such as nausea and dizziness, and in rat models there were observed teratogenic effects – although in levels far higher than would be used clinically.[119] Resistance in trials has been seen in various mutations to the coenzyme F420, and in one study the spontaneous rate of mutations conferring resistance was at a similar rate to isoniazid – suggesting monotherapy would result in resistant strains appearing at a fast rate.[119]

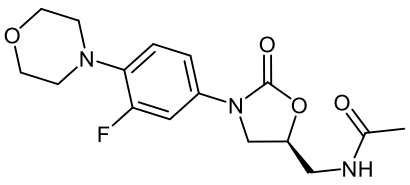

Figure 30. Linezolid structure

Linezolid has been in use for MDR-TB treatment since the early 2000's, despite its initial prognosis as a general antibacterial. It acts by binding at the 50S ribosomal subunit which in turn prevents the formation of the complete ribosome, halting protein synthesis by blocking the initiation step.[120] Resistance to linezolid arises primarily from mutations in the 23S rRNA gene, although growing research into the Cfr rRNA methyltransferase gene indicates it may traverse the bacterial species barrier, acting to methylate the 23S subunit preventing linezolid attachment.[120] Common side effects include diarrhoea and nausea, with cases observed of; thrush, pancreatitis, and liver damage.[121] It is used as a "last resort" treatment due to more severe side effects of myelosuppression and neuropathy.[122]

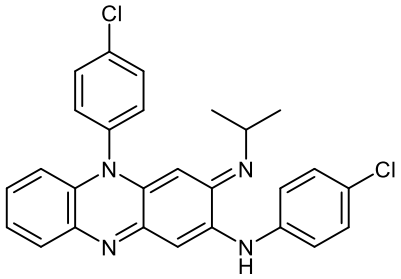

Figure 31. Clofazimine structure

Clofazimine is a repurposed drug, conventionally used to treat leprosy, which has recently been included on the WHO guidelines for a short treatment regimen.[123] Its mechanism of action is unclear although recent studies on *M. smegmatis* indicate it is most likely a prodrug which undergoes reduction by NADH dehydrogenase followed by reoxidation by O_2, releasing reactive oxygen species as a result.[70] As previously described, mycobacterial cells cannot resist oxidative stress and as such the cell will die. Resistance has been attributed to overexpression of membrane efflux pumps.[70] Common side effects are similar to most other anti-tuberculosis drugs, with nausea and stomach pains widely reported alongside more serious conditions such as skin discolouration.[124]

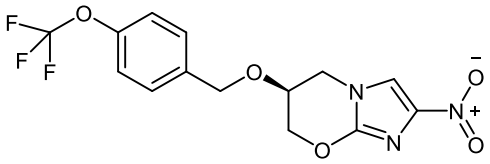

Figure 32. Pretomanid structure.

Pretomanid is a compound of the nitroimidazole class which has been approved in 2019 by the FDA for use against certain types of MDR-TB. It is given as part of a "drug cocktail" along with bedaquiline and linezolid. Its method of action is not clear although recent studies indicate it interferes with cell sugar phosphate metabolism creating an excess of methylglyoxal which is toxic to the bacterial cell.[125] Common side effects include peripheral neuropathy, anaemia, nausea, and indigestion.[126]

As can be seen in **Figure 33**, the coverage and scale of research into the efficacy of tuberculosis treatment regimens is truly worldwide, this level of dedication into ascertaining the spread of resistance is crucial for maintaining an effective outcome of the stop TB strategy.

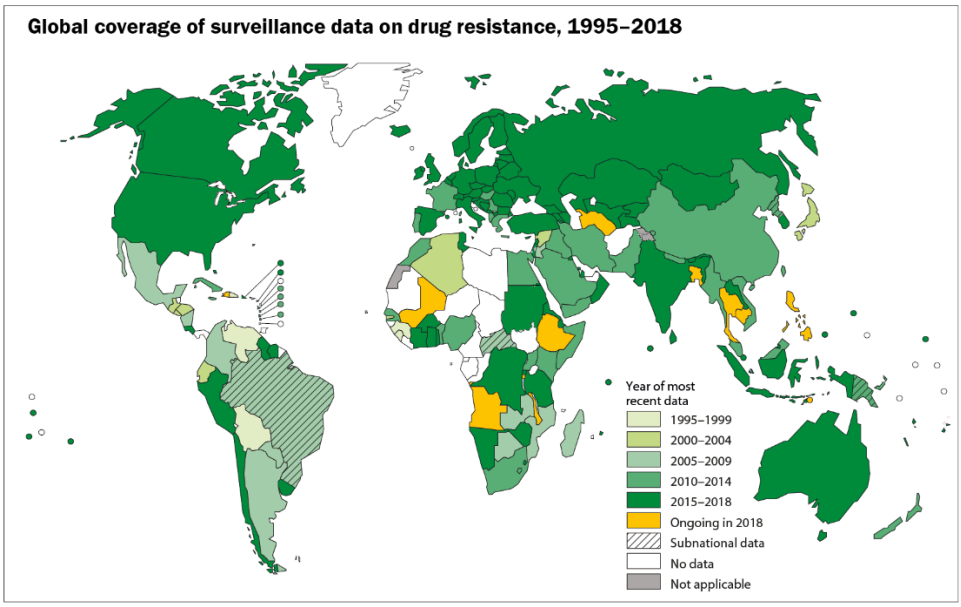

Figure 33. Global coverage of drug resistance surveillance.[4]

2.0 Literature Review - Structural Based Inhibition Studies for targeting InhA

2.1 Isoniazid-based inhibitors

As isoniazid is a highly potent and specific inhibitor of InhA in *Mycobacterium tuberculosis/bovis,* it is clear that compounds based upon or incorporating its structure may have a therapeutic effect, the subject of which has been widely reviewed.[127, 128] Rychtarčíková *et al* (2014) incorporated known antitubercular agents or structures with proposed anti-tubercular activity coupled with isoniazid by various linkers, recent work introduced a carbonyl linker to introduce various substituted phenyl rings (R = alkyl chain/halogen) as shown in **Scheme 3**, as well as further functionalisation of selected species to their corresponding oxadiazoles.[129]

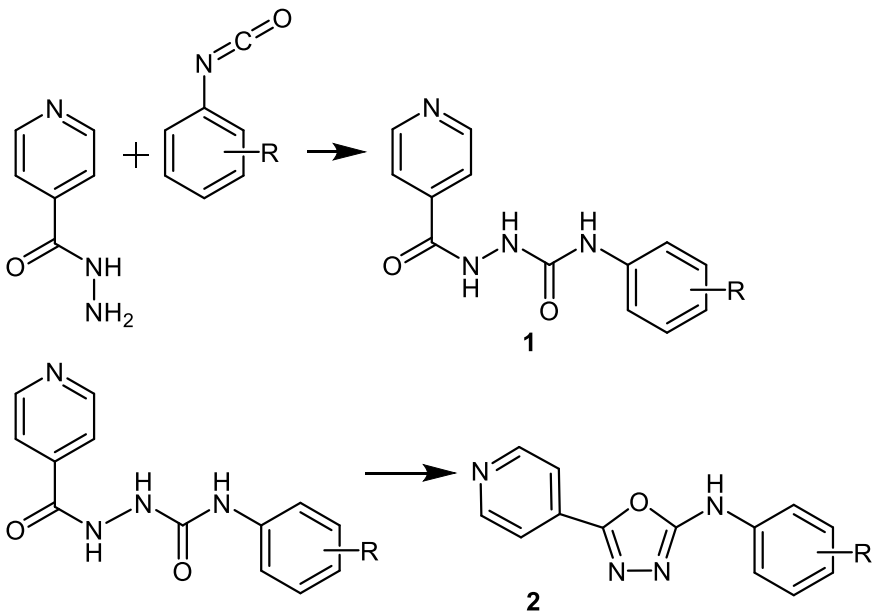

Scheme 3. General synthetic route for aryl derivatives.[98]

The compounds were evaluated for their *in vitro* antimycobacterial activity, with none exhibiting a lower minimum inhibitory concentration (MIC) than isoniazid (values between 1 and 125 μM)). Increasing the size of the alkyl chain on the substituted ring decreased the MIC and as the natural substrate of InhA is a long chain fatty acids this is logical; the best result was acquired by an *n*-octyl derivative of **1** which exhibited an almost equal MIC (1-2 μM) to isoniazid.

Docking studies confirmed the aryl group sits near a region surrounded by hydrophobic amino acid residues with the alkyl substituent directed into the hydrophobic binding pocket, supporting the theory that substrates with large hydrophobic sites will act as potent inhibitors. It also showed the pyridine group is positioned near the active site entrance, and the carboxamide is positioned directly adjacent to NADH where it might also hydrogen bond to Tyr158, these observances correlate with other reports.[84] Halogenated compounds adopted a similar conformation although the aryl group didn't occupy the space as well as the alkyl derivatives and as such resulted in weaker MIC values, although a trichloro-substituted species exhibited an MIC of 4 μM presumably due to its size. The oxadiazole compounds showed a drastic reduction in activity with MIC > 125 μM suspected to be caused by alterations in sterics or lipophilicity balance.[129]

2.2 Natural products as inhibitors

The idea of using natural products as antibiotics has been extensively investigated with a large literature precedent of potent compounds, and as such it is natural to examine naturally biosynthesised structures for their effect as potential anti-tuberculosis agents.

Thiolactomycin is a broad spectrum anti pathogenic drug as well as a potent tuberculosis inhibitor for the FASII pathway, and pyridomycin is also bactericidal against tuberculosis at concentrations ranging between 1.15 – 2.31 μM (MIC 0.72 μM), the structures of these two compounds are shown in **Figure 34**. Studies indicate pyridomycin occupies the NAD^+

binding site as well as inserting into the hydrophobic region within the active site of InhA, where hydrogen bonds are seen between active site residues and free alcohols of pyridomycin as well as several hydrophobic interactions with amino acid residues. This agrees with previously discussed binding ideas for isoniazid derivatives and shows there are a wide variety of structures that inhibit InhA reinforcing the notion that having a substituent with many hydrophobic interactions is vital for potent InhA inhibition. [130,131] The similarity in structure between thiolactomycin and L-ascorbic acid should also be noted for future reference in section **4.0** (**Figure 35**).

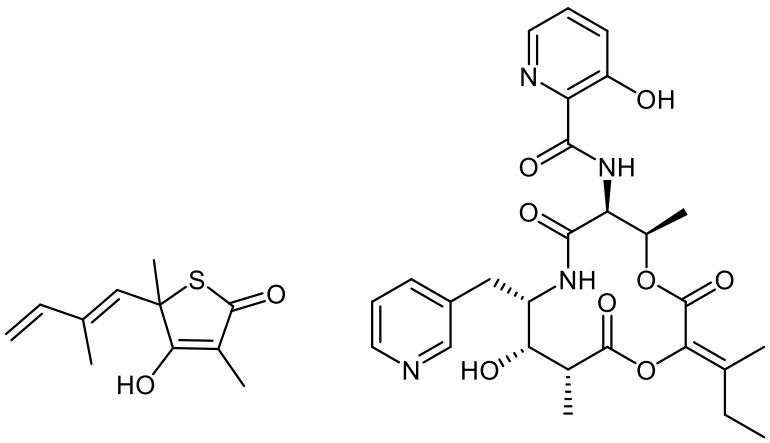

Figure 34. Structures of thiolactomycin and pyridomycin

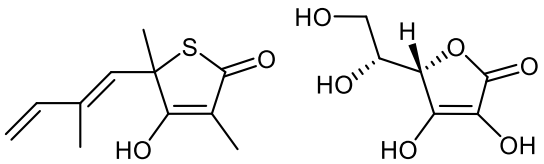

Figure 35. Structures of thiolactomycin and L-ascorbic acid

2.3 Triclosan derivatives

Triclosan (TRC), illustrated in **Figure 36**, is used in low concentrations in common household products such as toothpaste and deodorant as well as industrially in pesticides. It acts as a membrane disruptor halting bacterial growth and is bactericidal against tuberculosis even at low concentration.[132]

Triclosan has a modest MIC (12.5 μM), but as it targets InhA directly with no need for KatG activation any derivatives of triclosan or subsequent diaryl ether compounds may exhibit antitubercular activity foregoing isoniazid resistant mutations in KatG.[133] The key interactions between triclosan and InhA are hydrogen bonding between the hydroxyl group and Tyr158/NAD^+, and a π - π stacking interaction between the nicotinamide ring of NAD^+ and the hydroxylated aromatic ring.[134] It has been proposed that future compounds developed using triclosan as a lead may need to mask or remove the hydroxyl due to phase II metabolism risks.[135]

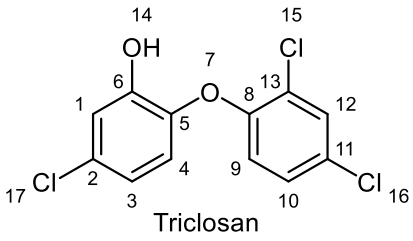

Triclosan

Figure 36. Structure of triclosan

The Stec group (2014) modified the structure by introducing various groups at positions two and eleven in order to assess the change in potency and to further develop understanding of SAR.[136] Selected compounds and their inhibition data are reported in **Table 1**. MIC in this study refers to inhibition of MTB-H37Rv, with compounds exhibiting similar or better values compared to triclosan subjected to percentage inhibition studies on the isolated InhA enzyme.[136]

Compound	Structure	MIC [μg/mL]	InhA Inhibition [%]
TRC	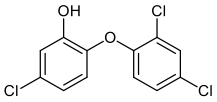	12.5	96 $\pm$ 0.65
1	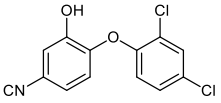	12.5	97 $\pm$ 0.06
2	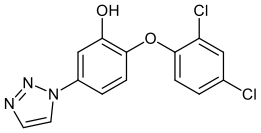	5	97 $\pm$ 0.14
3	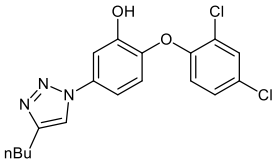	0.6	98$\pm$ 0.22
4	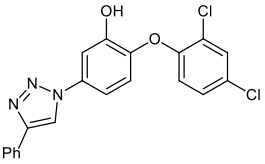	>100	nd
7	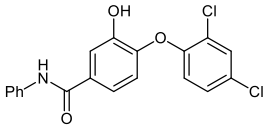	>100	nd
9	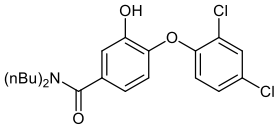	>100	nd
13	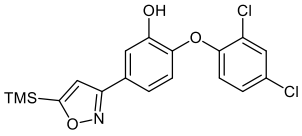	100	nd
15	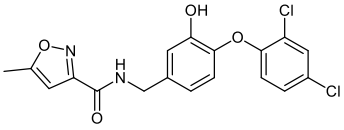	5	99 $\pm$ 0.28

18	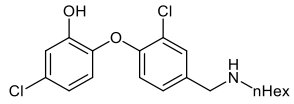	5	38 ± 0.15
20	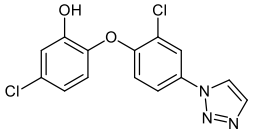	100	nd
22	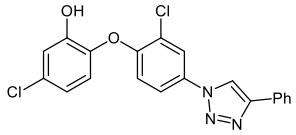	>100	nd
25	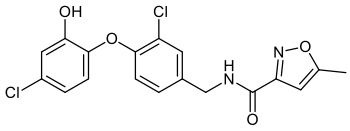	>100	nd

Table 1. Selected derivatives of triclosan with MIC of *Mtb* (H37Rv) and InhA inhibition values.[54] nd = not determined. Compounds numbers mirror those published by Stec *et al*.[136]

Compound **1** exhibited similar activity to triclosan, whereas introducing the bulkier triazole analogue **2** increased potency threefold. This demonstrates that larger groups can be tolerated and indeed the addition of an *n*-butyl substituent on triazole **3** further increased potency almost tenfold. A size limit appears to exist as **4** was completely inactive against InhA, with a phenyl substituent on triazole not tolerated. This suggests flexible substituents are preferred to rigid ones in terms of pocket binding, echoed by prior analysis of isoniazid based structures, as they would be able to conform to the shape of the binding pocket and therefore have a stronger interaction.[129]

The requirement for flexibility is further reinforced by **7** and **9** where the rigidity of the amide bond is presumed to create a non-rotational barrier with the opening of the binding pocket. This prevents the alkyl or aryl chains from pointing into the pocket resulting in no activity; this notion is further supported by **13** and **15** as the rigid oxazole group of **13** led to no activity, whereas the introduction of a methylene next to the amide in **15** gives

the molecule an increased point of rotation. This small change resulted in an increased potency by nearly threefold as compared to triclosan.

Modifications at position eleven replicated the trend as an *n*-hexyl substituent **18** was threefold more potent than triclosan, this concept was repeated by **20** and **22** having no activity due to no flexibility on the substituent but curiously the benzylamide **25** exhibited no activity in contrast to **15** suggesting the compound is unable to orientate itself for inhibitory purposes.

InhA inhibition data was obtained for compounds with an MIC value equal to or better than triclosan, tested at their respective MIC values. Results are also displayed in **Table 1**. The substituents at position two all had >97% enzyme inhibition although substitution at position eleven gave lower than 75% inhibition suggesting other targets are affected to provide whole cell activity.

These derivatives were also tested against resistant strains (INH-resistant (mc24977) and MDR strains (mc25855, CI12081)), all showing increased potency as compared to triclosan. The best analogue, **3**, was tested *in vivo* but was only weakly active at 100 and 300 mg/kg doses suggesting a low bioavailability due to solubility issues and rapid phase II metabolism.[135, 136]

2.4 Diphenyl compounds

The Kanetaka group (2015) generated a series of compounds by operating a matched molecular pair (MMP) approach and *in silico* screening. Starting from a lead (KES4) (**Figure 37**) they used MMP to narrow down > 460,000 compounds to 32, followed by docking analysis and filtering based on H-bond interactions to give 10 compounds to be taken forward for *in vitro* assays.[137, 138]

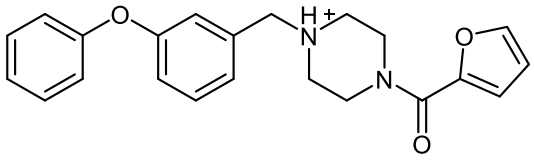

Figure 37. Structure of lead compound discovered by *in silico* docking "KES4" [55]

Modifications of KES4 replaced the furan with aryl derivatives except in one compound where a carbonyl was introduced on the methylene adjacent to the right-hand phenyl ring and piperazine. Binding modes of the ten derivatives were investigated by protein-ligand interaction fingerprint (PLIF) and ligand interaction (LI) analysis which supports prior work showing the diphenyl ether rings are located near NAD^+, interactions with known binding residues such as: Tyr158, Phe149, Met199 and Leu218 were also observed. The compounds were assessed for InhA inhibition at 50 μM, all were able to suppress InhA with two resulting in < 22% InhA activity (substituents of phenyl and 2-fluorobenzyl, **KEM4** and **KEM7** respectively, **Figure 38**).[137] The addition of a flexible alkyl chain was proposed but not attempted.

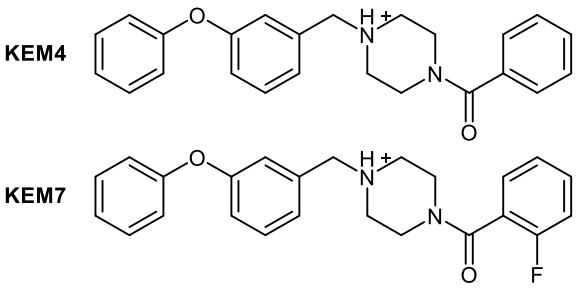

Figure 38. KEM4 and **KEM7** structures.[137]

A bacterial growth assay was performed on the non-pathogenic bacterium *M. smegmatis* which shares over 2000 genes with *M. tuberculosis* and has a broadly similar InhA

sequence: after 24 hours five compounds strongly inhibited growth whereas the others weakly inhibited growth. IC_{50} values were obtained for the strong inhibitors with phenyl and fluorophenyl having similar activity (12.0 μM and 17.3 μM respectively) to isoniazid (9.8 μM), and toxicity data showed no inhibition of growing mammalian cells or *E. coli.*

The Kamsri group (2014) used molecular dynamics simulations and a 3D-QSAR study to elucidate the activity of various ring substitutions based on the triclosan derivative shown in **Figure 39**.[139]

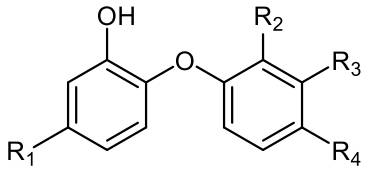

Figure 39. General structure of Kamsri group compounds.[57]

Their results agreed with the Stec group (2014) as longer alkyl chains at R_1 exhibited stronger binding affinities with *n*-octyl able to form more hydrophobic interactions with side chains in the pocket.[136] It is interesting to note that large substituents at the $R_{2/3/4}$ positions showed poor InhA inhibitory activity also agreeing with Stec group findings. Molecular dynamics simulations showed that $R_{2/3/4}$ groups sit near the pyrophosphate of NAD^+ and so small hydrophilic groups should be used for optimal binding affinity.

2.5 Pyrazole linked pyrimidine hybrids

Bhatt and co-workers (2015) designed compounds without the ether linkage (as described above for diphenyl compounds) and assessed pyrazole linked pyrimidine hybrids.[140] Triazolopyrimidines resemble purine, and have been incorporated in various treatments for cardiovascular diseases whereas pyrazole derivatives have been used as potent

antitubercular inhibitors.[140, 141] Modifications of pyrimidine structures by incorporating a carboxamide side-chain increased their pharmacological activity as reported before in the literature, as has the incorporation of pyrazole units.[142] As a result of this, hybrid structures were created to theoretically combine antitubercular activity with the core structure shown in **Figure 40**.

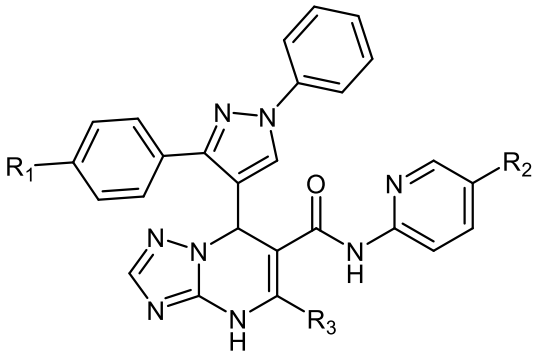

R_1 = H, CH_3, NO_2, Cl, F; R_2 = H, CH_3, Br; R_3 = CH_3, $CH(CH_3)_2$

Figure 40. Core structure of hybrid species developed by Bhatt *et al*. [58]

Thirty compounds were designed and synthesised before activity was evaluated against the harmless *MTB* strain H37Rv at 6.25 μg/mL concentration and those with ≥90% inhibition were further examined at increased dilutions to determine MIC with the results shown in **Table 2**.[143]

Compound	**R_1**	**R_2**	**R_3**	**% Inhibition at (6.25 μg/mL)**	**MIC μg/mL**
J3	H	Br	Me	95	3.13 ± 0.313
J15	NO_2	Br	Me	96	1.56 ± 0.083
J21	Cl	Br	Me	98	0.78 ± 0.039
J25	F	H	Me	99	0.78 ± 0.039
J27	F	Br	Me	99	0.39 ± 0.019

INH	-	-	-	99	0.3
Rifampicin	-	-	-	99	0.5
Ethambutol	-	-	-	99	3.125

Table 2. Inhibition data taken from Bhatt *et al*.[58] Compound number mirror those published by Bhatt *et al*.[140]

Substitution at R_1 by electron withdrawing groups exhibited the strongest effect on inhibition whereas methyl groups resulted in <90% inhibition, and fluorine resulted in the largest potency due to its hydrophobicity. Substitution of R_2 with bromine vastly increased potency as did retaining a methyl at R_3, also showing that longer alkyl chains are not tolerated here. It is important to note **J27** has very similar activity to isoniazid and as such could be used for future development.

Docking studies showed that the NH of the pyrimidine ring hydrogen bonds with the carboxyl group of Gly14, and the two phenyl rings π - π stack with the phenyl ring of Phe97 and amine of Arg43: a significant van der Waals interaction was also observed for all structures. Pharmacokinetics and ADME were considered and predictions fall within acceptable parameters although aqueous solubility is an issue, so solubility enhancers were recommended should the compounds be taken forward for development.[140]

2.6 Benzo[d]oxazol-2(3H)-ones

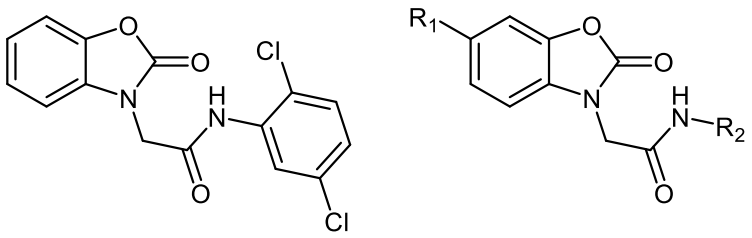

Figure 41. UPS14 and lead structure.[62]

Pedgaonkar and co-workers (2014) identified **UPS14** as a lead with an MTB IC_{50} of 22.12 ± 0.8 μM and developed a range of inhibitors based on the structure in **Figure 41** with selected promising results shown in **Table 3**.[144]

Compound	R_1	R_2	MTB MIC μM
19	NO_2	2-Pyridylmethyl	76.15
29	Cl	5-Nitrothiazol-2-yl	17.61
30	NO_2	5-Nitrothiazol-2-yl	17.11
32	Cl	2-Benzothiazolyl	17.37
33	NO_2	2-Benzothiazolyl	33.75

Table 3. Selected data from Pedgaonkar *et al*.[62] Compound numbers mirror those published by Pedgaonkar *et al*.[144]

Docking results for **UPS14** correlated well with prior work and showed the carboxyl of benzo[d]oxazol-2(3H)-one hydrogen bonds with Tyr158 as well as NAD^+ and the carboxamide ring system is able to project into the binding pocket and interact with the hydrophobic residues.[144] This correlates with docking and inhibition studies of the synthesised compounds as hydrophobic substitutes at R_2 exhibited greater potency and had extensive hydrophobic interactions in the pocket, the hydrophobic trend replicated at R_1 as hydrophobic substitutes were also found to be more potent. This further supports work indicating hydrophobic structures with hydrogen bonding regions should be incorporated into InhA inhibitors.

2.7 2-(4-Oxoquinazolin-3(4H)-yl)acetamide derivatives

Pedgaonkar *et al* (2014) continued their work on InhA inhibitors by working on 2-(4-oxoquinazolin-3(4H)-yl)acetamide derivatives based on **UPS17** with the core structure shown in **Figure 42**, selected derivatives are shown in **Table 4**.[145]

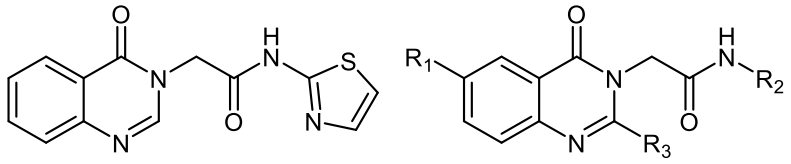

Figure 42. UPS17 and core structure.[63]

Compound	R_1	R_2	R_3	MTB MIC μM
12	Cl	2-furylmethyl	H	4.91
21	Cl	Phenyl	CH_3	4.76
25	Cl	2-furylmethyl	CH_3	4.70
37	H	6-nitro-2-benzothiazoyl	H	4.09

Table 4. Selected data from Pedgaonkar *et al*.[63] Compound numbers mirror those published by Pedgaonkar *et al*.[145]

This data correlates well with work on benzo[d]oxazol-2(3H)-ones (section **3.6**), with aryl groups at R_2 exhibiting the strongest effect upon InhA, crystal structures echo the hydrogen bonding network and hydrophobic interactions seen before.[144, 145]

2.8 4-Hydroxy-2-pyridones

Manjunatha *et al* (2015) screened a series of compounds from Novartis for antitubercular activity, resulting in > 20,000 hits with > 50% inhibition at 12.5 μM which were narrowed down by assessing: cytotoxicity; undesirable functional groups; scaffolds of known anti-TB compounds; Lipinski's rules and promiscuous pan-active compounds (non-selective).[84, 146]

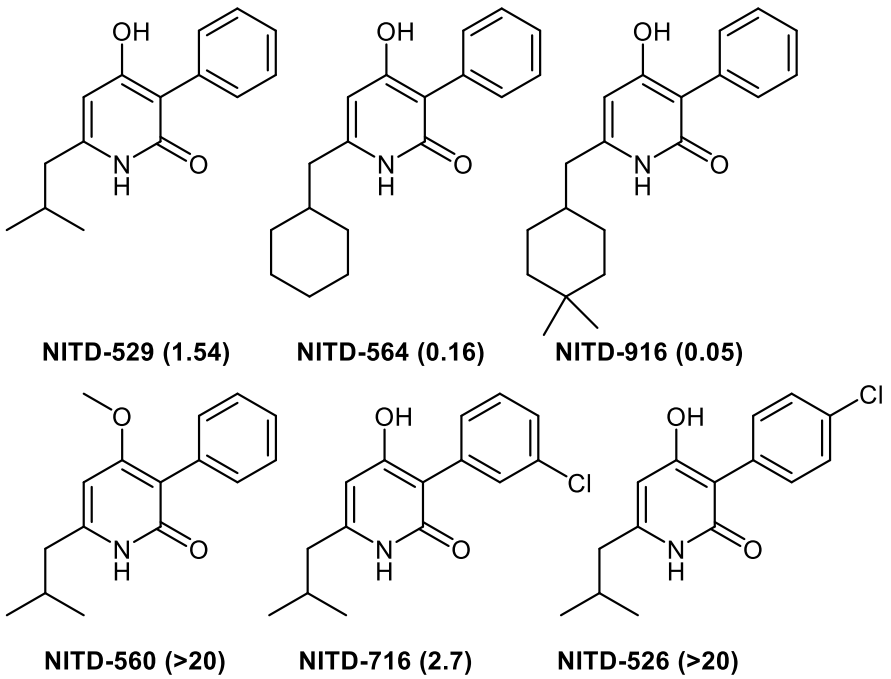

Figure 43. Novartis compounds with MIC values in μM.[31]

The six structures in **Figure 43** further reinforce structure activity relationships previously detailed in this chapter, as increasing the lipophilicity of the substituent from **NITD-529** to **NITD-564** and **NITD-916** increased potency as expected, a fact confirmed by docking data which puts the cyclohexyl/dimethylcyclohexyl group in the hydrophobic region of the binding pocket.[147]

Increased substituent size heightened potency due to a greater number of interactions with hydrophobic residues in the binding pocket. The importance of a hydrogen bonding system is reinforced as methylating the alcohol in **NITD-560** removes activity presumably resulting in a reduced hydrogen bonding capacity with Tyr158; moreover the addition of a chlorine atom onto the right hand phenyl ring hinders efficacy if placed in the *meta* position and removes it completely if placed in the *para* position as seen in **NITD-716** and **NITD-526**.

NITD-916 was identified as a promising lead, as it is more potent than isoniazid, with optimal toxicity results but relatively poor aqueous solubility and low lung–to-plasma ratio.[148]

2.9 3-(9H-Fluroren-9-yl)pyrrolidine-2,5-dione derivatives

Matviuuk *et al.* (2013) assessed 3-(9H-fluroren-9-yl)pyrrolidine-2,5-dione derivatives which have a similar structure to a known InhA inhibitor GEQ; selected compounds are shown in **Figure 44** that exhibited high levels of InhA inhibition (>79%).[149, 150]

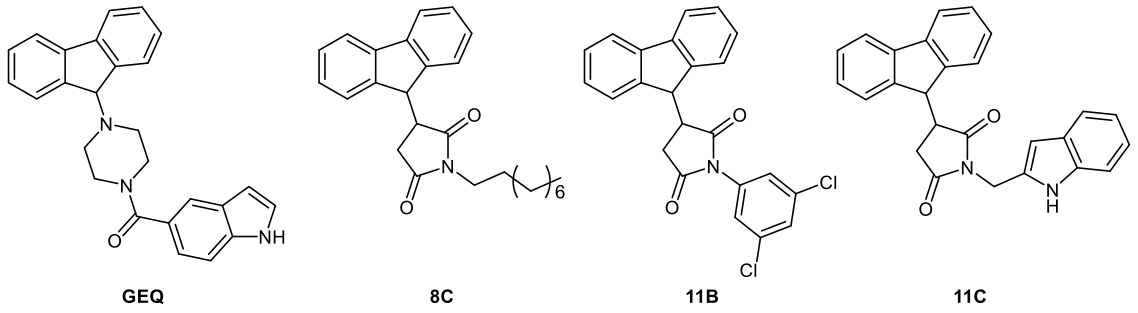

Figure 44. Selected 3-(9H-fluroren-9-yl)pyrrolidine-2,5-dione derivatives.[67]

The results correlated with data from other InhA inhibitors as inclusion of a flexible long chain or hydrophobic aryl structure increased efficacy, and rigid structures incorporating a carboxyl linker between the nitrogen and substituent gave poorer enzyme inhibition at 50 μM.

It is interesting to note that although these three structures inhibit InhA, only **11B** had good activity against whole cell growth. Using a carboxyl linker appeared to increase potency against whole cell growth, but these compounds are proposed to act at a different site as the inhibition of InhA is reduced in these structures, and docking reaffirmed that

hydrogen bonding and hydrophobicity (for region of inhibitor located inside the binding pocket) are vital components for potent inhibitors.[149]

2.10 Pyrroyl-1,3,4-thiadiazole inhibitors

Joshi *et al.* (2015) developed a series of compounds, the lead and two highest activity compounds shown in **Figure 45**. These are based on 1,3,4-thiadiazoles, which are well known to have a broad biological activity, as well as their prior work on pyrroyls.[151-154] Such a hybrid pharmacophore approach is not uncommon and yielded good data, with **9N** and **9Q** showing significant activity against *M. tuberculosis* with MIC's of 6.25 and 3.125 μg/mL respectively.

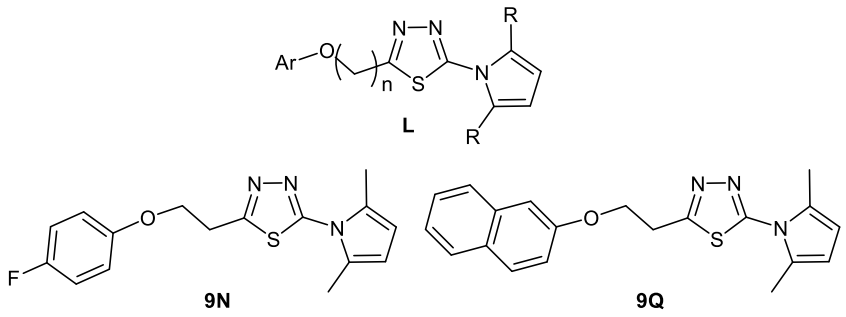

Figure 45. Lead structure and selected high activity inhibitors.[73]

Docking studies revealed compounds based on these structures with longer chains (n=2) were able to protrude more into the active site and the hydrophobicity of Ar groups allowed van der Waals interactions in the pocket whereas the thiadiazole ring coordinated with NAD^+ and Tyr158. A similar series of compounds was developed by More *et al* (2014) on a pyrroyl-phenyl derivative with a hydrazide linker on which aromatic groups were attached to assess the subsequent impact on InhA inhibition.[155] Results concurred and

indicated larger or hydrophobic aryl groups make good inhibitors with MIC values 0.2 - 0.8 μg/mL.

2.11 1,3,4-Oxadiazole derivatives

Desai and co-workers focused their efforts on compounds containing three key structural motifs – indole, pyridine, and oxadiazole.[156] Each were considered due to individual factors with the aim of combining those in aid of creating a potent and non-toxic inhibitor of InhA. Indoles are found in many naturally occurring and manmade compounds used for anticancer, antimicrobial, and antimalarial activity respectively and as such have become renowned constituents of many a researchers drug designs.[157-160] Pyridines and oxadiazoles share these features and in particular 1,3,4-oxadiazoles can be used as a bioisostere for both amide or ester functional groups, exhibiting hydrogen bonding with various receptors.[156, 161]

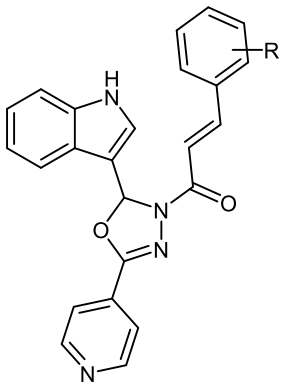

Figure 46. Desai and co-workers general structure, R group consists of various alkyl/halogen/alkoxy/nitrogen containing substituents[156]

Figure 46 shows the general structure of compounds tested with variety in the R group of the phenyl ring. Initial tests were undertaken to assess activity against dormant and active strains of *M.tb* and *M. bovis,* the newly synthesised compounds showed little to no

activity towards *M. tuberculosis* $H_{37}Ra$ with selectivity towards *M. bovis* BCG observed. R groups containing alcohols, halogens, and nitro groups performed best with regards to MIC and IC_{50}. The SAR basis for this with respect to docking was explored later.

Further studies were undertaken to ascertain toxicity against three human cancer cell lines with promising results showing little to no cytotoxicity as compared to Paclitaxel. This test also returned GI_{50} values allowing selectivity to be calculated, with results showing great specificity for *M. bovis* over human cell lines. Docking studies to elucidate binding modes of the most active compounds to InhA were performed using Glide and showed results comparative to other groups data, with non-polar interactions in the binding pocket along with hydrogen bonding interactions on the outside of the pocket helping direct the ligand and bind it into the site.[162]

2.12 *N*-Benzyl-4-((heteroaryl)methyl)benzamides

In 2016 Guardia and co-workers presented studies on *N*-benzyl-4-((heteroaryl)methyl)benzamides based off an initial hit as shown in **Figure 47**. SAR optimization was based around modifying four areas of the molecule: the pyrazole, the length of the amide linker, central phenyl unit, and the right hand phenyl unit.[163]

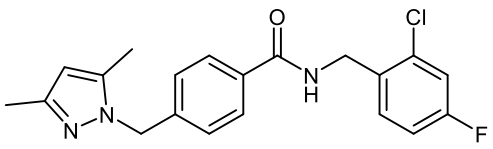

Figure 47. Initial hit in study performed by Guardia and co-workers.[163]

The biological aspects of the initial hit were promising, with an InhA IC_{50} of 0.05 μM accompanied with the somewhat more moderate antitubercular MIC_{90} of 10 μM. These

results, in addition to little to no cytotoxicity, suggest this hit was a reasonable starting point for SAR study.

The first set of compounds involved alterations to the RHS of the molecule to assess tolerance of *meta/ortho/para* substitution as well as differing substituents (halogen/nitro/sulfone). Results indicated *ortho/para* substitution was essential for InhA activity, albeit compounds with an aromatic *meta* carbamide proved the most successful with respect to whole cell studies. These came with suboptimal logP values and as such were not developed further.

2.13 Thiourea containing compounds with benzenesulfonamide moiety

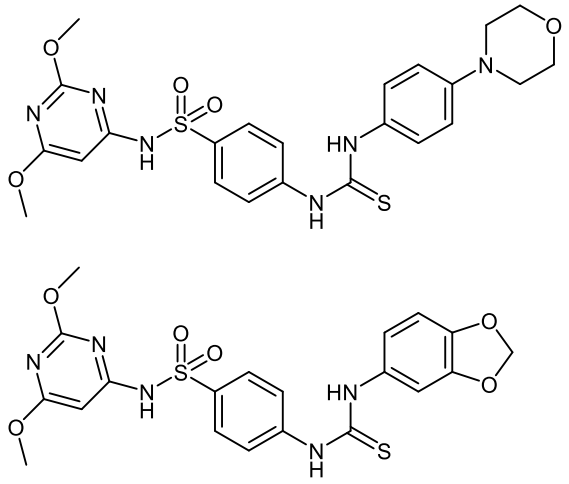

Figure 48. Derivatives with optimal results.[164]

Ghorab *et al.* designed, docked, and ran biological studies on a series of compounds connecting a benzenesulfonamide moiety via a thiourea linking group to various aryl species.[164] These style of compounds were chosen due to the use of thiourea containing species already in clinical use, such as thioacetamide and prothionamide.[164]

The most promising compounds are shown above in **Figure 48**. The MIC values were 3.13 μg/mL for the morpholine containing compound, and 6.25 μg/mL for the benzodioxole containing compound. Respective growth inhibition results were 74.9% and 59.2% respectively.

2.14 Summary of Literature

To summarise, a variety of structures have been synthesised and tested in an effort to attain a highly potent InhA inhibitor with varying success. Structure-activity-relationships have been reaffirmed with docking studies agreeing that hydrophobic interactions in the binding pocket, as well as co-ordination to NAD^+ and Tyr158 outside of the binding pocket, are vital for efficacy of a proposed InhA inhibitor.

A general pharmacophore can be deduced that a core containing a hydrogen bond donor and aromatic moiety coupled to a flexible hydrophobic species may act as a potent InhA inhibitor. It is promising that a large variance in structure can be tolerated, and some structures which do not inhibit InhA may affect whole cell growth and as such could be developed as general antibiotics for tuberculosis.

Several structures have excellent InhA activity and attention is now focused on improving *in vivo* activity with focus on pharmacokinetics and pharmacodynamics, as well as lowering toxicity.

3.0 Project Aims

The aim of my project is to synthesize compounds based on L-ascorbic acid which share the same hydrogen bonding system as the compounds developed by Manjunatha *et al.* (2015) (section **3.8**), the pharmacophore and general structure are shown in **Figure 49** alongside **NITD-529**, with the initial targets illustrated in **Figure 50**.[84]

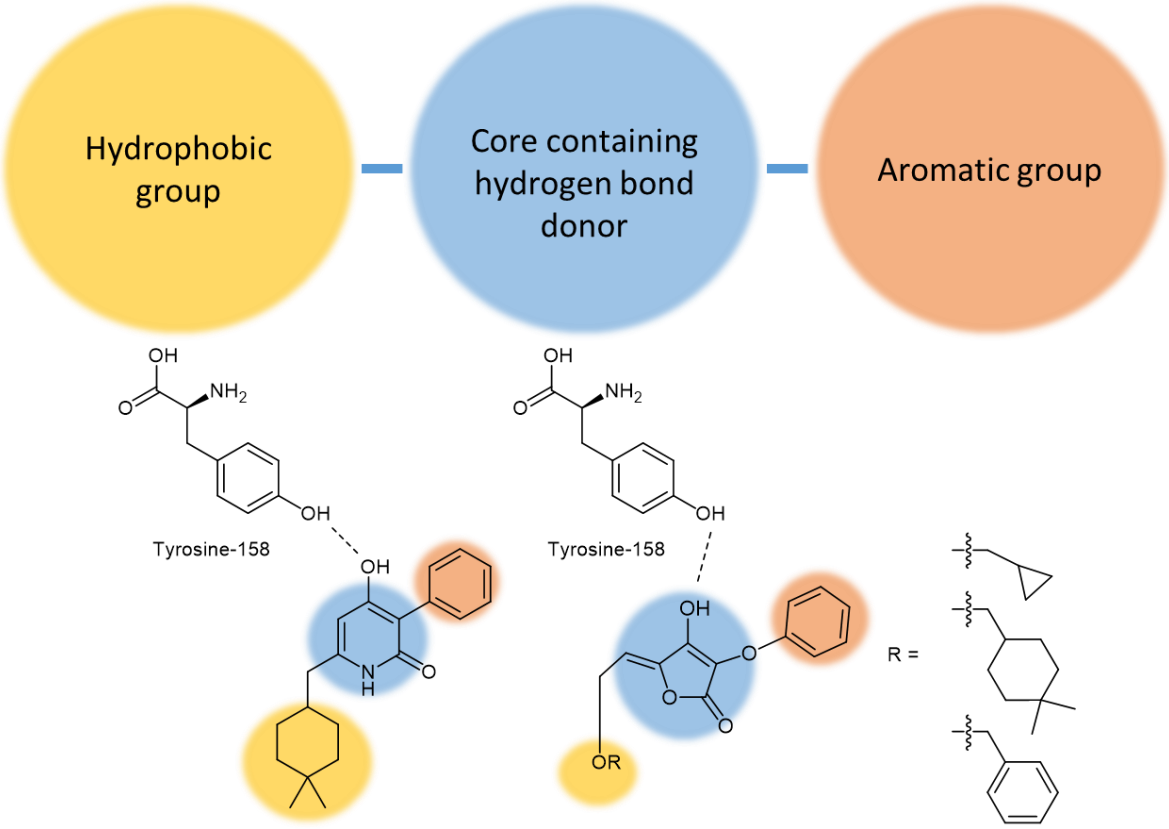

Figure 49. NITD-529 and target compound showing structure comparison as well as hydrogen bonding with tyrosine-158 therefore potential for similar reactivity.

They will be tested for their activity against InhA, initially in an isolated enzyme assay, to determine percentage inhibition followed by calculation of IC_{50} values. Compounds exhibiting strong inhibition will be subjected to whole cell work. If results are promising then a series of compounds will be designed to improve upon their potency by varying substituents on the left and right side of the molecule, using molecular modelling to aid selection.

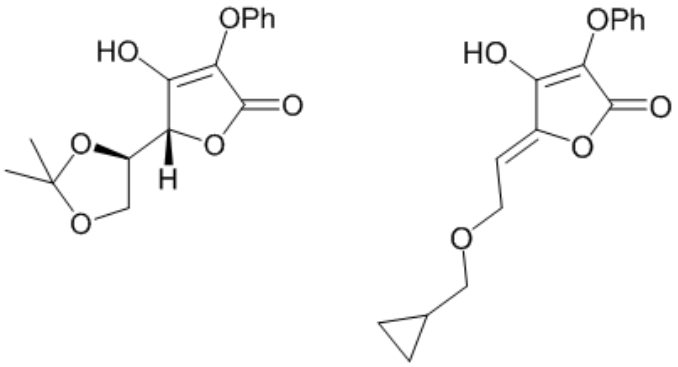

Figure 50. Initial target compounds

As previously discussed, docking data shows the 4-hydroxy-2-pyridones coordinate in the expected way as is illustrated in **Figure 51** and as such it is expected that L-ascorbic acid derivatives (who share a similar proposed pharmacophore) may co-ordinate in a similar way and as such inhibit InhA. It is also important to note that L-ascorbic acid exhibits little to no toxicity in the body and as such provides an exciting, sustainable, and novel starting material for inhibitors. As discussed in section **3.2**, thiolactomycin shares a similar conformation to L-ascorbic acid and as such any derivatives of L-ascorbic acid are predicted to orientate in a similar fashion to thiolactomycin therefore inhibit InhA.

An important aim for the WHO is that "no TB-affected household" should face extortionate costs to treat the disease and as such the relatively low cost of L-ascorbic acid may appeal more to companies developing antitubercular medication. Ultimately this cost effectiveness should be passed on to the patient/organisation funding the healthcare which would be particularly important to those in regions such as Africa who may be unable to afford expensive treatment regimens.[3]

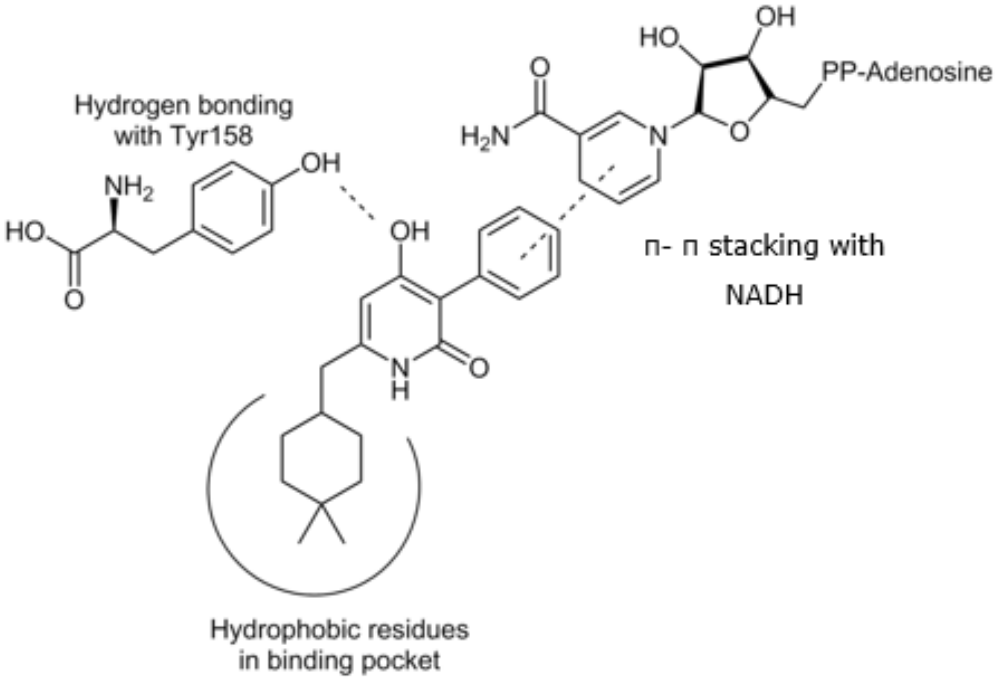

Figure 51. Illustration showing position of 4-hydroxy-2-pyridone NITD-916 in active site of InhA coordinating with InhA-NADH complex via π stacking with NADH, hydrogen bonding with Tyr158 and the alkyl group pointing into the binding pocket.[84]

4.0 Results and Discussion

4.1 Synthesis of target A

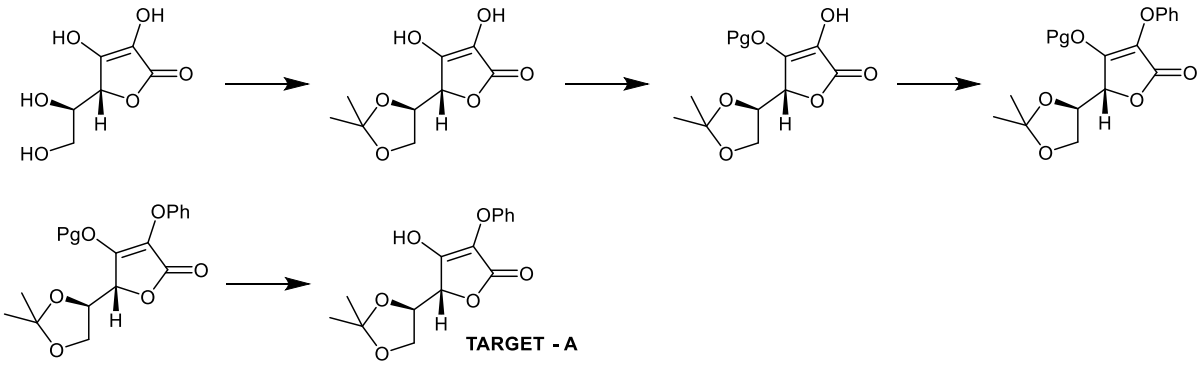

Scheme 4. Proposed general reaction scheme for synthesis of target **A.**

Detailed above in **Scheme 4** is the proposed reaction pathway for synthesis of target molecule **A**, the foreseen difficulties in the synthesis were accurate and efficient protection of the acrylic alcohol. The differences in the respective pKa values between it and the alcohol on the adjacent carbon are fairly large (pKa of 4.1 and 11.8 respectively) but as the adjacent alcohol is fairly unhindered it can also react giving undesirable by-products.[165] The difference in pKa values is due to the resonance of the acrylic alcohol with the carbonyl, resonance structures are shown in **Scheme 5**.

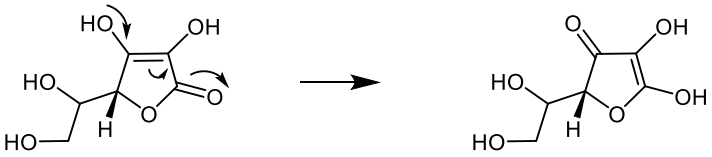

Scheme 5. Resonance of L-ascorbic acid

The first step in the synthesis was protection of the diol using acetyl chloride in acetone to form an acetal, which on first attempt was achieved in reasonable yield (68%) as shown in **Scheme 6** and after modification of the procedure to reduce reaction time and increase dilution the yield improved to > 90%.[166]

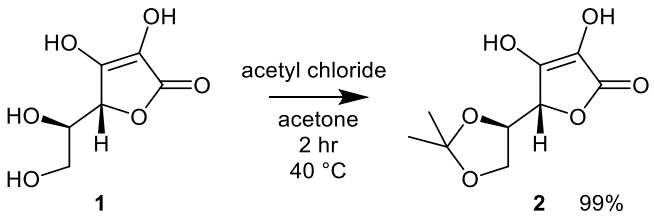

Scheme 6. Acetal formation conditions.[167]

4.1.1 Protection by methyl ether

The next step was the selection of a protecting group which would be stable to both acidic and basic conditions due to uncertainty over conditions which may be needed for future steps in the synthesis and so formation of a methyl ether was chosen for study.

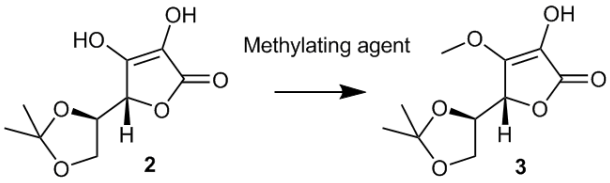

Scheme 7. Protection of 3-*O* on **2** with methylating agent before arylation of 2-*O*.

Conditions	Yield
MeI, K_2CO_3, DMSO:THF (9:8) (r.t) [162]	N/A
MeI, $NaHCO_3$, DMSO:THF (9:8) (r.t) [162]	N/A
MeI, NEt_3, MeOH (r.t) [161]	10 - 26%
DMS, NEt_3, MeOH (r.t) [161]	15 - 19%
MeI, NEt_3, DMSO (r.t)	N/A
MeI, NEt_3 (trace MeOH) (r.t)	N/A

Table 5. Methylation conditions investigated for formation of **3**.

Selective methylation of **2** (**Scheme 7**) was attempted using a range of conditions which are detailed in **Table 5**, the determination of which alcohol is alkylated can be performed by ^{13}C analysis of changes in ppm of the peaks corresponding to the alkene. Initial attempts using K_2CO_3 and methyl iodide in DMSO:THF (9:8) appeared to give pure product and so this product was taken forward for arylation of the adjacent alcohol albeit these

reactions failed.[168] After repeated attempts with stronger bases and different conditions (detailed in **Table 7** later in text) closer analysis was made of the "methylated" species, which showed that dimethylation had occurred and as such any desired alkylation would fail.

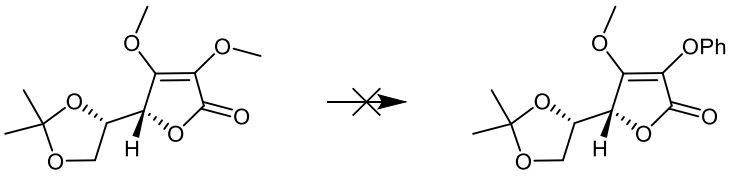

Figure 52. Illustration of blocked reaction due to overmethylation

Separation of the mono and di protected products by column chromatography failed as no column conditions gave adequate separation for the two products to be isolated on gradients of 100% hexane to 100% ethyl acetate, or DCM with varying percentages of methanol. Different reaction conditions were utilised to provide only mono protection by changing the base to the weaker sodium hydrogen carbonate but this did not aid selectivity, neither did shortening the reaction time from 16 hours (2,4,6,8 hours respectively).

Changing the base to triethylamine solved the selectivity problem but low yields were observed, this was only marginally improved by using fresh methylating agent and any future work using triethylamine for methylation ought to use non-nucleophilic solvents to minimise quenching of alkylating reagent.[167] Small scale reactions with new conditions were attempted to improve upon the poor yields observed, with DMSO as a solvent and also trying the reaction neat (with a trace of methanol to aid solubility) but these reactions failed.

4.1.2 Protection by ethyl ether

Due to the low yields observed with methylating agents, the decision was made to alter the protecting group to an ethyl ether instead as the additional size (however small) should give adequate separation via column chromatography. The range of conditions used are shown later in **Table 6**.

The switch to ethylation proved successful as the conditions first attempted for methylation worked although in poor yield due to diprotection, but unlike methylation both mono and di protected species were able to be isolated via column chromatography.

The low yields were improved upon by changing the reaction conditions, changing reagents as well as reaction times and temperatures. Using triethylamine, as expected, improved the yield two-fold due to improved selectivity over the adjacent alcohol. It is important to note that while increasing the temperature increased reaction yield this was offset somewhat by an increased amount of diprotected product and so yields never reached a range which could be considered "good". As expected, increasing the equivalents of base and alkylating reagent did not increase the desired yield, only the yield of diprotected product.

A procedure using TBAB increased the yield somewhat, but the best conditions comprised sodium hydrogen carbonate in DMSO at 50 °C which gave the reasonable yield of 55 – 62%.[169, 170] This step does not give the same yields when performed at larger scale, due to a large portion of the base used collecting on the bottom of the flask and hardening into a gum-like layer thus being unable to affect the reaction.

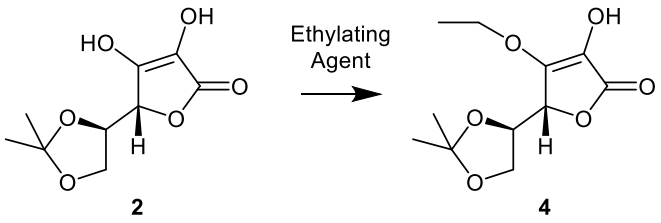

Scheme 8. Ethyl protection with conditions shown in **Table 6**.

Conditions	Yield
EtI, K_2CO_3, DMSO:THF (9:8) (r.t) [162]	17 - 20%
EtI, NEt_3, MeOH (r.t) [161]	31 - 44%
EtI, K_2CO_3, Ac (reflux) [162]	34%
EtI (1.5 eq), K_2CO_3 (1.5 eq), Ac (reflux) [162]	10% (Majority diprotected)
EtI, K_2CO_3, TBAB (cat), Ac:DMSO (4:1) (30°C) [163]	44 - 50%
EtI, $NaHCO_3$, DMSO (50°C) [164]	55 - 62%

Table 6. Ethylation conditions investigated for formation of **4**.

4.1.3 Arylation

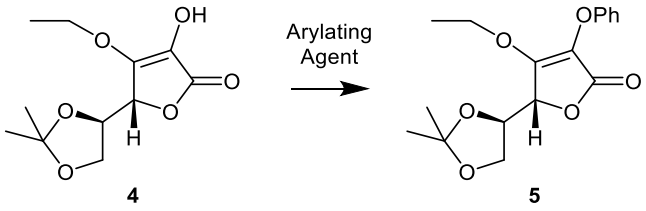

Scheme 9. Arylation step with conditions investigated listed below in **Table 7**.

Conditions	Yield
CuI, PhI, K_2CO_3, Tol (reflux) [166]	N/A
CuI, 1,10 – Phenanthroline, PhI, K_2CO_3, Tol (reflux) [166]	N/A
Ph_2IOTf, K_2CO_3, Ac (reflux) [162]	20 – 30%
Ph_2IOTf, NaOH (60 °C) [168]	N/A

Table 7. Arylation conditions investigated to form compound 5. Yields termed "N/A" afforded no reaction.

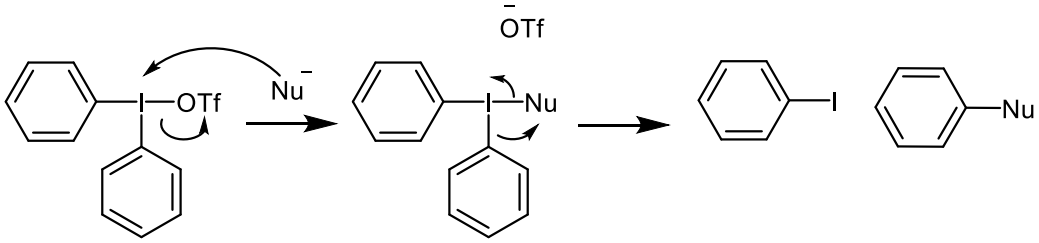

Scheme 10. Mechanism for arylation using diphenyliodonium triflate.[171]

Arylation was first attempted using copper catalysed chemistry (CuI, 1,10-phenanthroline, PhI, K_2CO_3, Tol) with and without 1,10-phenanthroline at reflux but this reaction failed, possibly due to weak base and bulky ligands as the literature procedure referenced unhindered alcohols.[172] Success came when using diphenyliodonium triflate as an arylating reagent which was initially purchased but due to the cost (approximately a hundred pounds per gram) a route was found for in house synthesis which can be completed in two hours in high yield (>90%).[173] Using this route arylation was completed in relatively low yield which may be improved upon in future by altering the base used and potentially solvent to increase the maximum reflux temperature. A further attempt was made using aqueous sodium hydroxide but this also failed.[174] **Table 7** is a summary of the reaction conditions investigated.

4.1.4 Deprotection of ethyl ether

The conditions used for removing the ethyl group are shown in **Table 8**. TMSI was investigated for removal of the ethyl group but failed, both old and new reagents. Producing TMSI *in situ* also proved ineffective as did altering equivalents of the reagent and reaction time/temperature. HCl (1M) with trace THF to aid solubility generated product visible in the mass spectrometry data, but this could not be isolated, the product obtained appeared to consist of the compound without the ethyl ether and diol deprotection as shown in **Scheme 11**.

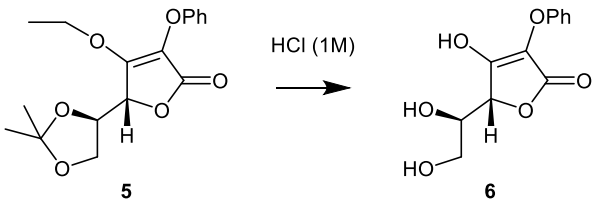

Scheme 11. Product obtained from HCl mediated deprotection.

Conditions	Yield
TMSI (fresh), (r.t/reflux)	0
NaI, TMSCl, H_2O, AcN (40 °C)	0
HCl (1M), THF (trace), (40 °C)	Analysis indicates product but majority double deprotection

Table 8. Conditions investigated for removal of ethyl ether

Due to the difficulty in removing the ethyl group, the decision was made to trial alternate protecting groups which should be more labile for later points in the synthesis so as to avoid the unnecessary reprotection of the diol.

4.1.5 Evaluating alternate protecting groups

4.1.5.1 Allyl

Protecting groups previously discounted were now investigated for their efficacy in shortening the reaction pathway by one step – foregoing the need for diol re-masking after the acidic conditions necessary to remove the ethyl group. Allyl groups are generally removed by palladium catalysis and this should not affect other functional groups in the molecule. The product from this reaction could not be completely purified, instead giving a mixture of products as shown below in **Figure 53**. These products have been seen in the literature previously, with the rearrangement shown in **Figure 54**.[175]

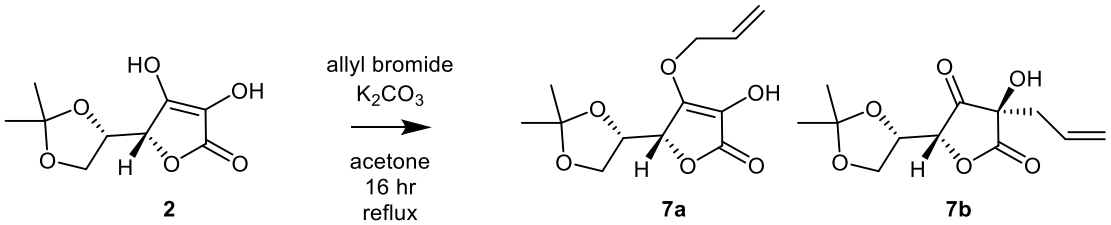

Figure 53. Mixture of products obtained after allyl use.

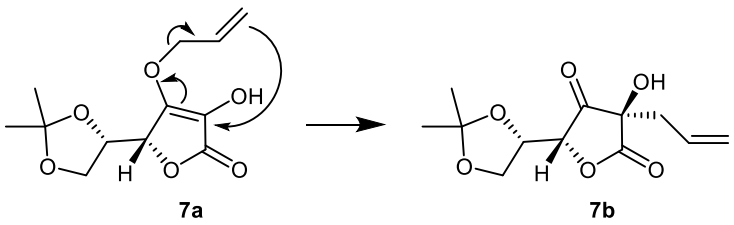

Figure 54. Claisen rearrangement.[175]

These products appeared as one spot on TLC in a number of eluent mixtures, in a ratio of 42:58 as calculated in the NMR. Proton and carbon NMR are shown below for reference in **Figure 55** and **Figure 56**.

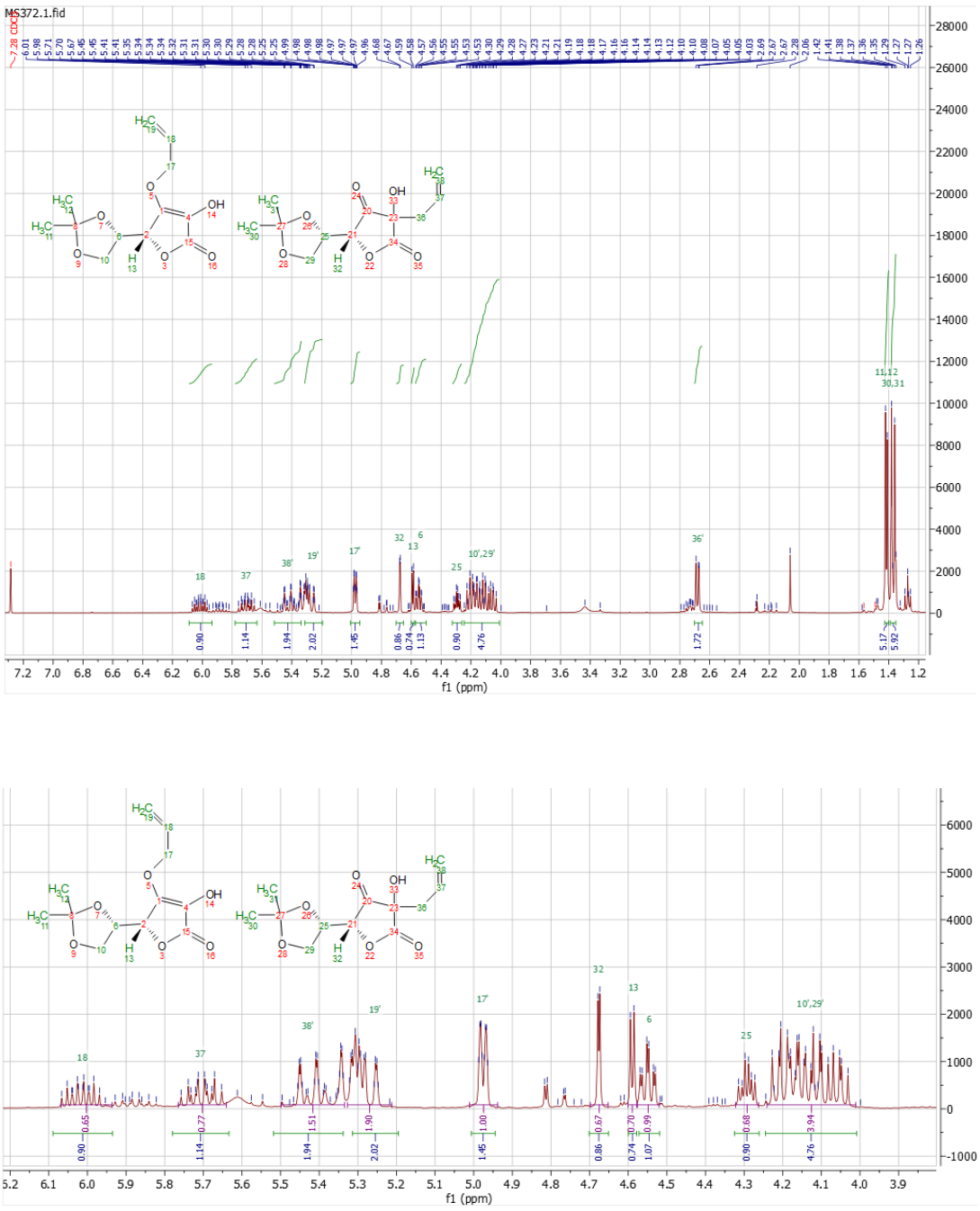

Figure 55. Proton NMR of allyl ether formation showing mixture of products, region of 3.9 – 6.1 ppm enlarged for clarity.

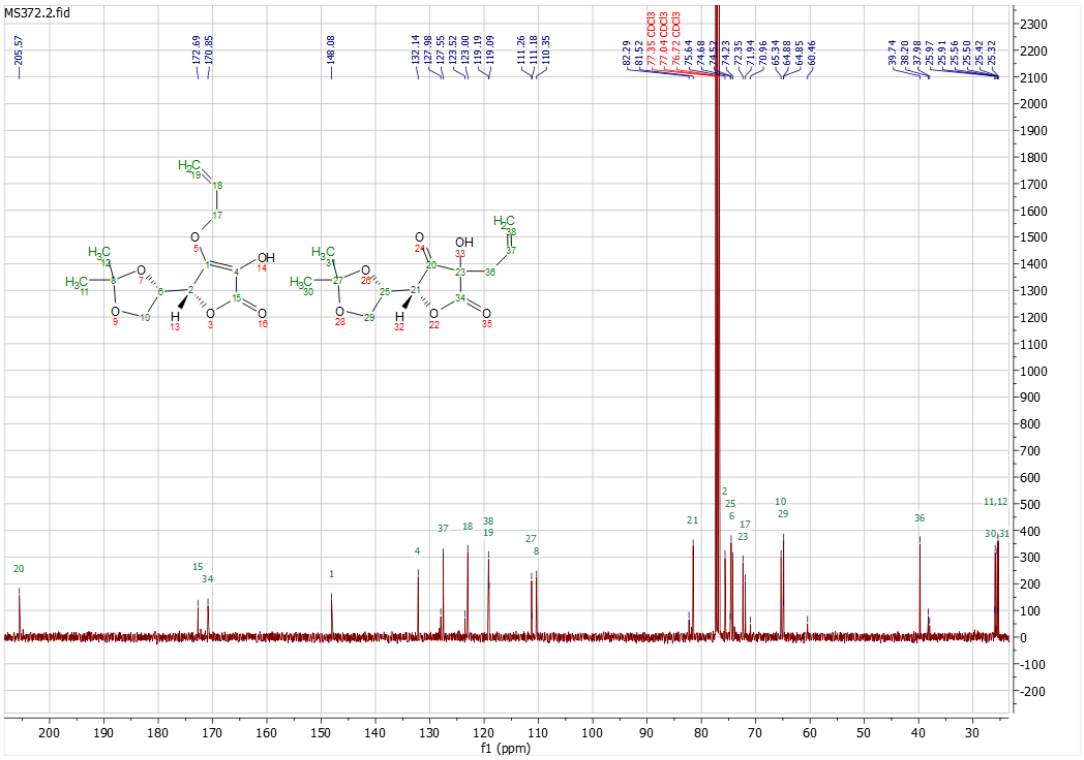

Figure 56. Carbon NMR of allyl ether formation showing mixture of products.

This mixture of materials was taken forward to the arylation step (**Scheme 12**) but no product was observed, only a further conversion between allyl products to a ratio of 31:69 as can be seen in the NMR below (**Figure 57**).

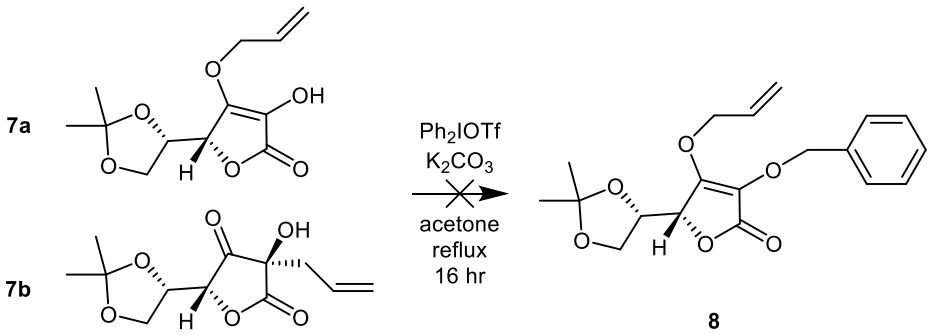

Scheme 12. Failed arylation step of allyl compounds due to rearrangement exacerbated by heat.

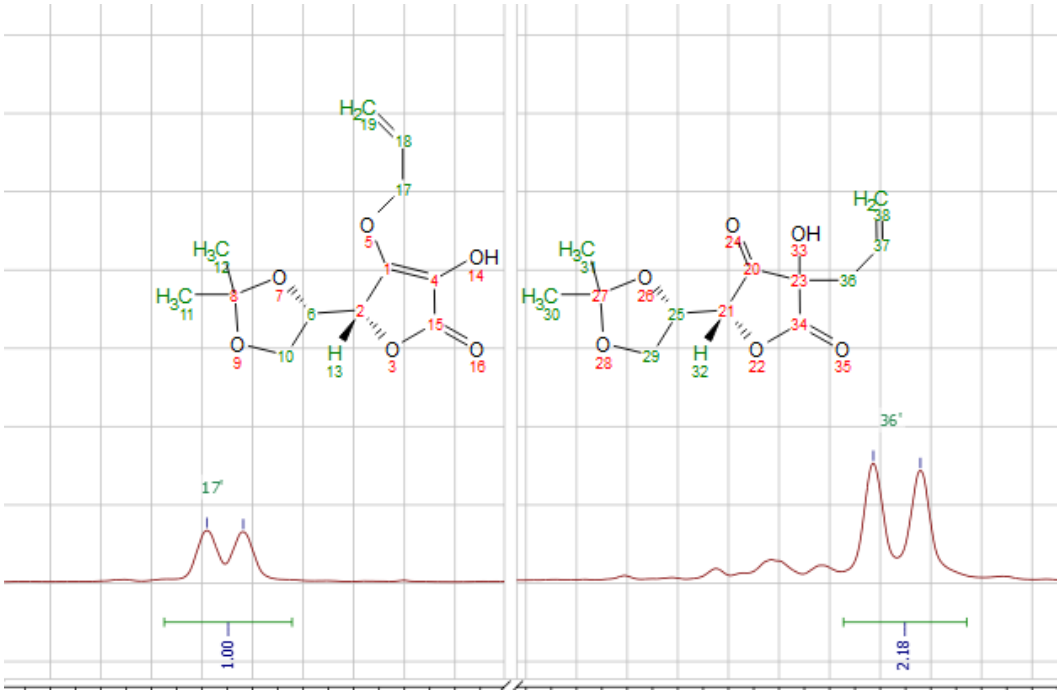

Figure 57. Proton NMR of allyl conversion with peaks corresponding to ethylene group adjacent to alkene as reference.

Due to the mixture of products seen when trialling allyl as a protecting group and the failure of the subsequent arylation step, this method was not used again.

4.1.5.2 Benzyl

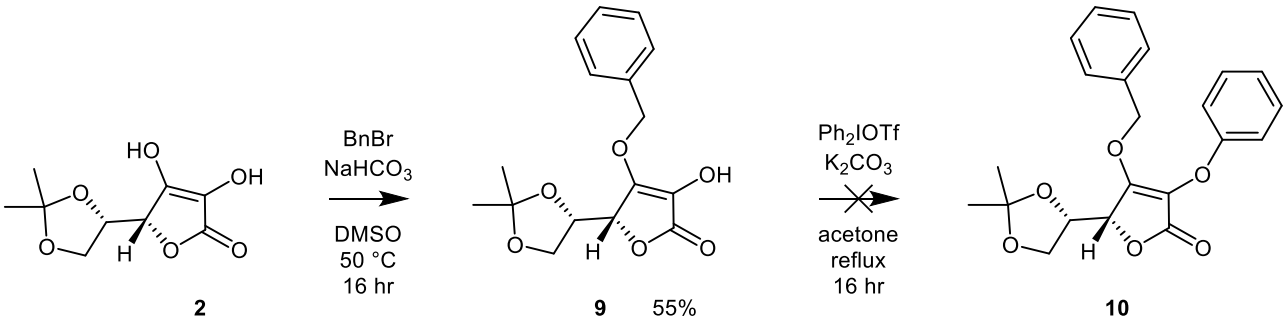

Scheme 13. Failed conditions for arylation following benzyl protection.

Benzyl protection was achieved in reasonable yield (55%) although arylation attempts proved unsuccessful (**Scheme 13**). This could be due to steric clashes between the benzyl

group and Ph_2IOTf, as stronger bases have been used with no success such as NaH and ^tBuOK.[170]

4.1.5.3 Silyl

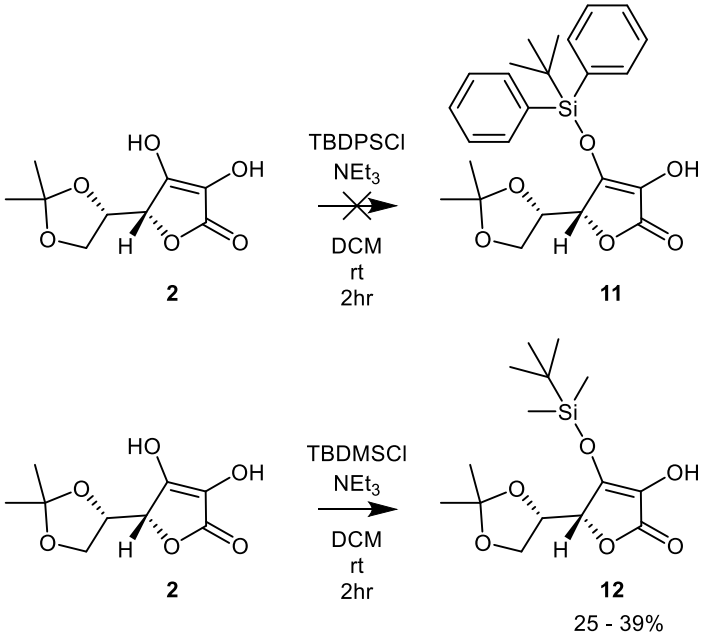

Scheme 14. Scheme to show size of substituents on silyl group affects reactivity.

TBDPS protection failed, possibly due to the diphenyl group being too bulky and hindered for the 3-*O* alcohol to attack (**Scheme 14**). TBDMS protection was successful although arylation failed due to steric hindrance between the silyl group and Ph_2IOTf, as it is possible to attach a benzyl group to this alcohol after TBDMS protection (shown in **Scheme 15**).

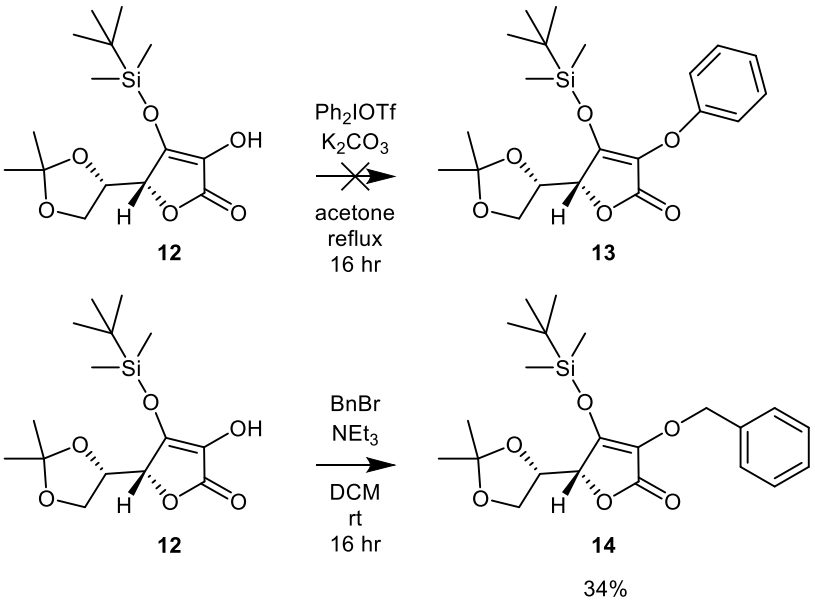

Scheme 15. Illustration of steric hindrance in attaching aryl groups to silyl protected compounds.

Smaller groups were clearly necessary and so TES protection was utilised, which was achieved in low yield (30%). This may be improved upon by increasing the temperature of the reaction, increasing reaction time did not aid the yield. Despite the smaller silyl group, arylation was unsuccessful suggesting the close proximity of the silyl group to the bulky arylating agent is preventing the alcohol from being in close proximity to the arylating reagent (**Scheme 16**).

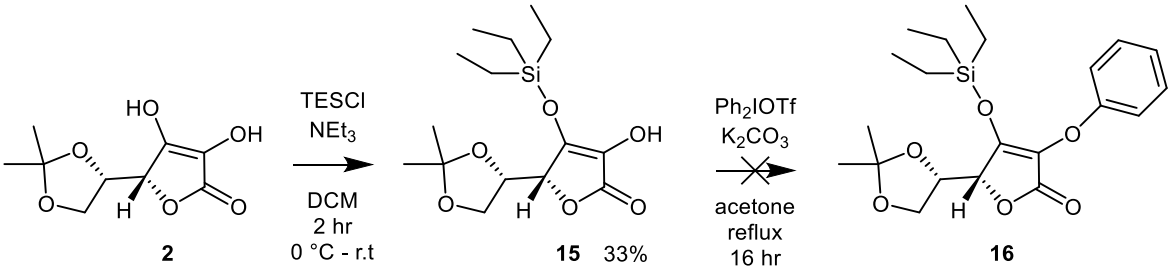

Scheme 16. Illustration of failed arylation reaction following triethylsilyl protection.

4.1.5.4 Methoxymethyl

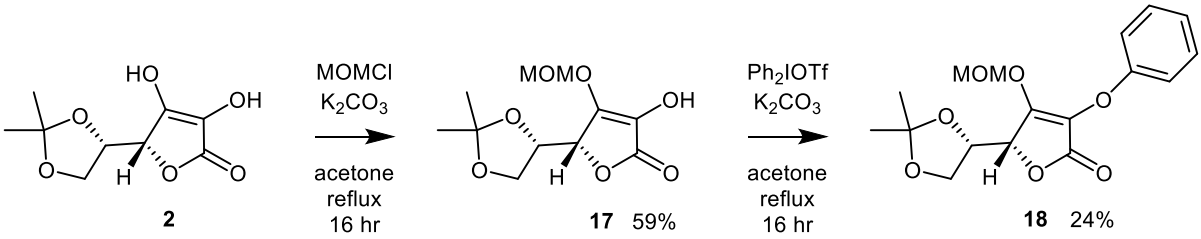

Scheme 17. Methoxymethyl protecting route.

Due to the apparent size constraints involved in the selection of a protecting group another small group was chosen for synthetic analysis, methoxymethyl (MOM). This group is easier to remove than an ethyl ether (in general more labile when using acid) so would be advantageous for the final deprotection step in the synthesis of target **A**.

Attachment of the MOM group to form **17** was achieved using methods described previously in section **5.1.2** using K_2CO_3 in acetone (60 °C) with yields ranging from 25 – 60% (higher yield observed using oven dried apparatus). Arylation of the remaining alcohol to form **24** was achieved in a similar yield to previous efforts when using ethyl as a protecting group. An illustration of this is shown in **Scheme 17**.

Removal of the MOM group was attempted first using 1M HCl, which also afforded removal of the acetal group to give **19**, re-acetylation was then achieved in good yield using acetyl chloride in acetone to form **A** as shown in **Scheme 18**. To remove the need for the reacetylation step, attempts were made to use non aqueous methods for the removal of the MOM group. This includes using acetyl chloride and CSA in DCM, but these also removed the acetal protecting group.

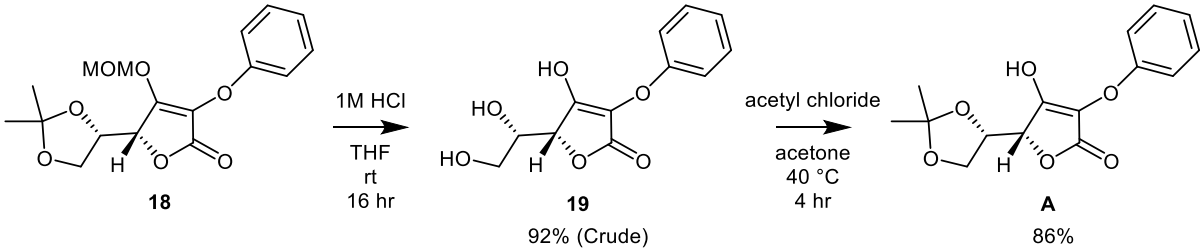

Scheme 18. Methoxymethyl route to target **A** comprising of unwanted acetal deprotection and reformation following removal of MOM ether.

Target **A** satisfies Lipinski's rules: with a molecular weight of 292 which is significantly below the recommended limit (500), one hydrogen bond donor (recommended limit 5), six hydrogen bond acceptors (recommended limit 10), and a predicted logP (using ChemDraw Professional 16.0) of 2.16 (recommended between 0 and 5).

4.2 Synthesis of target B

4.2.1 Deacetylation

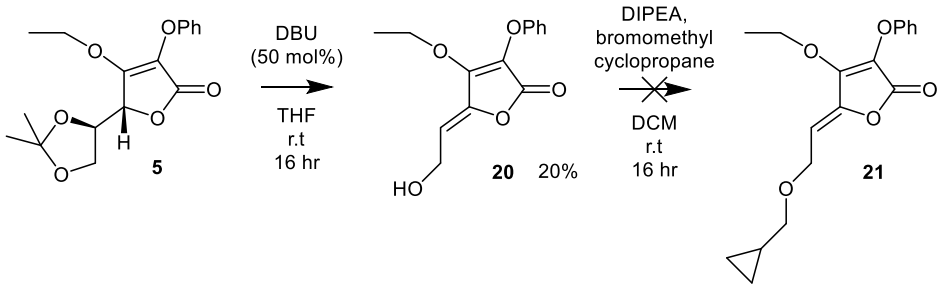

Scheme 19. Deacetylation to form alkene followed by unsuccessful attempt at alkylation

Deacetylation of **5** was attempted using DBU (50 mol %) in THF with no success, increasing the amount of base did not help as did altering the reaction dilution and temperature/time.[169] Success was achieved when doing the reaction on a larger (gram) scale presumably due to the addition of DBU needing to be very slow, although only in very low yield (20%). This step was not reproducible and so an alternative methodology was followed as will be discussed in a future chapter.

Alkylation of **20** to form **21** appeared to be successful upon using bromomethylcyclopropane and DIPEA, as mass spec analysis of the crude mixture showed a peak corresponding to the desired product, although it could not be isolated by column chromatography and as the previous alkene formation step (formation of **20**) was unable to be reproduced, a new method was attempted.

4.2.2 Alkene formation

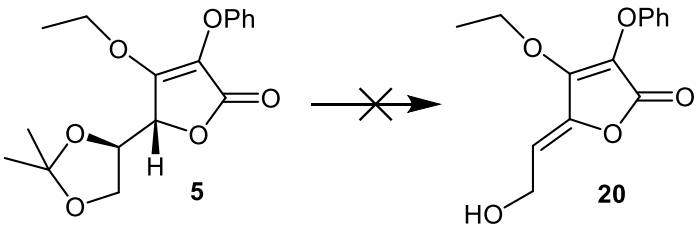

Scheme 20. Failed deacetylation to form alkene.

As briefly discussed before in section **5.2.1**, deprotonation of **5** to remove a molecule of acetone to form the desired alkene **20** as shown in **Scheme 20** failed under conditions using DBU which was attributed to steric issues. Alternative bases were used with similar results including triethylamine, sodium hydride, DIPEA, pyridine and DMAP. No starting material was recovered from these reactions which delayed synthesis of targets significantly. Usage of a small base (sodium hydride) without success suggested that sterics may not be the problem, that it may be electronic issues hindering progress.

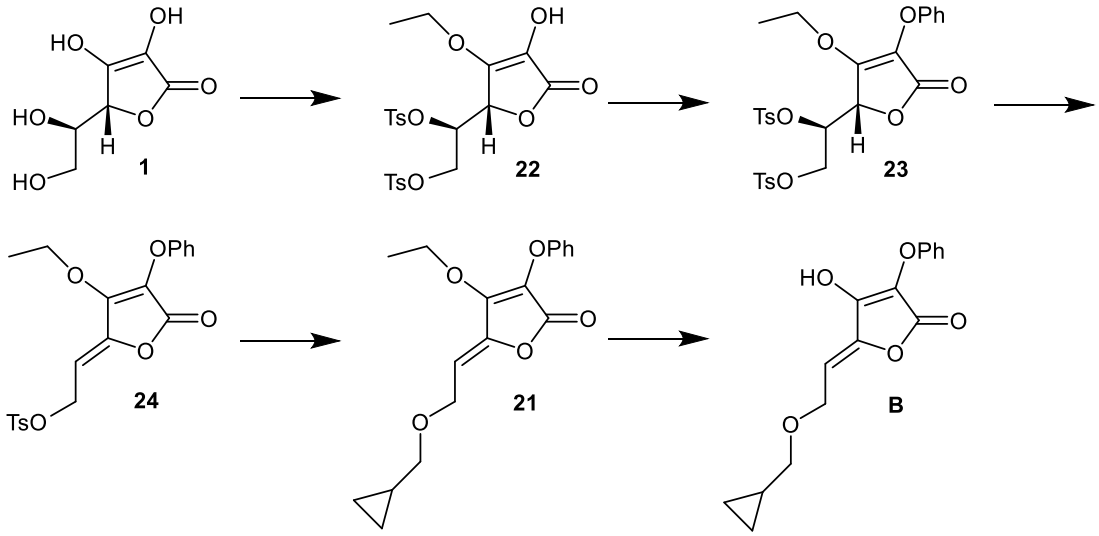

Scheme 21. Proposed scheme using tosyl derivatives.

An alternate route was considered involving use of tosyl groups to act as a better leaving group for alkene formation as shown in **Scheme 21**.

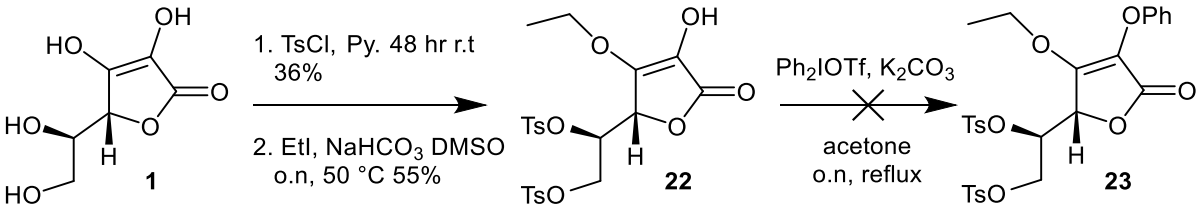

Scheme 22. Tosyl route attempted with L-ascorbic acid as starting material showing failure of arylation step.[176]

Ditosylation and ethylation to give **22** were successful albeit arylation failed with conditions shown in **Scheme 22**, sodium hydride as a base for the arylation was also tested without success. This meant a new strategy was needed as shown in **Scheme 23**.

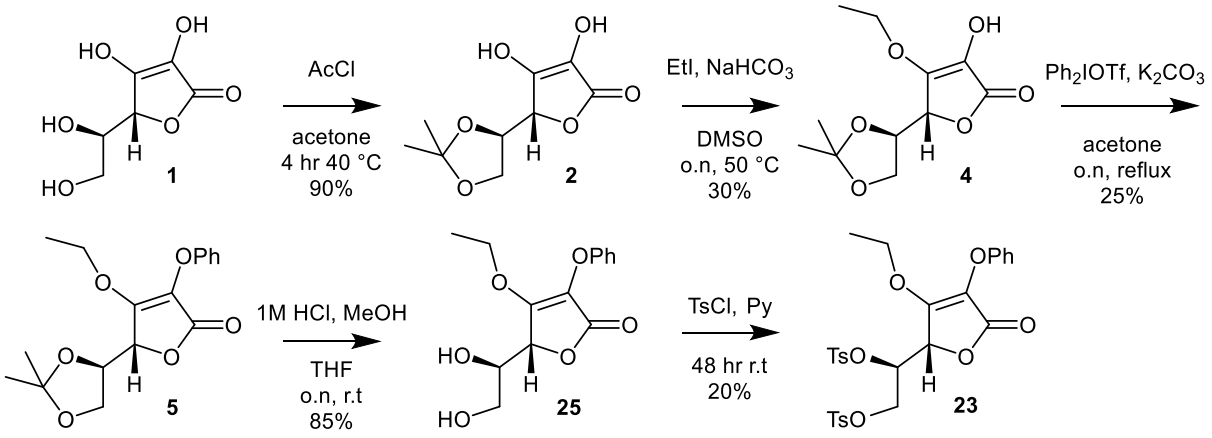

Scheme 23. Second tosylation strategy forming phenyl ether before tosyl addition to diol.

Ditosylation of **25** to give **23** was achieved but in very poor yield with impurities in the ^{1}H NMR although new tosyl peaks were observed to indicate reaction had proceeded. The next step of forming the alkene **24** failed using DBU and it was presumed that the size of the leaving groups may be preventing the desired reaction from working with a clash between the aryl groups and the relatively large DBU and so the strategy was changed in order to utilise mesylate groups. Mesyl groups were also chosen as they are smaller than tosyl and electronically more labile, as NaH also failed with tosyl derivatives and as such should improve the yield.

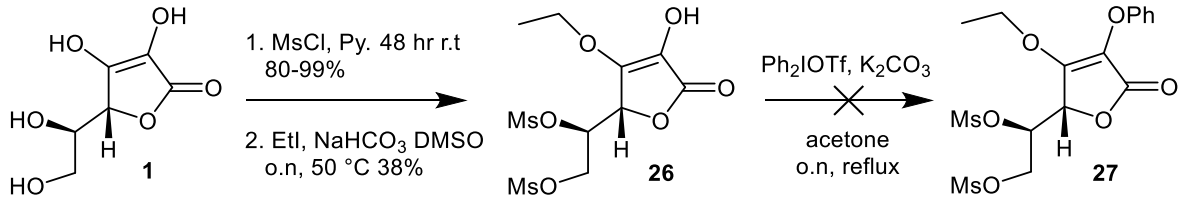

Scheme 24. Mesyl route attempted with L-ascorbic acid as starting material showing failure of arylation step.[176]

Scheme 24 details initial attempts at using mesylation to achieve alkene **30** formation which shared the same outcome as the tosyl equivalent. Alkylation to form **26** was

achieved in a lower yield than observed in the tosyl route, attributed to mesylate groups being more labile under reaction conditions of ethyl ether formation (heating) than tosyl groups. Arylation to form **27** also failed so the same strategy employed in **Scheme 23** whereby mesylation was attempted after aryl ether formation was adapted, the procedure followed is shown in **Scheme 25**.

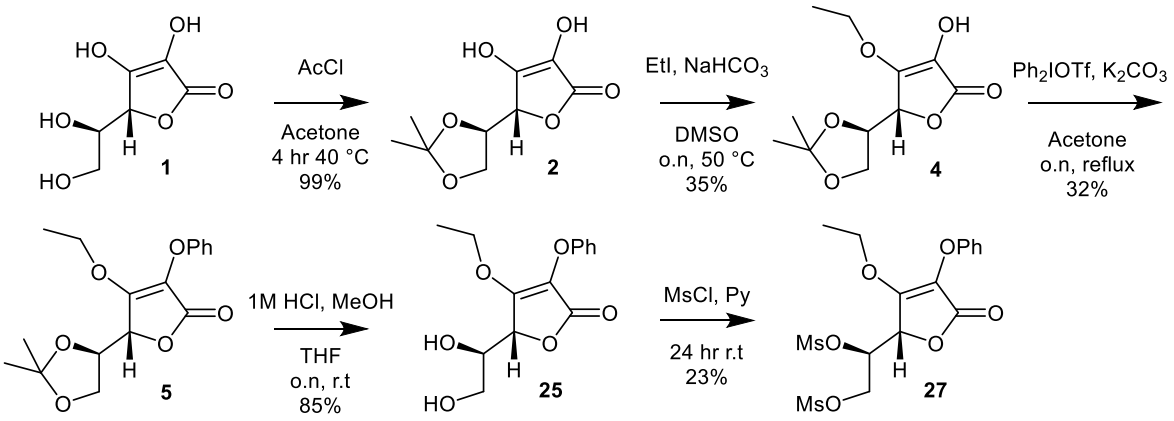

Scheme 25. Second mesylation strategy.

27 was produced using the method in **Scheme 25** although the final mesylation step was in poor yield, efforts to generate the alkene **30** shown in **Scheme 26** failed under the same conditions as used in the deacetylation step, with no starting material observed or identifiable products. Closer analysis of the most recent attempt using triethylamine indicated the reaction had produced the charged species **31** as shown in **Figure 58**. The exact mass was observed in the mass spectrum (**Figure 59**) and a mix of the desired alkene product **30** and the nitrogen species was seen in the crude NMR as well. In particular, the peak in the proton and carbon spectra which correlates to the methylene group (N-CH_2-CH) in **Figure 58** has two peaks dependent on if a mesyl group or ammonium group is next to it. A portion of the C^{13} spectra is shown in **Figure 60**.

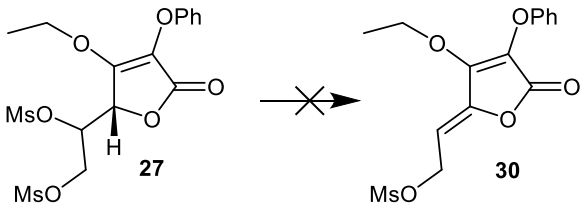

Scheme 26. Alkene formation from mesyl species.

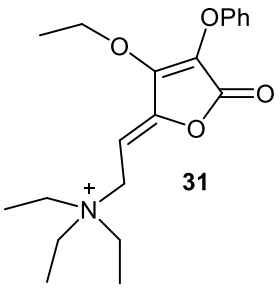

Figure 58. Triethylamine adduct formed.

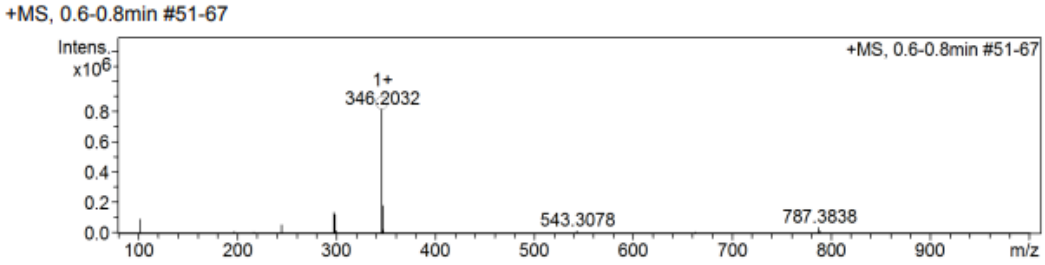

Figure 59. HRMS showing peak at 346.2032 which correlates with exact mass (346.2018) of compound in **Figure 58**.

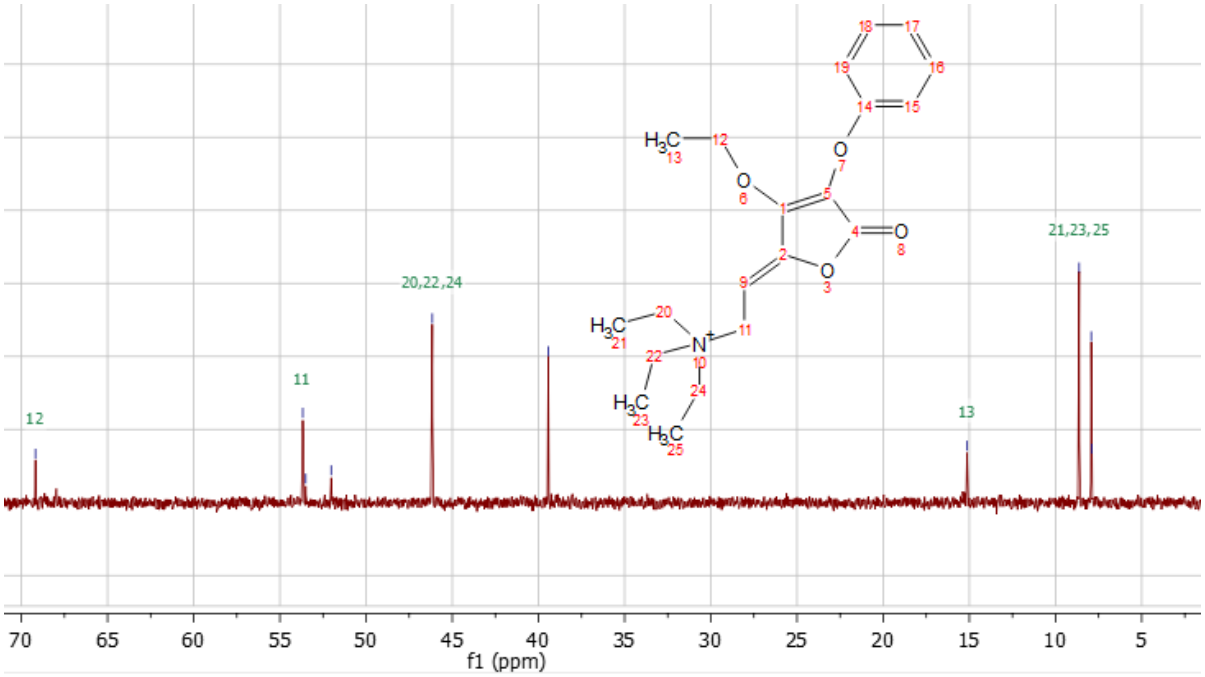

Figure 60. A region of the crude ^{13}C NMR of compound in **Figure 58**. Peak at ~ 39 ppm assigned to methyl group of mesylated species in crude mixture, small peak at ~ 53 ppm assigned to carbon 11 of mesylated species in crude mixture.

As the compound was fixed to the baseline on the TLC plate and no starting material was observed, the decision was made to proceed with synthesis and purify after the next step. Procedure shown in **Scheme 27**.

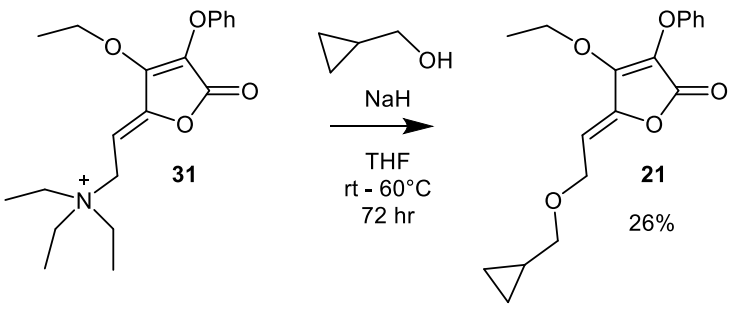

Scheme 27. Procedure for adding cyclopropylmethyl ether to compound.[176]

The alkylation in **Scheme 27** to form **21** initially failed using a "one-pot" method of adding all reagents together at the same time. However, stirring the alcohol separately with NaH

addition for thirty minutes before adding dropwise to a solution of starting material **31** in solvent caused a colour change of yellow to deep red which got darker overnight. Mass spec analysis indicated the reaction was proceeding, but incomplete, and so a further equivalent of alcohol and base was added to the stirring solution, which after 16 hours was left to reflux over the weekend in order to aid reaction completion. The pure product **21** was obtained in 26% yield, with the final step being removal of the ethyl group masking the vinylic alcohol.

Conditions used earlier in the synthesis of target **A** were attempted here with similar results, in that no progression of the reaction was observed. Conditions used included: TMSI (both reagent and synthesised *in situ*), HCl, and BBr_3. Due to the inability to remove the ethyl protecting group, an alternate derivative of **B** was chosen to produce.

4.2.3 Towards the synthesis of benzyl alternative of target B

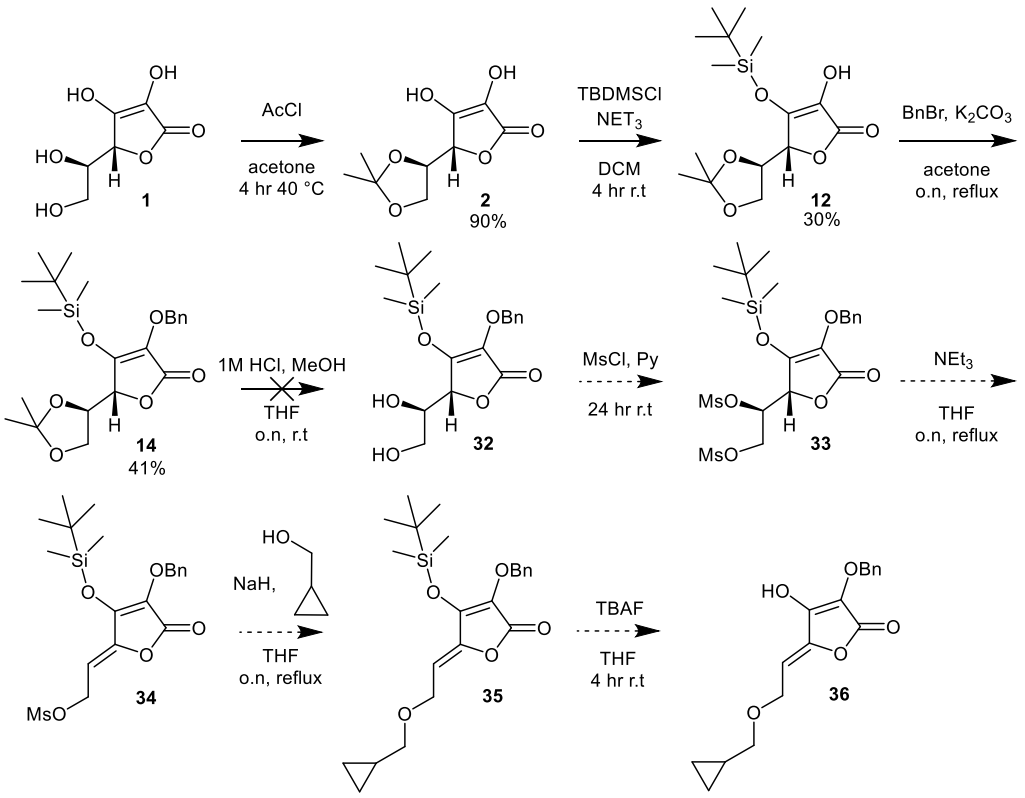

Scheme 28. Silyl route towards synthesis of benzyl analogue of target **B**

Whereas silyl protection had previously been discounted due to steric clashes upon arylation of the adjacent alcohol, a benzyl group should afford enough distance to remove this obstacle. Silyl groups are commonly used for quick and efficient protection of alcohols due to their ease of deprotection using fluorine based reagents, it is for this reason that the route depicted in **Scheme 28** was followed.[177]

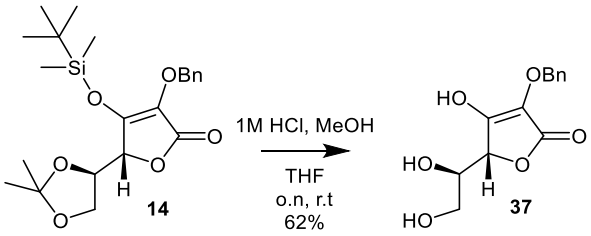

Scheme 29. Product formed under aqueous acidic conditions.

Acetal formation of **2** was achieved in high yield (>90%), with silyl protection forming **12** completed in 30% yield. Subsequent benzyl addition to give **14** was achieved in 41% yield although acetal deprotection to afford **32** did not yield the desired product, instead additionally removing the silyl group to give **37** as shown in **Scheme 29**. An attempt was made to mesylate the diol formed but was unsuccessful. A non-aqueous method of acetal deprotection using camphorsulfonic acid in DCM was investigated but this also removed the silyl group.

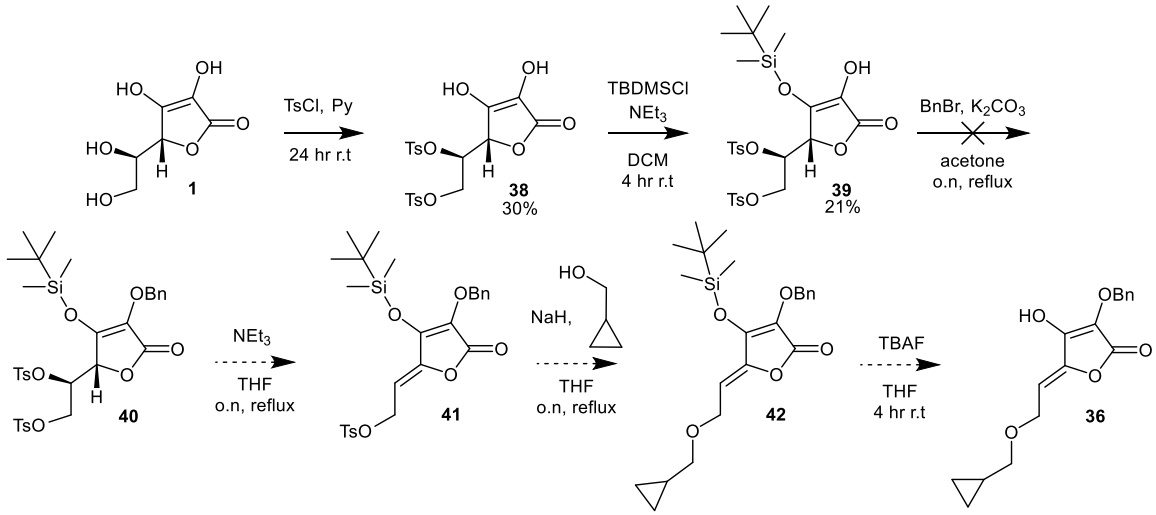

Scheme 30. Proposed scheme using diol conversion as first step in synthesis to avoid silyl removal under acidic conditions as seen in **Scheme 29**.

Due to the problems encountered, a process whereby the diol was converted into a leaving group prior to silyl and benzyl addition was examined as shown in **Scheme 30**. The number of steps required in this synthesis meant a more stable leaving group of tosyl was utilised in place of the more labile mesyl group.

Ditosylation to give **38** was achieved in 30% yield, and silyl protection of the 3-*O* followed in a similar fashion to give **39** although purification was an issue due to co-elution of starting material and product. This was taken forward for benzyl addition to the remaining 2-*O* which afforded the desired product **40** in an inseparable mixture alongside a di-benzylated species illustrated below in **Figure 61**.

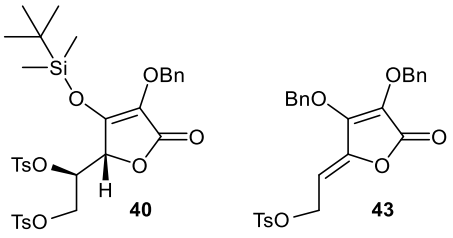

Figure 61. Inseparable products from benzylation.

These were taken forward for alkene formation using conditions in section **5.2.2** (triethylamine in THF at reflux) which after 16 hours showed no remnants of starting material (ditosyl species) by mass spectrometry. After purification by column chromatography, NMR indicated the presence of additional peaks in the aryl and alkyl regions suggesting a mixture of products **41** and **44** had eluted as shown in **Figure 62**.

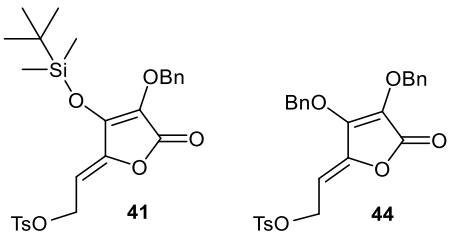

Figure 62. Products obtained from alkene formation step.

No desired product was obtained from the attempted ether formation shown in **Scheme 31**, if this route is attempted in future then mesyl groups may be considered for their higher lability as compared to tosyl. Alternately conversion of tosyl to an alcohol before methylcyclopropane alkylation could be performed as shown in **Scheme 32**.

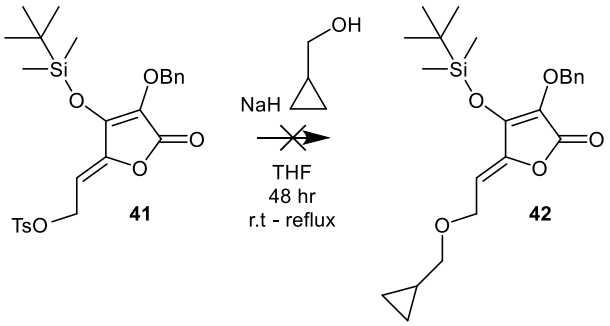

Scheme 31. Failed conditions for ether formation.

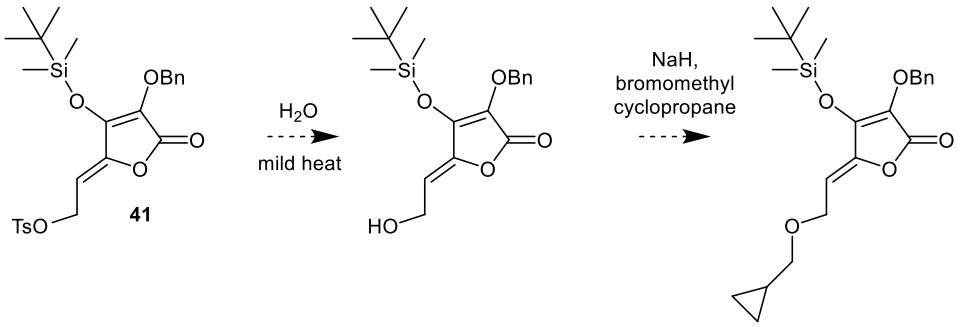

Scheme 32. Proposed route converting tosyl into hydroxyl for reaction with bromomethyl cyclopropane.

4.3 Benzyl ether synthesis

4.3.1 One-pot silyl approach [178]

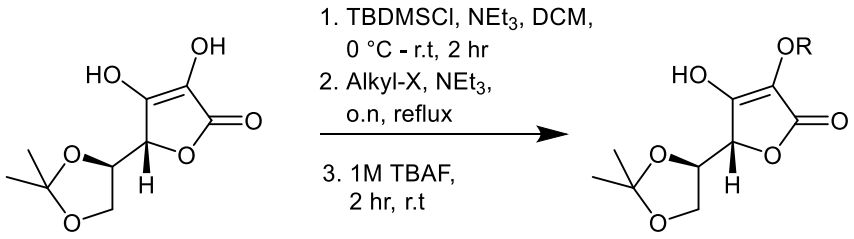

Scheme 33. General conditions for one-pot synthesis of compounds.[178] R = Benzyl, PMB, *p*-iodobenzyl, *p*-nitrobenzyl, ethylcyclohexane, propylbenzene

A less time consuming route for production of functionalised ascorbic acid was discovered which should allow for fast production of final compounds with the need for only one purification step at the end of the route as shown in **Scheme 33**.

This method allows an investigation into the region on the right hand side of the molecule to assess whether increased distance between the aryl group and the core of the molecule affects activity, as well as altering the electrophilicity of the aryl group. Non-aromatic groups were also chosen as a proof of concept as they will not share the same π–π stacking interaction with NADH and as such ought to be poor inhibitors/show no activity towards InhA.

The reasoning behind this is that the free alcohol remaining is expected to coordinate to Tyr158 residing near the binding pocket on InhA (interaction described in section **4**) and so moving this region into closer proximity is expected to increase interaction strength and make the compound a better inhibitor. Making the aromatic group more electrophilic is expected to alter its interaction with NADH, making it more electron rich is thought to increase the π–π stacking interaction.

The reaction was to proceed in a stepwise manner of addition, whilst maintaining a "one-pot" approach to purification. Addition of TBDMSCl in DCM accompanied by NEt_3 was to silyl protect the left-hand alcohol, and after two hours one equivalent of alkylating reagent in DCM with a further portion of NEt_3 was added before a second two hour wait. After this time an equivalent of TBAF was used to deprotect the silyl-alcohol with a half an hour wait.

A range of compounds were chosen for synthesis comprising of the R group being: benzyl, PMB, *p*-iodobenzyl, *p*-nitrobenzyl, ethyl cyclohexane and propyl benzene. Overall yields were poor, with final compounds produced in less than 20% yield. An increase in time between steps was attempted in a ratio of 4:16:2 (silyl protection:alkylation:silyl deprotection) for each step respectively but this did not aid in yield or purity. Poor yields are attributed to the base used in the method, and to increase these a stronger base may be necessary as well as splitting the reaction up into its constituents and optimising the conditions.

The compounds obtained had impurities in the NMR as well as a mix of products observed with R groups attached to either alcohol (**Scheme 34**) as shown in the NMR below for a nitrobenzyl derivative, with the satellite peaks aside the major peaks attributed to unwanted alcohol alkylation.

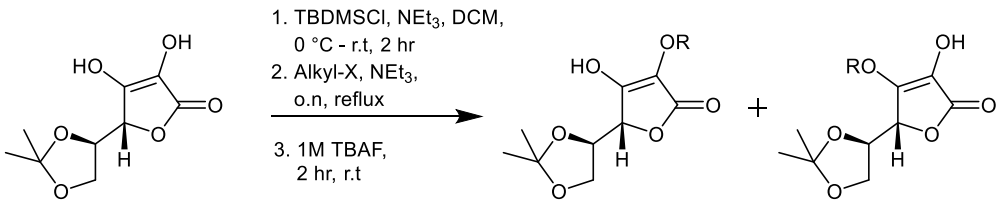

Scheme 34. Products obtained from one-pot alkylation methodology with alkylation on both alcohols.

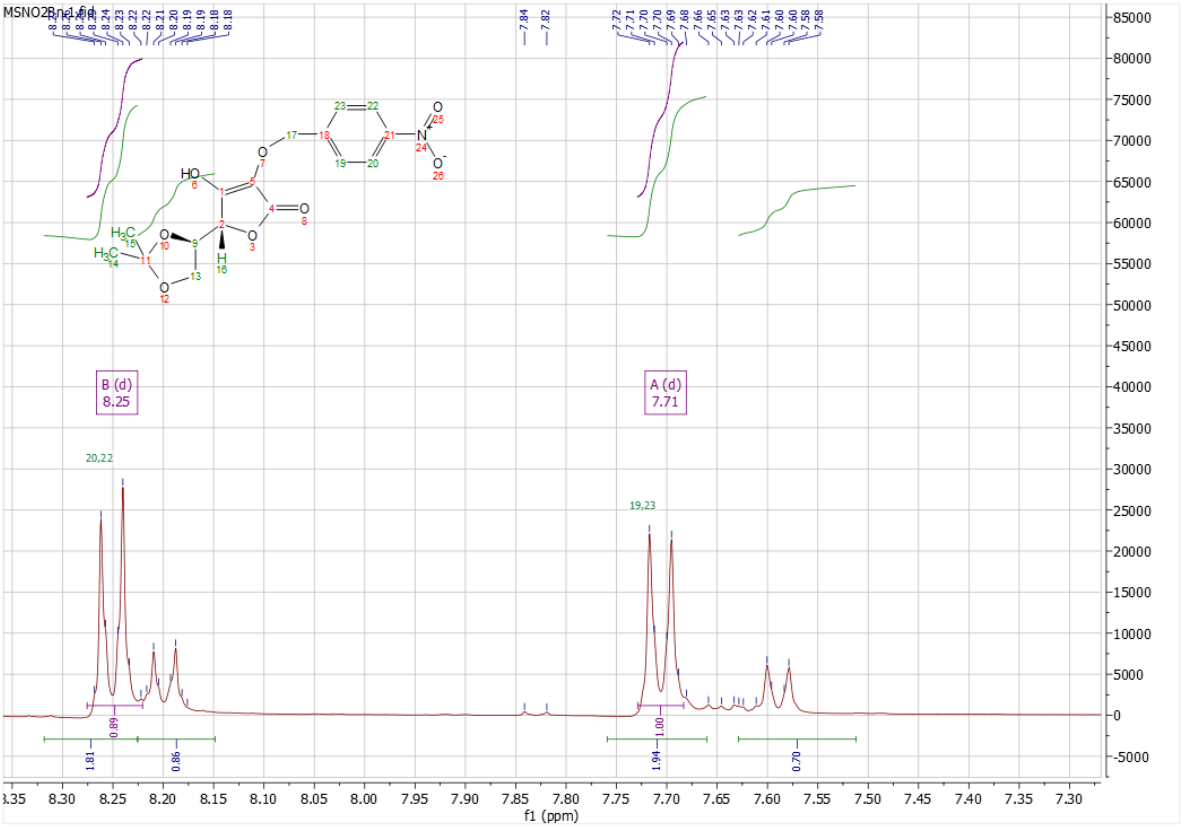

Figure 63. ^{1}H NMR showing mixture of products from reaction in **Scheme 33** for a nitrobenzyl derivative.

Further enforcing previous statements regarding proximity issues with groups directly attached to the right hand alcohol is the fact that attempts to introduce a cyclohexyl or phenyl moiety were unsuccessful which is attributed to steric clashes with the silyl protecting group.

4.3.2 Direct 2-*O* alkylation approach

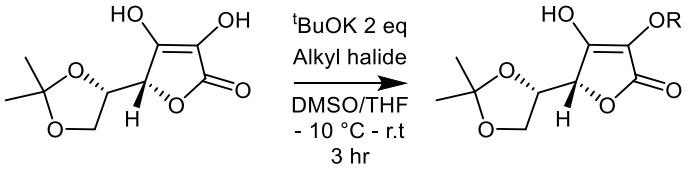

Scheme 35. General reaction conditions for direct 2-*O* alkylation. [179]

An alternate approach was used, following work carried out by Olabisi and Wimalasena, which determined reaction pathways using considerations of electrostatic potential caused by basic environments around the 5,6-*O*-isopropylidene-L-ascorbic acid.[179] An image of the changes in electrostatic potential obtained from Olabisi *et al* is shown below in **Figure 64**.[179]

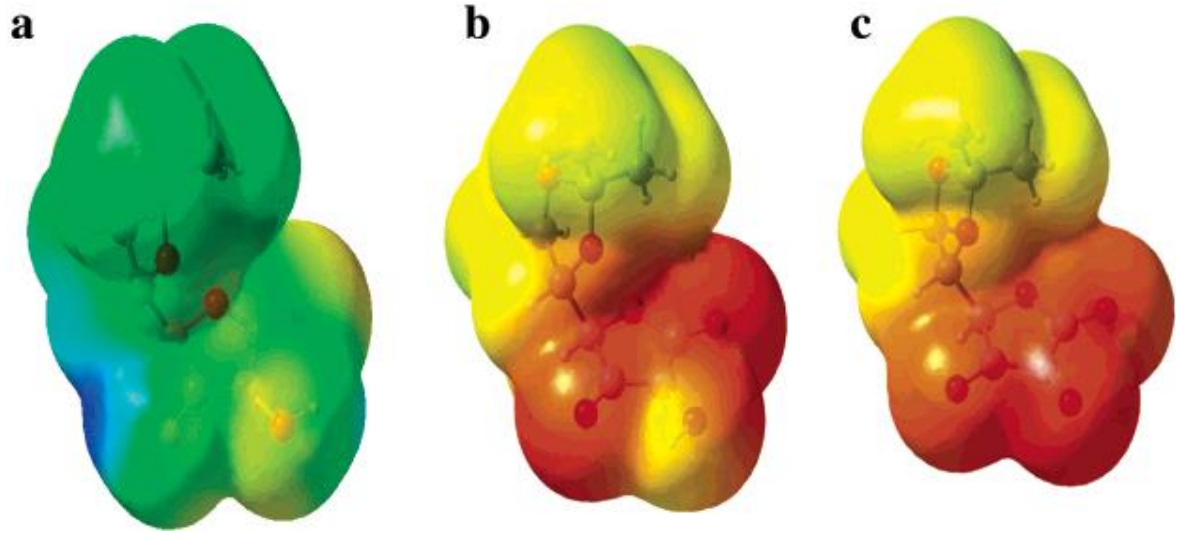

Figure 64. Calculated electrostatic potential diagrams of the neutral, monoanionic, and dianionic forms of 5,6-*O*-isopropylidene-L-ascorbic acid. Calculated electron density diagrams of (a) neutral, (b) monoanionic, and (c) dianionic forms. Order of electron density: blue < green < yellow < red

This figure shows clearly the shift in electron density upon conversion between neutral, mono, and dianionic forms of 5,6-*O*-isopropylidene-L-ascorbic acid. One equivalent of base directs the electron density primarily towards the 3-*O* where the charge can be delocalised via resonance into the carbonyl as previously described in **Scheme 5**. A second equivalent of base to afford the dianion therefore makes the 2-*O* the primary source of reaction with electrophilic agents.

Two equivalents of ^{t}BuOK added to 5,6-*O*-isopropylidene-L-ascorbic acid **2** in DMSO/THF followed by addition of the alkylating reagent was therefore attempted for a one-pot method of producing benzyl based derivatives. It is important to note that addition of the base must be done under lower temperatures as addition at room temperature exuded heat, which turned the solvent from liquid to a jelly-like substance thereby preventing stirring of the reaction.

Using alkylating agents with chlorine as the leaving group as opposed to more labile halogens gave no product under the described reaction conditions, presumably due to the relative strength of the carbon-chlorine bond (~ 84 kcal mol^{-1} compared to a C-C bond of ~ 90 kcal mol^{-1}).[180]

An ethylene-cyclohexyl derivative exclusively formed the double alkylated product as was shown in mass spec and NMR, ^{13}C peaks from the assigned alkyl region are shown below in **Figure 65**.

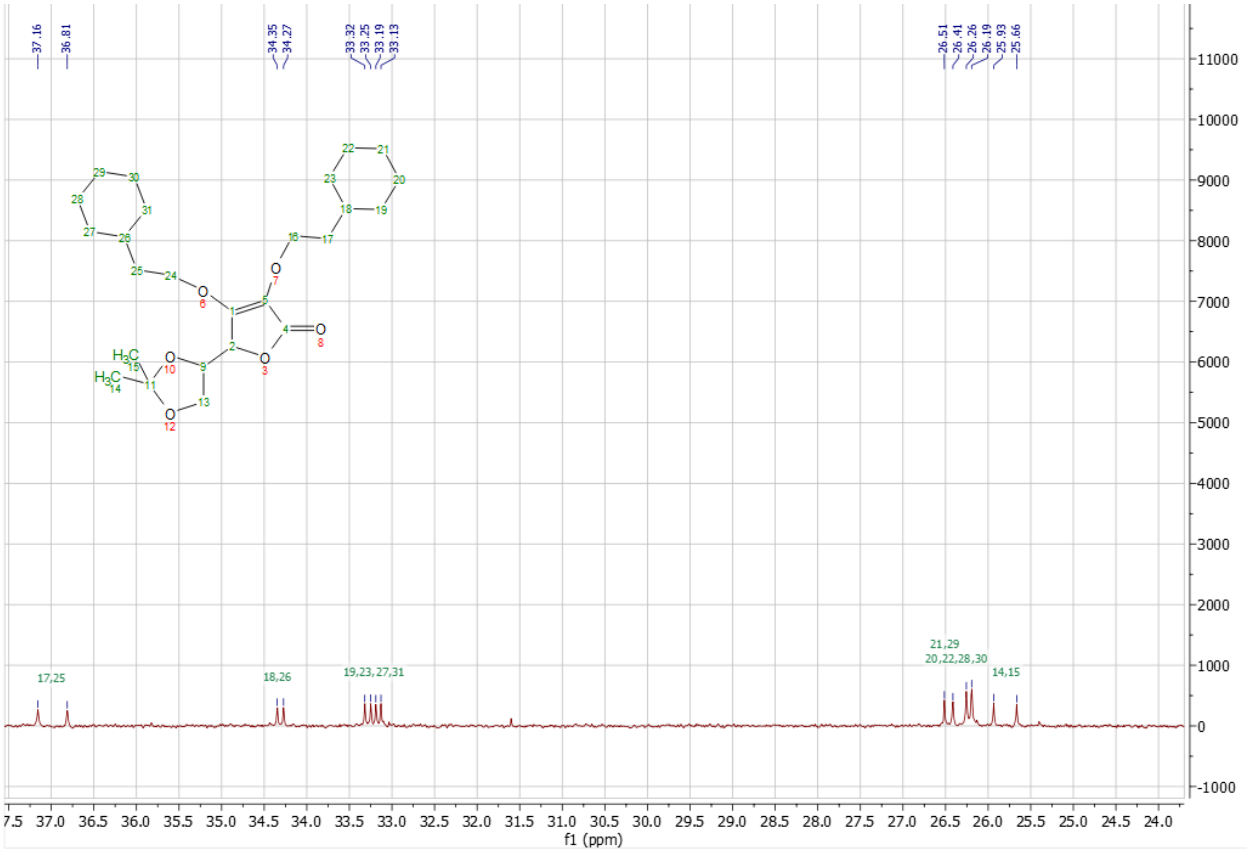

Figure 65. ^{13}C NMR of dialkylated product.

A *para*-iodo benzyl derivative also gave double alkylation, with the relevant peaks from the assigned proton NMR shown below in **Figure 66**.

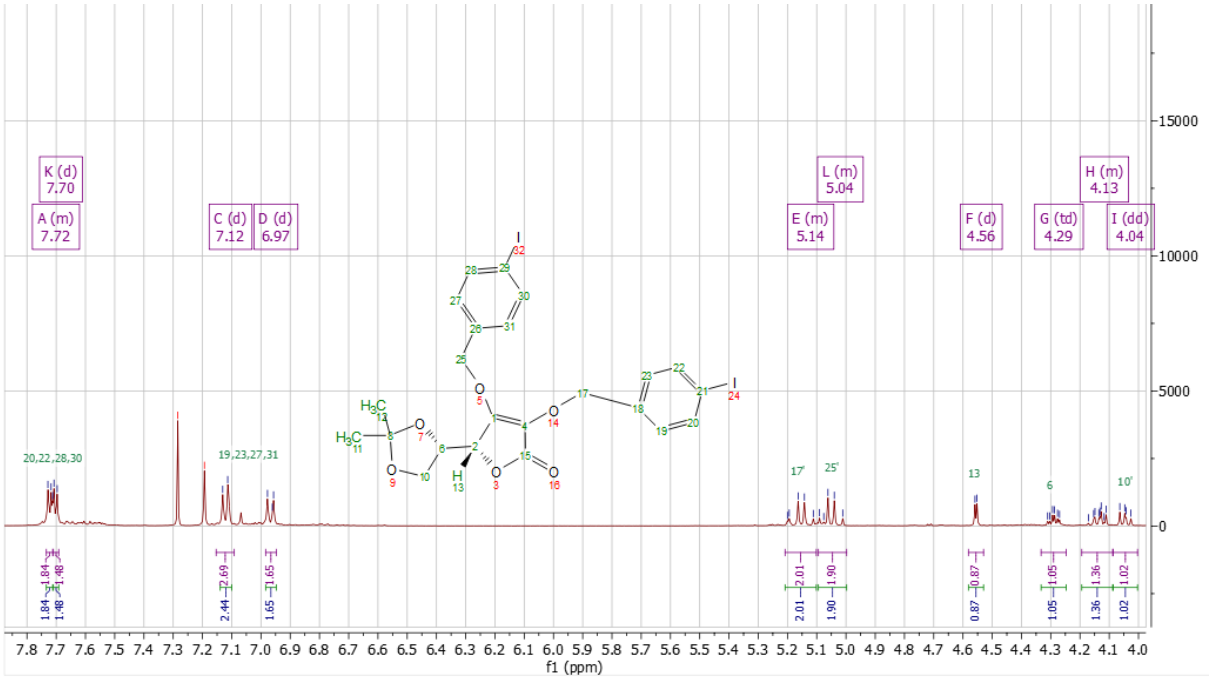

Figure 66. ^{1}H NMR of dialkylated iodobenzyl derivative.

After a *para* isopropane - benzyl derivative gave the same result, the other reactions were analysed by mass spec before workup and all showed that double alkylation had taken place with none of the desired mono-alkylation observed.

These results indicate that one-pot/direct alkylation approaches beginning with 5,6-*O*-isopropylidene-L-ascorbic acid are not viable for producing benzyl ethers so a stepwise silyl route was investigated.

4.3.3 Silyl stepwise approach

This route adapted the procedure used in section **5.3.1** into a stepwise approach, with a purification step at each stage of the synthesis. This was done in order to improve product purity throughout the route which will aid in selectivity of 3-*O* alkylation over unwanted dialkylation as was seen in sections **5.3.2** and **5.3.1**.

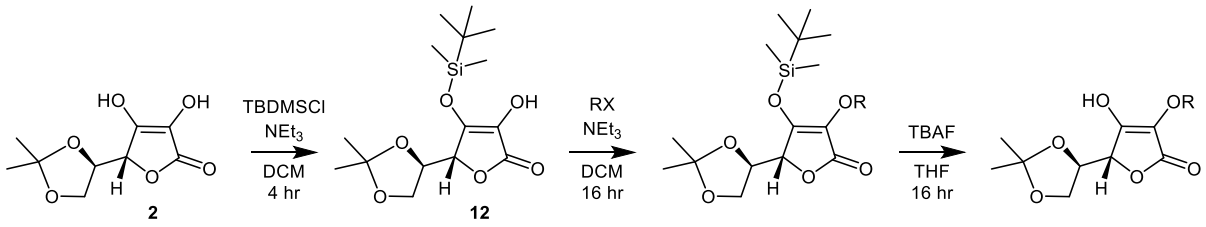

Scheme 36. Scheme to illustrate stepwise approach

TBDMSCl was chosen over other silyl protecting agents for a compromise over stability and also size of the methyl substituents. Prior work to attain target **A** had shown that silyl groups with larger substituents than a methyl afforded steric clashes when adding a bulky R group (direct attachment of cyclohexyl/phenyl) onto the 2-*O* with no hydrocarbon chain and so TES and TBDPS were discounted. TMS was not used due to its relative poor stability as compared to TBDMS.

Alkylation of **12** was achieved in varying yields (10 – 30%), with reagents incorporating chlorine as a leaving group unsurprisingly giving the poorest yields. Subsequent silyl deprotection was achieved in generally high yields (>80 %), although a nitrobenzene species was unable to be isolated due to TLC overlap with leftover ^{t}butyl-amine from the TBAF used in the reaction.

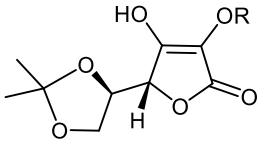

No	R	Yield	Amount (mg)	MW	H-bond donors	H-bond acceptors	Predicted logP
54	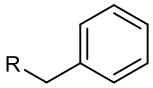	34%	70	306.11	1	6	1.79
53	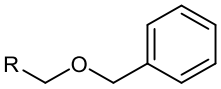	10%	1.8	350.14	1	7	1.71
64	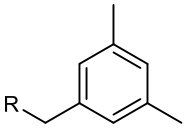	28%	30	334.14	1	6	2.79
67	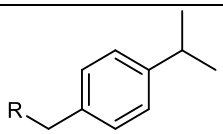	29%	50	348.16	1	6	3.22
57	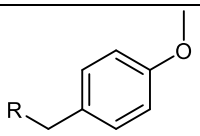	28%	70	336.12	1	7	1.71
58	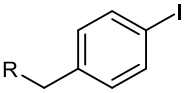	18%	10	432.01	1	7	2.91
61	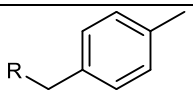	25%	10	320.13	1	6	2.29
62	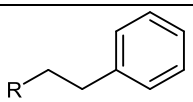	27%	15	320.13	1	6	2.26
65	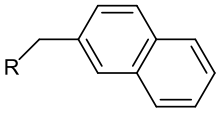	31%	70	356.13	1	6	1.09

Table 9. Benzyl ethers synthesised with corresponding values relating to Lipinski's rules. Yield corresponds to alkylation step.

Table 9 shows the structures of benzyl ethers synthesised along with their values showing satisfaction of Lipinski's rules (logP predicted in ChemDraw Professional 16.0). This shows all the compounds synthesised would have good "druglikeness" scores with the only negative aspect being the existence of a free alcohol making the compounds subject to phase two metabolism, however many drugs in clinical use contain free alcohols so this is not a primary concern.

In summary, a range of ethers were synthesised to be taken forward for isolated enzyme assay testing against InhA. In order for this route to be better utilised, different conditions for the alkylation step are necessary, with alterations of solvent used to aid higher temperatures as well as a stronger base to make the alcohol more reactive.

4.4 Towards the synthesis of 2-Deoxy-L-ascorbic Acid

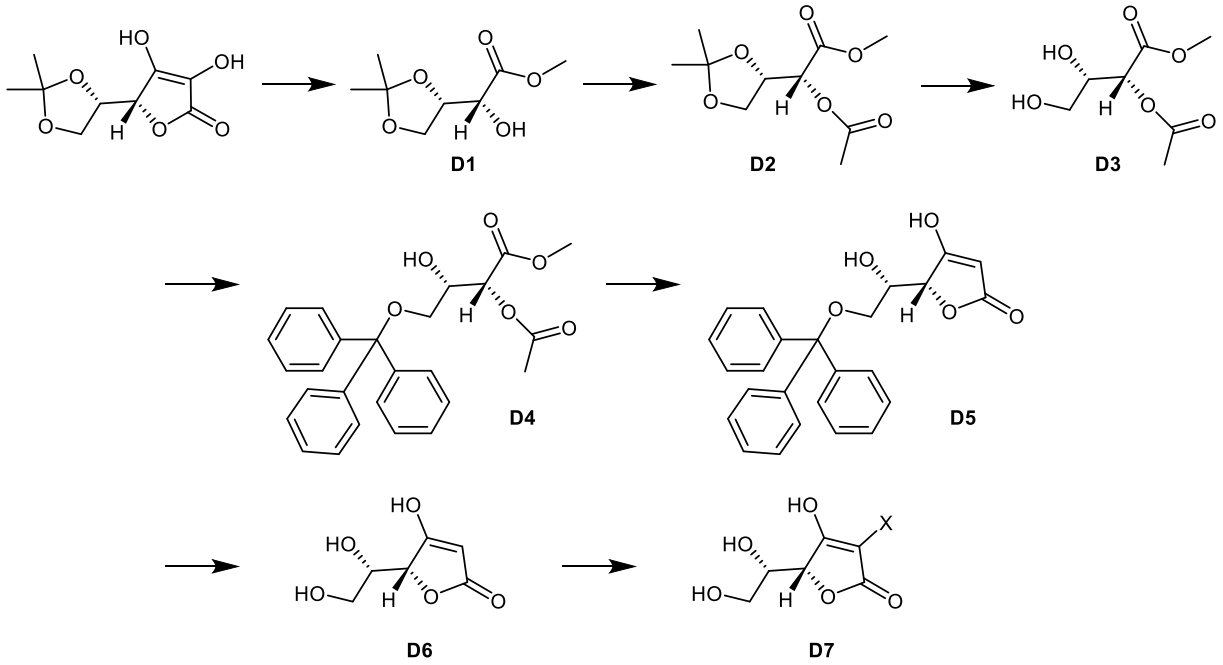

Scheme 37. General procedure for synthesis of 2-halo-L-ascorbic acid.

The low yields observed in section **5.1.3** prompted considerations of alternate routes to direct arylation of **3**, and indeed a route utilising 2-halo-L-ascorbic acids was investigated.[181, 182] The route proceeds via a peroxide mediated ring opening followed by methylation (**D1**), acetylation (**D2**), and addition of a trityl group to the unmasked diol (**D4**). Ring reformation (**D5**) is then accomplished before acidic removal of the trityl group to afford 2-deoxy-L-ascorbic acid (**D6**). This is converted to the corresponding halo-acid by utilisation of the appropriate N-X-succinimide (N-iodo-succinimide for an iodo species for example). An illustration of this is shown in **Scheme 37**.

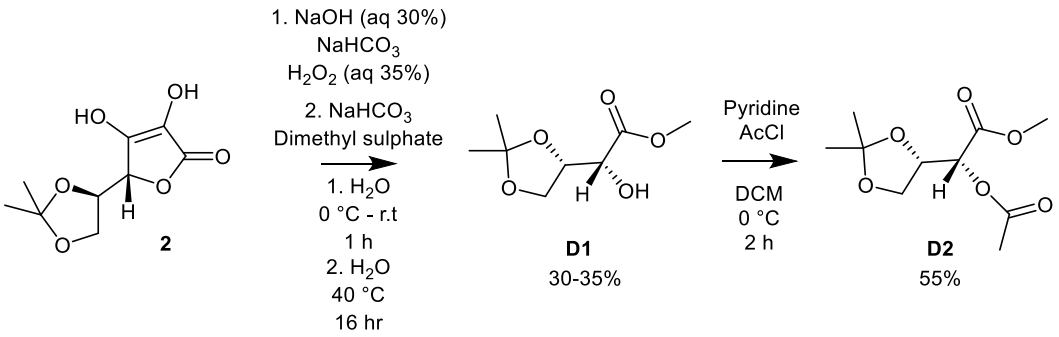

Scheme 38. Formation of **D1** and **D2.**

The formation of **D1** was achieved in reasonable yield (typically between 30 – 35%), in repeat reactions the reaction was done in a larger flask and base added at a slower rate to reduce the risk of excess gas evolution on addition of $NaHCO_3$. Acetylation to form **D2** was achieved in good yield (55%).

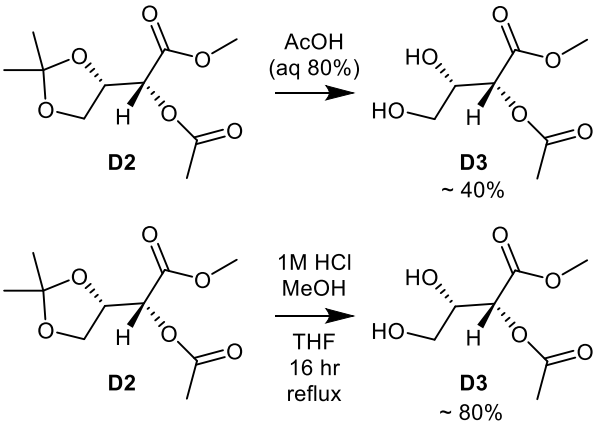

Scheme 39. Conditions to form **D3**

Formation of **D3** using AcOH (aq 80%) did not give complete conversion from the acetal to the diol. Purification was an issue as the pure product was unobtainable after silica gel column chromatography. To maximise the desired product moving forward, conditions used to form **7.15** were utilised – a 1:1:1 mixture of MeOH:THF:1M HCl (aq) heated at reflux overnight – which afforded no starting material seen in the mass spec. The crude product was taken forward to form **D4**.

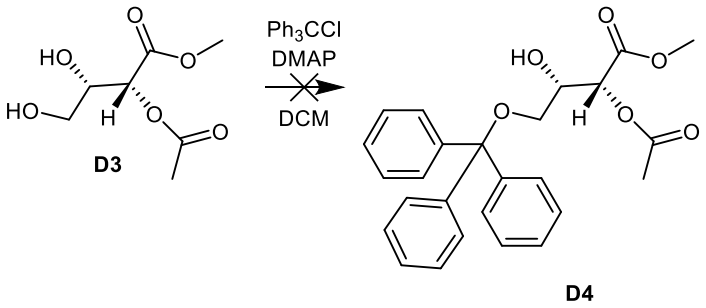

Scheme 40. Failed conditions for trityl addition.[182]

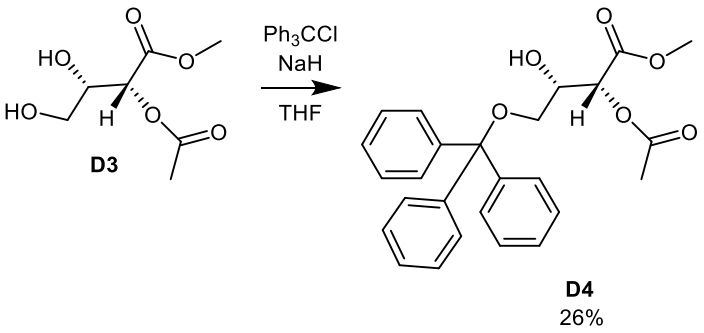

Scheme 41. Successful tritylation conditions.

Literature conditions advised using trityl chloride and DMAP to produce the trityl ether **D4**, but this gave no product as seen in the mass spec when the reaction was performed at room temperature or reflux. The bulky intermediate formed using these reagents is presumed to be too hindered for nucleophilic attack and as such a different procedure was used, involving sodium hydride left to stir with **D3** for half an hour before dropwise addition of trityl chloride and stirring overnight. This afforded the desired product albeit in low yield (26%). As this route had given poor yields throughout, it was discarded for continued work.

5.0 InhA Inhibition Assay

5.1 Background to Inhibition Assay

Compound inhibition data was obtained using an isolated enzyme assay first developed by former Thomas group member Aneesa Ahmed and optimised by current group member Malcolm Lamont (PhD student, University of Nottingham).[183]

The assay works on the basis of the commonly used method of comparing enzyme activity in the presence and absence of the proposed inhibitor, measured using an approach applicable to the Michaelis-Menten model. This model allows an observation of enzyme activity relating to first order kinetics by monitoring the conversion of substrate to product

over a set period of time – in this case the conversion of NADH to NAD^+ as monitored by UV absorbance at 340 nm, which decreases upon NADH oxidation.

$$E + S \rightleftharpoons [ES] \longrightarrow E + P$$

Equation 1. First order Michaelis-Menten schematic. E = Enzyme. S = Substrate, P = Product

The *in vivo* function of the InhA enzyme is to reduce a thioester in the growing mycolic acid chain by donating a hydride from NADH. This step is commonly adapted for assay work by replacing the natural thioester with *trans*-2-octenoyl CoA which acts as a mimic.[183] The full structure of *trans*-2-octenoyl CoA is shown in section **6.3** with a shortened version depicted in **Scheme 42** taking part in the reduction which comprises the assay.

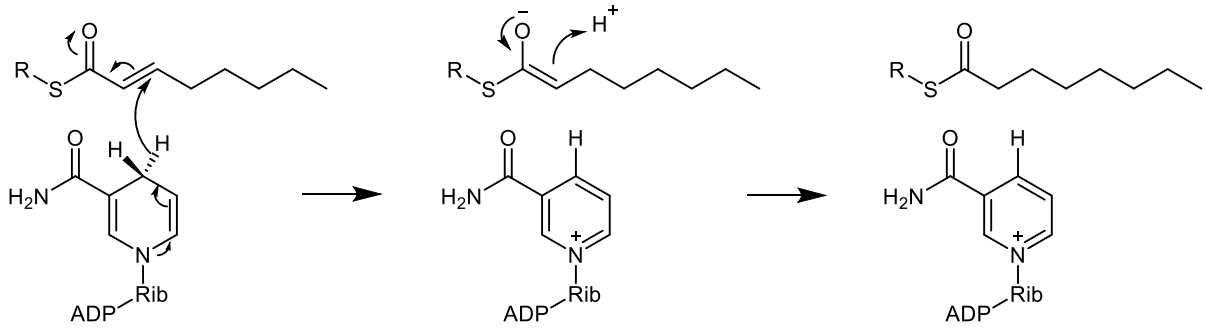

Scheme 42. Schematic showing reduction of *trans*-2-octenyl CoA by NADH.

5.2 Materials

All materials were purchased from Sigma-Aldrich apart from the following items. InhA constructs were prepared as stated in section **6.4** and thawed on ice prior to use. NADH sodium salt was purchased from PanReac AppliChem and a 10 mM stock solution freshly prepared in 30 mM PIPES buffer at pH 6.8 (assay buffer) on ice before dilution dependant on the required concentration for the assay which was run on the same day. *trans*-2-

Octenoyl CoA was prepared by Tom Armstrong (University Of Nottingham) according to a procedure outlined in section **6.3** and stored dry in 3.56 mg aliquots at -80 °C prior to use. Aliquots were thawed on ice and dissolved in 800 µL assay buffer on the day of use to give a 5 mM stock solution. Concentrations were confirmed before testing with a TECAN spark plate reader for both NADH (340 nM) and substrate (254 nM) with respective extinction coefficients of 6220 $M^{-1}cm^{-1}$ and 20,400 $M^{-1}cm^{-1}$ and addition volumes adjusted according to results.

All compounds tested were prepared in stock solution of 100 mM in DMSO. **NITD-564** (section **3.8**) was used as a control to reference % inhibition and IC_{50} against. Compounds selected for testing were diluted in assay buffer to a concentration of 500 µM, giving a final percentage of 0.5% v/v DMSO or 1M NaOH. The final assay volume is 100 µL.

5.3 OcCoA synthesis

This was synthesised by Tom Armstrong (PhD student, University of Nottingham). The route followed to synthesise the InhA substrate *trans*-2-octenoyl CoA was previously described by Aneesa Ahmed (originally from literature).[183-185] CoA trilithium salt was dissolved in water along with potassium carbonate and the apparatus covered in foil to avoid light interference. *Trans*-2-octenoic acid, THF, and PyBOP were added and the reaction stirred in the dark for 16 hours under a nitrogen atmosphere. Organic solvent was then removed under reduced pressure and water removed by lyophilisation. The resulting crude material was twice purified by semi-prep HPLC on an Eclipse XDB-C18 column (9.4 x 150 mm; 5 µm) with a gradient of ammonium acetate buffer (pH: 5.9, 20 mM) (buffer A) and acetonitrile (buffer B). Percentages are given as composition of buffer A. Variable wavelength detector set at 254 nm. The method was as follows: 0 – 1 mins (100%), 1 – 2 mins (90%), 2 – 5 mins (80%), 5 – 15 mins (75 -> 70%), 15 – 17 mins (70 -> 5%), 17 – 18 mins (5%), 18 – 19 mins (5 – 100%), 19 – 21 mins (100%). Fractions containing pure product were pooled and lyophilised three times to ensure complete

removal of water and residual ammonium acetate which was confirmed via hydrogen NMR). The combined product was split into 3.56 mg fractions and stored at -80 °C prior to use.

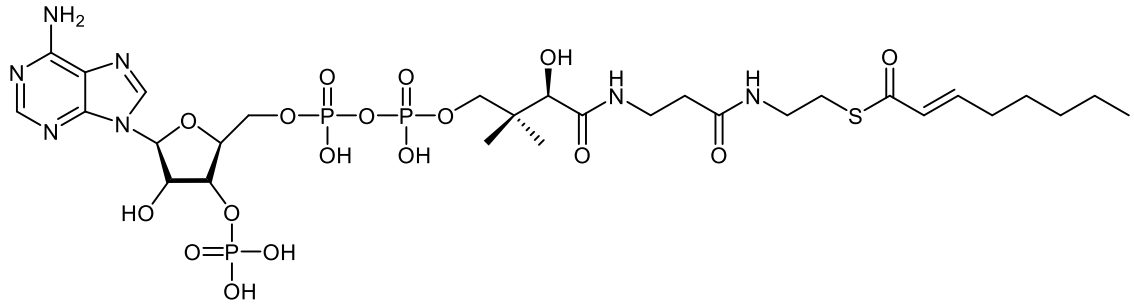

Figure 67. Assay substrate *trans*-2-octenoyl-CoA.

5.4 Protein Expression and Purification

Work in this section (**5.4**) to express and purify the protein was carried out by Malcolm Lamont (PhD student, University of Nottingham). The InhA:pET15a construct was kindly provided by Prof. Peter Tonge (Stony Brook University). A single colony from a BL21 InhA agar plate was grown overnight in 10 mL LB media containing 100 µg/mL ampicillin at 37 °C with 180 rpm shaking. Expression of InhA was induced with 1 mM IPTG in Luria Bertani (LB) broth (containing ampicillin 100 µg/mL) and grown at 30 °C for 6 hours until an OD_{600} of 0.6 - 0.7 was reached. The protein was isolated by cell lysis using sonication followed by centrifugation at 30,000 *g* for 30 min at 4 °C. Purification was performed using a Ni-affinity His-Trap 5 mL column (GE Healthcare). The column was washed with 150 mL binding buffer [Tris HCl (20 mM), NaCl (300 nM), imidazole (500 mM), pH 7.5] in a 0 – 100% gradient of the elution buffer. The protein was analysed with SDS-PAGE and then exchanged to a storage buffer (PIPES, 30 mM, pH 6.8) and concentrated to 10 mg/mL using a 10 kDa Amikon centrifugal filter (Millipore). Aliquots were mixed with 10% glycerol and stored at -80 °C. The molecular weight (29,806 Da), pI (6.10), and extinction

coefficient were determined using the ExPasy translate tool. The extinction coefficient 37.5 $mM^{-1}cm^{-1}$ at λ_{280} was used in calculation of the protein concentration.

5.5 Assay Conditions

In vitro enzyme inhibition studies were performed by Malcolm Lamont (PhD student, University of Nottingham). Compounds were screened at a concentration of 50 μM using the thermostated UV-Vis spectrophotometer (Tecan Sunrise) at 340 nm as detailed below.

The assay conditions were as follows for a 100 μL total volume: InhA (5 μL, 150 nM), NADH (10 -11 μL, 100 μM), OcCoA (9 – 11 μL, 400 μM), and compound (10 μL, 50 μM) made up to 100 μL with buffer (pH 6.8, 30 mM PIPES).

Percentage inhibition was calculated by ascertaining loss of activity vs absence of the inhibitor with the equation shown below. Positive controls were ran alongside every row of 12 reactions and each compound was assessed in duplicate.

$$\left(\frac{[V_0 - V_1]}{V_0} \right) * 100$$

Equation 2. Calculation of % inhibition where V_0 corresponds to rate in absence of inhibitor and V_1 corresponds to rate in presence of inhibitor ($\mu M.min^{-1}$)

Compounds showing promising inhibition data at 50 μM would be subjected to further testing to ascertain IC_{50} values. This would be accomplished by running the assay with varying concentrations of inhibitor from 0 – 50 μM before plotting reaction rates against the log of concentrations used. This would give a curve at which the IC_{50} can be determined by inputting data into the GraphPad Prism four-parameter model shown below.

$$Y = \text{Bottom} + \frac{(\text{Top} - \text{Bottom})}{\left(1 + 10^{((\log IC_{50} - X) * \text{HillSlope})}\right)}$$

Equation 3. IC_{50} four parameter model. Top and bottom corresponds to respective velocity plateau's, Hillslope corresponds to incline of slope, IC_{50} corresponds to concentration where the response is hallway between top and bottom

The positive control used was hydroxypyridone **NITD-564** (discussed in section **3.8**) which has an IC_{50} literature value of 0.59 μM.[84, 136] Experimental IC_{50} obtained using this control was 0.75 μM, correlating with literature value of 0.59 μM.[84] IC_{50} graph for **NITD-564** is shown below in **Figure 68**. As the obtained IC_{50} value is within threefold range of the literature value the assay can be seen as working accurately. Percentage inhibition studies alongside tested compounds at 50 μM resulted in 70.9% inhibition seen for **NITD-564**, the highest data point in **Figure 68** was taken at 10 μM so this correlates well with the plateau seen in **Figure 68**.

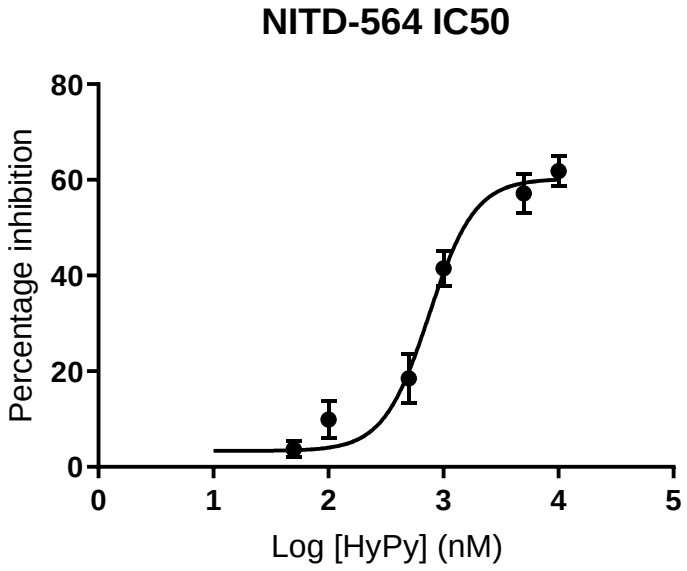

Figure 68. IC_{50} curve for NITD-564 inhibition of InhA.

Percentage inhibition studies were carried out on the benzyl ethers synthesised in section 4**.3.3** as well as target **A** with none of the compounds trialled showing activity against InhA. To better understand this, molecular modelling should be undertaken so as to direct future generations of compounds.

6.0 Conclusions and Future Work

To summarise, work has been carried out to synthesise targets **A** and **B** as well as benzyl analogues of **A**. These compounds can be considered a "second generation" of inhibitors as compared to the 4-hydroxy-2-pyridones synthesised by Manjunatha *et al* as they share a similar pharmacophore.[84] The synthesis of target **A** was completed as well as nine benzyl derivatives, with varied substituents (alkyl, halogen, ether) and alkyl chain lengths (n = 1,2) as well as non-substituted products. The production of a *p*-nitrobenzyl compound was achieved but could not be isolated. Progress has been made in the production of target **B** but difficulty in removal of the protecting group on the 3-*O* position as well as alkene formation from the acetal protected diol has hindered progress with this route.
The benzyl ethers synthesised in section **4.3.3** (compound **7.43** omitted due to loss of compound) were screened for activity against InhA in an isolated enzyme assay at 50 μM to first determine their percentage inhibition, promising results would then direct future synthesis and strongly inhibiting compounds would be taken forward for IC_{50} calculation.

Unfortunately none of the compounds tested showed any inhibitory activity towards InhA and so molecular modelling should be used to better understand these results and to direct future iterations of potential inhibitors.

Future work may involve a library of compounds based on the designs shown below in **Figure 69**, as the introduction of nitrogen in the core would better mimic the compounds described in section **2.8**. The removal of the 2-*O* to allow direct attachment of alkyl/aryl groups to the core would also better mimic the compounds described in section **2.8**.

Completion of target **B** synthesis will aid understanding of L-ascorbic acid based compounds inhibition of InhA.

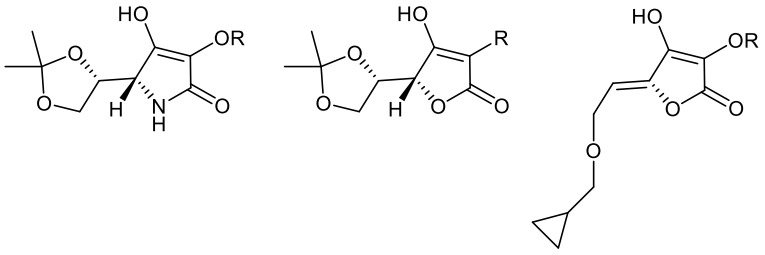

Figure 69. Proposed compounds for future work.

7.0 Experimental

Commercial reagent grade solvents purchased from Fischer Scientific® were used for all reactions, anhydrous DMF was purchased from Sigma Aldrich®. All reagents were purchased from either Sigma Aldrich®, Alfa Aesar®, Merck Chemicals Ltd, or Strem Chemicals Inc.

All ^{1}H NMR spectra were recorded on a BrukerTM AV400 spectrometer at 400 MHz, and at ambient temperature. All spectra were recorded relative to residual solvent peaks. Spectra were recorded in solutions of deuterated chloroform ($CDCl_3$, δsolv = 7.26), deuterated water (D_2O, δsolv = 4.79), or deuterated DMSO ($(CD_3)_2SO$, δsolv = 2.50). All ^{13}C NMR spectra were recorded on a Bruker™ AV400 spectrometer at 100 MHz and at ambient temperature. All spectra were recorded relative to residual solvent peaks. Spectra were recorded in solutions of deuterated chloroform ($CDCl_3$, δsolv = 77.1), or deuterated DMSO ($(CD_3)_2SO$, δsolv = 39.5). Chemical shifts (δ) are given in parts per million (ppm) and J values in Hertz (Hz). Multiplets are designated by the following notations: singlet (s), doublet (d), triplet (t), quartet (q), double doublet (dd), double triplet (dt), multiplet (m).

High resolution mass spectroscopy (HRMS) was recorded on a BrukerTM microTOF, an orthogonal Time of Flight instrument with electrospray ionisation (ESI, both positive and

negative ion) sources as indicated. Values of mass to charge ratio (m/z), are given to four decimal places. The mass of the counter ions are H^+ 1.0078, and Na^+ 22.9898.

Thin layer chromatography was performed using Merck Kieselgel 60 F254 plates. Visualisation was by UV light and staining with phosphomolybdic acid (PMA) with heating. Flash column chromatography was performed using Merck Kieselgel silica gel 60 Å, 230-400 mesh, 40-63 μm, unless otherwise stated.

Melting points were determined on a Stuart Scientific melting point apparatus (SMP3), values are given in degrees Celsius (°C) and are uncorrected.

Optical rotations were obtained at ambient temperature using a Bellingham and Stanley Ltd ADP 220 polarimeter.

7.1 5,6-*O*-Isopropylidene-L-ascorbic acid (2) [166]

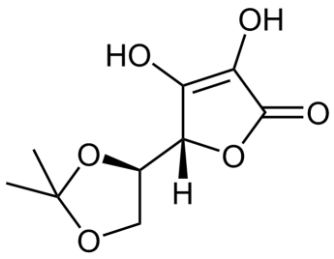

L-ascorbic acid (10.0 g, 56.8 mmol) was suspended in acetone (120 mL) and acetyl chloride (4.4 mL, 61.9 mmol) added in one portion. The suspension was heated at 40 °C for 2.5 hours before being cooled to -10 °C and filtered, washed with cold acetone (2 x 50 mL) then left to dry. Pure product obtained as off white solid (11.6 g, 54.0 mmol, 95%). $[\alpha]_D$ + 25.50 (*c* 1.00 in H_2O); ^1H NMR (400 MHz, D_2O) δ ppm 1.31 (s, 6 H, CH_3), 4.11 (dd, 1H, *J* = 9 Hz, 5 Hz CH_2), 4.25 (dd, 1H, *J* = 9 Hz, 7.4 Hz, CH_2), 4.53 (m, 1H, CH), 4.85, (d, 1H, *J* = 2.1 Hz); ^{13}C NMR (100 MHz, D_2O) δ ppm 24.0 (CH_3), 24.7 (CH_3), 65.0 (CH_2), 73.1

(CH), 75.8 (CH), 110.8 (C_{quat}), 117.8 (C_{quat}), 155.7 (C_{quat}), 173.4 (C_{quat}); HRMS (ESI) required for $C_9H_{12}O_6Na^+$ 239.0532 observed $C_9H_{12}O_6Na^+$ 239.0529

7.2 3-*O*-Methyl-5,6-*O*-isopropylidene-L-ascorbic acid (3) [168]

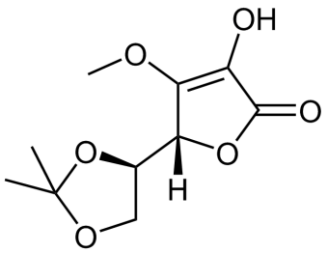

5,6-*O*-Isopropylidene-L-ascorbic acid (1.00 g, 4.63 mmol) was dissolved in methanol (30 mL) before addition of triethylamine (0.7 mL, 4.63 mmol). Solution was stirred for 30 minutes before DMS (0.42 mL, 4.63 mmol) was added in one portion and allowed to stir for 16 hours at room temperature. Methanol was removed under reduced pressure and the residue left was dissolved in brine (30 mL) and extracted with ethyl acetate (3 x 30 mL). Organic layers were combined and dried over sodium sulfate. After filtration, solvent was removed under reduced pressure and residue purified by column chromatography using ethyl acetate:hexane as eluent (1:3) to give a yellow viscous oil (0.3 g, 1.30 mmol, 28%). $[\alpha]_D$ + 14.50 (*c* 2.00 in MeOH) (lit + 14.16 *c* 2 MeOH)[168]; ^{1}H NMR (400 MHz, $CDCl_3$) δ ppm 1.40 (s, 3 H, CH_3), 1.42 (s, 3 H, CH_3), 3.86 (s, 3H, OMe), 4.11 (m, 2H, CH_2), 4.30 (m, 1H, CH), 4.53 (d, 1H, *J* = 3.2 Hz, CH); ^{13}C NMR (100 MHz, $CDCl_3$) δ ppm 25.5 (CH_3), 25.8 (CH_3), 59.5 (OMe) 65.3 (CH_2), 74.0 (CH), 74.6 (CH), 110.8 (C_{quat}), 123.0 (C_{quat}), 156.0 (C_{quat}), 169.0 (C_{quat}); HRMS (ESI) required for $C_{10}H_{14}O_6Na^+$ 253.0688 observed $C_{10}H_{14}O_6Na^+$ 253.0682

7.3 3-*O*-Ethyl-5,6-*O*-isopropylidene-L-ascorbic acid (4) [170]

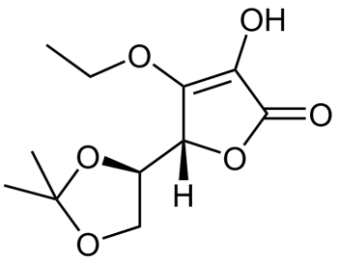

5,6-*O*-Isopropylidene-L-ascorbic acid (7.32 g, 33.8 mmol) was dissolved in DMSO (50 mL) before addition of sodium hydrogen carbonate (4.30 g, 33.8 mmol). Solution was stirred for 30 minutes before iodoethane (4.35 mL, 33.8 mmol) was added in one portion and allowed to stir for 16 hours at 50°C. Solution was neutralised with HCl (1M) and diluted with brine (50 mL) then extracted with ethyl acetate (3 x 100 mL). Organic layers were combined and washed several times with brine then dried over sodium sulfate. After filtration, solvent was removed under reduced pressure and residue purified by column chromatography using ethyl acetate:hexane as eluent (1:3) to give a yellow viscous oil (5.11 g, 20.9 mmol, 62%). $[\alpha]_D$ + 20.88 (*c* 0.30 in $CHCl_3$) (lit + 21.44 *c* 0.30 $CHCl_3$)[168]; ^{1}H NMR (400 MHz, $CDCl_3$) δ ppm 1.42 (m, 9 H, CH_3), 4.06 (dd, 1H, *J* = 9 Hz, 5 Hz CH_2), 4.16 (dd, 1H, *J* = 9 Hz, 7.4 Hz, CH_2), 4.28 (dt, 1H, *J* = 8.5 Hz, 3.8 Hz, CH), 4.55 (m, 3H, CH_2); ^{13}C NMR (100 MHz, $CDCl_3$) δ ppm 15.0 (CH_3) 25.5 (CH_3), 26.0 (CH_3), 65.0 (CH_2), 68.1 (OCH_2) 74.0 (CH), 76.0 (CH), 110.8 (C_{quat}), 118.0 (C_{quat}), 148.0 (C_{quat}), 171.4 (C_{quat}); HRMS (ESI) required for $C_{11}H_{16}O_6Na^+$ 267.0845 observed $C_{11}H_{16}O_6Na^+$ 267.0842

7.4 2-*O*-Phenyl-3-*O*-Methyl-5,6-*O*-isopropylidene-L-ascorbic acid (45) [168]

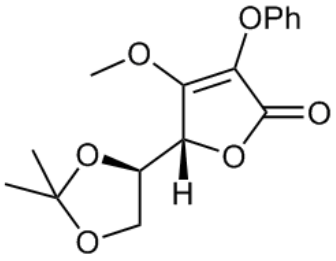

3-O-Methyl-5,6-O-Isopropylidene-L-ascorbic acid (500 mg, 2.20 mmol) was dissolved in acetone (50 mL) and potassium carbonate (300 mg, 2.20 mmol) added. After addition of diphenyliodonium triflate (930 mg, 2.20 mmol) suspension turned yellow. Suspension was heated to reflux overnight. Solvent was removed under reduced pressure and residue dissolved in water (100 mL) then extracted with ethyl acetate (3 x 100 mL). Organic layers combined and dried over magnesium sulfate before filtration. Solvent removed under reduced pressure and crude material purified by column chromatography using petroleum ether:ethyl acetate as eluent (4:1) to give the pure material as a dark yellow oil (200 mg, 0.58 mmol, 28%). ^{1}H NMR (400 MHz, $CDCl_3$) δ ppm 1.39 (s, 3 H, CH_3), 1.46 (s, 3 H, CH_3), 3.87 (s, 3H, OMe) 4.09 (m, 2H, CH_2), 4.42 (m, 1H, CH), 5.03 (m, 1H, CH), 7.33 (m, 5H, CH_{Ar}) ; ^{13}C NMR (100 MHz, $CDCl_3$) δ ppm 25.5 (CH_3), 26.4 (CH_3), 56.7 (OMe) 65.3 (CH_2), 74.4 (CH), 75.1 (CH), 110.0 (C_{quat}), 123.0 (C_{quat}), 128.0 (C_{Ar}), 129.0 (C_{Ar}), 129.8 (C_{Ar}), 156.7 (C_{quat}), 172.0 (C_{quat}); HRMS (ESI) required for $C_{16}H_{19}O_6$ 307.1176 observed $C_{16}H_{19}O_6$ 307.1176

7.5 2-*O*-Phenyl-3-*O*-Ethyl-5,6-*O*-isopropylidene-L-ascorbic acid (5) [168]

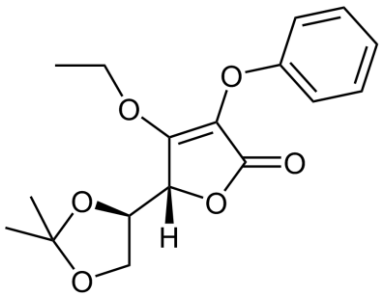

3-O-Ethyl-5,6-O-Isopropylidene-L-ascorbic acid (50 mg, 0.22 mmol) was dissolved in acetone (5 mL) and potassium carbonate (30 mg, 0.22 mmol) added. After addition of diphenyliodonium triflate (93 mg, 0.22 mmol) suspension turned yellow. Suspension was heated to reflux overnight. Solvent was removed under reduced pressure and residue dissolved in water (30 mL) then extracted with ethyl acetate (3 x 30 mL). Organic layers combined and dried over magnesium sulfate before filtration. Solvent removed under reduced pressure and crude material purified by column chromatography using petroleum ether:ethyl acetate as eluent (4:1) to give the pure material as a dark yellow oil (21.2 mg, 0.062 mmol, 30%). ^{1}H NMR (400 MHz, $CDCl_3$) δ ppm 1.42 (m, 9 H, CH_3), 4.06 (dd, 1H, *J* = 9 Hz, 5 Hz CH_2), 4.16 (dd, 1H, *J* = 9 Hz, 7.4 Hz, CH_2), 4.28 (dt, 1H, *J* = 8.5 Hz, 3.8 Hz, CH), 4.55 (m, 2H, CH_2), 7.29 (m, 5H, CH_{Ar}); ^{13}C NMR (100 MHz, $CDCl_3$) δ ppm 15.0 (CH_3) 25.5 (CH_3), 26.0 (CH_3), 65.0 (CH_2), 68.5 (O-CH_2), 74.0 (CH), 76.0 (CH), 110.8 (C_{quat}), 118.0 (C_{quat}), 129.1 (CH_{Ar}), 129.7 (CH_{Ar}), 129.9 (CH_{Ar}), 148.0 (C_{quat}), 171.4 (C_{quat}); HRMS (ESI) required for $C_{17}H_{21}O_6$ 320.1333 observed $C_{17}H_{21}O_6$ 321.1333

7.6 (Z)-4-Ethoxy-5-(2-hydroxyethylidene)-3-phenoxyfuran-2(5H)-one (20) [169]

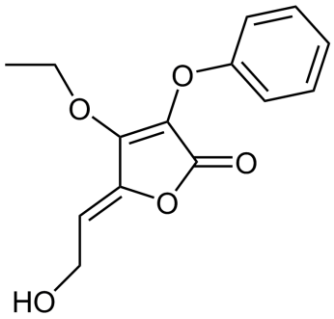

2-O-Phenyl-3-O-ethyl-5,6-O-isopropylidene-L-ascorbic acid (1.04 g, 3.25 mmol) was dissolved in THF (50 mL) and DBU added (0.5 mL 50 mol%) dropwise. Reaction was heated to reflux overnight. Solvent removed under reduced pressure and residue dissolved in ethyl acetate (20 mL) then washed with brine (3 x 20 mL). Dried over sodium sulfate then filtered. Solvent removed under reduced pressure and crude material purified by column chromatography using petroleum ether:ethyl acetate (3:1) as eluent to give the pure compound as a dark yellow oil (0.17 g, 0.65 mmol, 20%). HRMS (ESI) required for $C_{14}H_{15}O_5$ 263.0914 observed $C_{14}H_{15}O_5$ 263.0937

7.8 Diphenyliodonium triflate (46) [173]

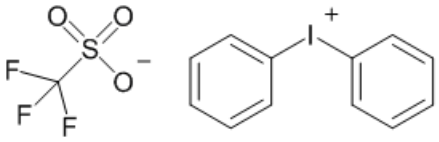

m-Chloroperbenzoic acid (1.00g, 5.12 mmol, 1.1 eq) and iodobenzene (0.5 ml, 4.65 mmol, 1 eq) were dissolved in DCM (30 mL) in a sealed tube. Benzene (0.5 mL, 5.12 mmol, 1.1 eq) was added and the solution cooled to 0°C before dropwise addition of trifluromethylsulfonic acid (1.3 mL, 14.0 mmol, 3 eq). Solution turned dark yellow. Solution was allowed to warm to room temperature and was stirred for one hour. Solvent removed under reduced pressure and solid suspended in diethyl ether (70 mL). Flask stored in freezer for 30 minutes to ensure complete precipitation. Suspension filtered and washed with cold diethyl ether (3 x 30 mL) to give pure product as a white solid (1.90 g, 4.42 mmol, 95%). mp 178 – 180 °C (lit value 177 – 179 °C)[186]; ^{1}H NMR (400 MHz, DMSO) δ ppm 7.55 (t, 4H, *J* = 8 Hz, ArCH), 7.68 (t, 2H, *J* = 8 Hz, ArCH), 8.26 (d, 4H, *J* = 8 Hz, ArCH); ^{13}C NMR (100 MHz, DMSO) δ ppm 117.0 (ArCH), 122.8 (CF_3), 132.2 (ArCH), 132.5 (ArC), 135.6 (ArCH); MS (ESI) required for $C_{12}H_{10}I^+$ 280.9822 observed $C_{12}H_{10}I^+$ 280.9822

7.9A 3-O-Allyl-5,6-O-isopropylidene-L-ascorbic acid (7a) [170]

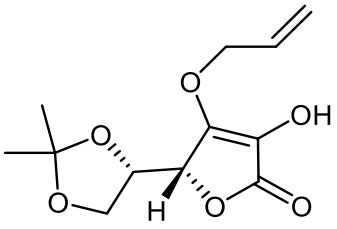

5,6-O-Isopropylidene-L-ascorbic acid (9.00 g, 41.6 mmol) was dissolved in DMSO (60 mL) before addition of sodium hydrogen carbonate (3.50 g, 41.6 mmol). Solution was stirred for 30 minutes before allyl bromide (3.50 mL, 41.6 mmol) was added in one portion and allowed to stir for 16 hours at 50°C. Solution was neutralised with HCl (1M) and diluted with brine (50 mL) then extracted with ethyl acetate (3 x 100 mL). Organic layers were combined and washed several times with brine then dried over sodium sulfate. After filtration, solvent was removed under reduced pressure and residue purified by column chromatography using ethyl acetate:hexane as eluent (1:3) to give a yellow viscous oil (3.00 g, 11.7 mmol, 28%). ^{1}H NMR (400 MHz, $CDCl_3$) δ ppm 1.41 (s, 3H, CH_3), 1.42 (s, 3H, CH_3), 4.01 – 4.24 (m, 2H, CH_2), 4.55 (td, 1H, *J* = 6.9, 2 Hz, CH), 4.59 (d, 1H, *J* = 3.8 Hz, CH), 4.98 (d, 2H, *J* = 5.8 Hz, CH_2), 5.21 – 5.33 (m, 2H, alkene CH_2), 5.97 – 6.07 (m, 1H, alkene CH); ^{13}C NMR (100 MHz, $CDCl_3$) δ ppm 25.6 (CH_3), 25.9 (CH_3), 65.3 (CH_2), 71.9 (CH_2), 74.2 (CH), 75.6 (CH), 110.3 (C_{quat}), 119.1 (alkene CH_2), 123.0 (alkene CH), 132.1 (C_{quat}), 148.1 (C_{quat}), 172.7 (C_{quat}); HRMS (ESI) required for $C_{12}H_{17}O_6Na^+$ 278.0845 observed $C_{12}H_{17}O_6Na^+$ 279.0841

7.9B (5R)-3-Allyl-5-((S)-2,2-dimethyl-1,3-dioxolan-4-yl)-3-hydroxyfuran-2,4(3H,5H)-dione (7b) [170]

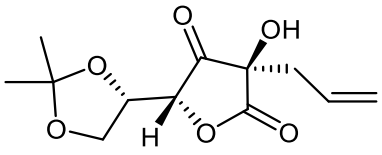

^{1}H NMR (400 MHz, $CDCl_3$) δ ppm 1.36 (s, 3H, CH_3), 1.38 (s, 3H, CH_3), 2.68 (d, 2H, *J* = 8 Hz, CH_2), 4.03 – 4.23 (m, 2H, CH_2), 4.29 (td, 1H, *J* = 6.7, 3.7, CH), 4.68 (d, 1H, *J* = 2 Hz, CH), 5.33 – 5.50 (m, 2H, alkene CH_2), 5.65 – 5.76 (m, 1H, alkene CH); ^{13}C NMR (100 MHz, $CDCl_3$) δ ppm 25.3 (CH_3), 25.5 (CH_3), 39.7 (CH_2), 64.9 (CH_2), 72.3 (C_{quat}), 74.5 (CH), 81.5 (CH), 111.3 (C_{quat}), 119.2 (alkene CH_2), 127.6 (alkene CH), 170.9 (C_{quat}), 205.6 (C_{quat})

7.10 3-O-Benzyl-5,6-O-isopropylidene-L-ascorbic acid (9) [170]

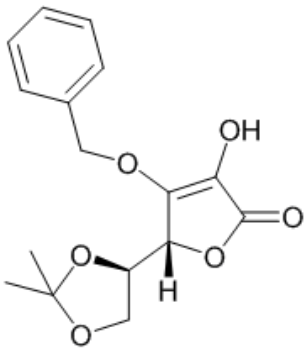

5,6-O-Isopropylidene-L-ascorbic acid (5.00 g, 23.11 mmol) was dissolved in DMSO (50 mL) before addition of sodium hydrogen carbonate (1.94 g, 23.11 mmol). Solution was stirred for 30 minutes before benzyl bromide (4.20 mL, 23.11 mmol) was added in one portion and allowed to stir for 16 hours at 50 °C. Solution was neutralised with HCl (1M) and diluted with brine (50 mL) then extracted with ethyl acetate (3 x 100 mL). Organic

layers were combined and washed several times with brine then dried over sodium sulfate. After filtration, solvent was removed under reduced pressure and residue purified by column chromatography using ethyl acetate:hexane as eluent (1:3) to give a yellow viscous oil (2.90 g, 9.48 mmol, 41%). $[\alpha]_D$ + 35.90 (*c* 1.00 in MeOH) (lit + 36.20 *c* 1.00 MeOH)[175]; ^{1}H NMR (400 MHz, $CDCl_3$) δ ppm 1.38 (s, 3 H, CH_3), 1.42 (s, 3 H, CH_3), 4.10 (m, 2H, CH_2), 4.29 (m, 1H, CH), 4.60 (d, 1H, *J* = 3.8 Hz, CH), 5.53 (s, 2 H, CH_2), 7.37 (m, 5H, CH_{Ar}); ^{13}C NMR (100 MHz, $CDCl_3$) δ ppm 25.7 (CH_3), 25.9 (CH_3), 65.3 (CH_2), 73.8 (CH_2) 74.0 (CH), 74.7 (CH), 110.3 (CH), 110.8 (C_{quat}), 121.3 (C_{quat}), 128.1 (CH_{Ar}), 128.7 (CH_{Ar}). 129.0 (CH_{Ar}), 134.0 (C_{Ar}), 156.5 (C_{quat}), 169.2 (C_{quat}); HRMS (ESI) required for $C_{16}H_{19}O_6$ 307.1176 observed $C_{16}H_{19}O_6$ 307.1171

7.11 3-O-TBDMS-5,6-O-isopropylidene-L-ascorbic acid (12) [178]

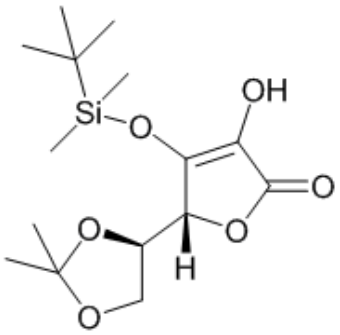

5,6-O-Isopropylidene-L-ascorbic acid (5.00 g, 23.15 mmol) was dissolved in DCM (40 mL) before addition of triethylamine (3.00 mL, 23.15 mmol). Solution was stirred for 30 minutes before being cooled to 0 °C. A solution of TBDMSCl (3.86 g, 23.15 mmol) in DCM (12 mL) was added in one portion and allowed to stir for 2 hours at room temperature. Solvent was removed under reduced pressure and the residue left was dissolved in brine (75 mL) and extracted with ethyl acetate (3 x 75 mL). Organic layers were combined and dried over sodium sulfate. After filtration, solvent was removed under reduced pressure and residue purified by column chromatography using ethyl acetate:hexane as eluent

(1:3) to give a yellow viscous oil (3.00 g, 9.09 mmol, 39%). ^{1}H NMR (400 MHz, $CDCl_3$) δ ppm 0.26 (s, 6 H, $SiCH_3$), 0.99 (s, 9 H, Si^tBu), 1.39 (s, 3 H, CH_3), 1.44 (s, 3 H, CH_3), 4.07 (m, 2H, CH_2), 4.48 (m, 1H, CH), 4.77 (d, 1H, *J* = 3.8 Hz, CH); ^{13}C NMR (100 MHz, $CDCl_3$) δ ppm -4.4 ($SiCH_3$), 25.1 (CH_3), 25.7 (Si^tBu), 25.9 (CH_3), 64.8 (CH_2), 73.5 (CH), 75.1 (CH), 110.6 (C_{quat}), 119.1 (C_{quat}), 154.1 (C_{quat}), 169.6 (C_{quat}); HRMS (ESI) required for $C_{15}H_{26}O_6SiNa^+$ 353.1396 observed $C_{15}H_{26}O_6SiNa^+$ 353.1397

7.12 3-O-TES-5,6-O-isopropylidene-L-ascorbic acid (15) [178]

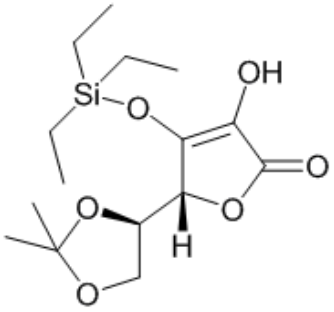

5,6-O-Isopropylidene-L-ascorbic acid (6.50 g, 30.95 mmol) was dissolved in DCM (56 mL) before addition of triethylamine (4.16 mL, 30.95 mmol). Solution was stirred for 30 minutes before being cooled to 0 °C. TESCl (4.00 g, 30.95 mmol) (12 mL) was added in one portion and allowed to stir for 2 hours at room temperature. Solvent was removed under reduced pressure and the residue left was dissolved in brine (75 mL) and extracted with ethyl acetate (3 x 75 mL). Organic layers were combined and dried over sodium sulfate. After filtration, solvent was removed under reduced pressure and residue purified by column chromatography using ethyl acetate:hexane as eluent (1:3) to give a yellow oil (1.00 g, 3.03 mmol, 9.75%). ^{1}H NMR (400 MHz, $CDCl_3$) δ ppm 0.54 (q, 6 H, *J* = 8.0, $SiCH_2$), 0.96 (t, 9 H, *J* = 8.2, $SiCH_3$), 1.28 (s, 3 H, CH_3), 1.44 (s, 3 H, CH_3), 4.14 (m, 2H, CH_2), 4.48 (m, 1H, CH), 4.75 (d, 1H, *J* = 3.8 Hz, CH); ^{13}C NMR (100 MHz, $CDCl_3$) δ ppm 6.6 ($SiCH_2$), 6.8 ($SiCH_3$), 25.1 (CH_3), 25.9 (CH_3), 64.8 (CH_2), 73.5 (CH), 75.1 (CH), 110.6

(C_{quat}), 119.1 (C_{quat}), 154.1 (C_{quat}), 169.6 (C_{quat}); HRMS (ESI) required for $C_{15}H_{27}O_6Si$ 331.1571 observed $C_{15}H_{27}O_6Si$ 331.1568

7.13 3-O-Methoxymethyl ether-5,6-O-isopropylidene-L-ascorbic acid (17) [168]

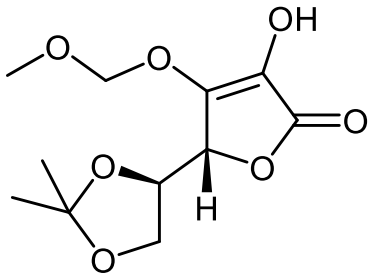

5,6-*O*-Isopropylidene-L-ascorbic acid (35.0 g, 162 mmol) was dissolved in acetone (500 mL) before addition of potassium carbonate (16.0 g, 162 mmol). Solution was stirred for 30 minutes before a solution of MOMCl (10.8 mL, 162 mmol) in acetone (50 mL) was added dropwise and allowed to stir for 5 hours at 60 °C. Solution was neutralised with HCl (1M) and diluted with brine (50 mL) then extracted with ethyl acetate (3 x 100 mL). Organic layers were combined and washed several times with brine then dried over sodium sulfate. After filtration, solvent was removed under reduced pressure and residue purified by column chromatography using ethyl acetate:hexane as eluent (1:3) to give a yellow viscous oil (25 g, 96.2 mmol, 59.5%). $[\alpha]_D$ + 13.05 (*c* 2.00 in MeOH) (lit + 13.00 *c* 2.00 MeOH)[187]; ^{1}H NMR (400 MHz, $CDCl_3$) δ ppm 1.35 (s, 3 H, CH_3), 1.36 (s, 3 H, CH_3), 3.59 (s, 3H, CH_3-O-CH_2-O), 4.10 (m, 2H, CH_2) 4.31 (m, 1H, CH), 4.61 (d, 1H, *J* = 3.8 Hz, CH) 5.36 (s, 2H, O-CH_2-O); ^{13}C NMR (100 MHz, $CDCl_3$) δ ppm 25.6 (CH_3), 25.8 (CH_3), 57.3 (CH_3), 65.2 (CH_2), 73.8 (CH), 74.7 (CH), 96.1 (CH_2), 110.4 (C_{quat}), 120.9 (C_{quat}), 145.8 (C_{quat}), 169.3 (C_{quat}); HRMS (ESI) required for $C_{11}H_{17}O_7$ 261.0969 observed $C_{11}H_{17}O_6$ 261.0966

7.14 3-O-Methoxymethyl ether-2-O-phenyl-5,6-O-isopropylidene-L-ascorbic acid (18) [168]

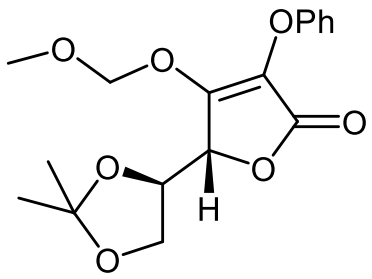

7.13 (10.0 g, 38.4 mmol) was dissolved in acetone (300 mL) and potassium carbonate (10.0 g, 38.4 mmol) added. After addition of diphenyliodonium triflate (16.5 g, 38.4 mmol) suspension turned yellow. Suspension was heated to reflux overnight. Solvent was removed under reduced pressure and residue dissolved in water (200 mL) then extracted with ethyl acetate (3 x 200 mL). Organic layers combined and dried over magnesium sulfate before filtration. Solvent removed under reduced pressure and crude material purified by column chromatography using petroleum ether:ethyl acetate as eluent (4:1) to give the pure material as a dark yellow oil (3.00 g, 8.93 mmol, 24%). ^{1}H NMR (400 MHz, $CDCl_3$) δ ppm 1.44 (s, 3 H, CH_3), 1.47 (s, 3 H, CH_3), 3.56 (s, 3 H, CH_3-O-CH_2), 4.22 (m, 2 H, CH_2), 4.50 (m, 1H, CH), 4.77 (d, 1H, *J* = 3.8 Hz, CH), 5.38 (s, 2H, O-CH_2-O) 7.07 (m, 3H, ArCH) 7.34 (m, 2H ArCH); ^{13}C NMR (100 MHz, DMSO) δ ppm 24.8 (2 x CH_3), 56.3 (CH_3), 74.7 (CH), 99.1 (CH_2), 115.3 (ArCH), 122.5 (ArCH), 129.9 (ArCH), 157.2 (ArC), 164.5 (C_{quat}), 172.2 (C_{quat}); HRMS (ESI) required for $C_{17}H_{20}O_7Na^+$ 359.1101 observed $C_{17}H_{20}O_7Na^+$ 359.1104

7.15 2-O-Phenyl-isopropylidene-L-ascorbic acid (19) [188]

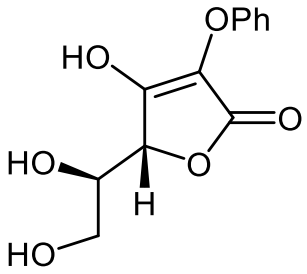

A solution of **7.14** (290 mg, 0.863 mmol) in methanol (3 mL), 1 M HCl (3 mL) and THF (3 mL) was heated for 16 hours at reflux. The solvent was removed in vacuo, and the residue was diluted with EtOAc. The organic layer was washed with water, dried, and concentrated to give the crude product as a yellow oil (200 mg, 92%) which was used without further purification. HRMS (ESI) required for $C_{12}H_{13}O_6$ 253.0707 observed $C_{12}H_{13}O_6$ 253.0710

7.16 2-O-Phenyl-5,6-O-isopropylidene-L-ascorbic acid (A) [166]

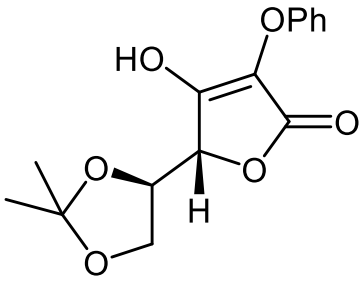

7.15 (200 mg, 0.79 mmol) was dissolved in acetone (2 mL) and acetyl chloride (0.1 mL, 7.9 mmol) added in one portion. The solution was heated at 40 °C for 2.5 hours before solvent was removed in vacuo. Pure product obtained as yellow oil. (200 mg, 0.68 mmol, 86%); ^{1}H NMR (400 MHz, DMSO) δ ppm 1.30 (s, 3H, CH_3), 1.32 (s, 3H, CH_3), 3.96 – 4.08 (m, 2H, CH_2), 4.21 – 4.26 (m, 1H, CH), 4.31 (d, 1H, *J* = 4 Hz, CH), 6.88 – 7.27 (m, 5H, ArCH); ^{13}C NMR (100 MHz, $CDCl_3$) δ ppm 26.1 (CH_3), 26.6 (CH_3), 65.4, (CH_2), 75.5 (CH),

77.1 (CH), 108.9 (C_{quat}), 115.2 (ArCH), 121.1 (ArCH), 129.5 (ArCH), 129.7 (ArC); HRMS (ESI) required for $C_{15}H_{17}O_6^+$ 293.0950 observed $C_{15}H_{17}O_6^+$ 293.1002

7.17 5,6-O-Tosyl-L-ascorbic acid (38) [176]

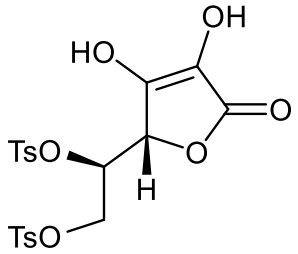

To a solution of L-ascorbic acid (10.0 g, 56.8 mmol) in dry pyridine (60.0 mL) at 0 °C was added tosyl chloride (20.0 g, 113.6 mmol) in portions and the mixture stirred under inert atmosphere for 36 hours at room temperature. Solution was diluted with DCM (300 mL) and washed with 3M aq HCl (3 x 300 mL) followed by brine (300 mL) and dried over sodium sulfate. Evaporation of solvent unveiled the title compound as a puffy dark brown resin. (9.90 g, 20.4 mmol, 35.9%). $[\alpha]_D$ + 33.15 (*c* 1.00 in MeOH); ^{1}H NMR (400 MHz, $CDCl_3$) δ ppm 2.42 (s, 6 H, CH_3), 4.15 (m, 2H, CH_2), 4.33 (m, 1H, CH), 4.82 (d, 1H, *J* = 4Hz, CH), 7.33 (m, 4H, ArCH), 7.81 (m, 4H, ArCH); ^{13}C NMR (100 MHz, $CDCl_3$) δ ppm 21.7 (Ts-CH_3), 21.8 (Ts-CH_3), 67.0 (CH_2), 69.1 (CH), 75.2 (CH), 113.2 (C_{quat}), 128.0 (ArCH), 128.9 (ArCH), 130.1 (ArCH), 130.1 (Ar-CH), 130.7 (ArC_{quat}), 131.9 (ArC_{quat}), 145.5 (ArC-CH_3), 146.8 (ArC-CH_3), 164.1 (C_{quat}), 166.9 (C_{quat}) ; HRMS (ESI) required for $C_{20}H_{21}O_{10}S_2$ 485.0571 observed $C_{20}H_{21}O_{10}S_2$ 485.0567

7.18 3-O-Ethyl-5,6-O-tosyl-L-ascorbic acid (22) [170]

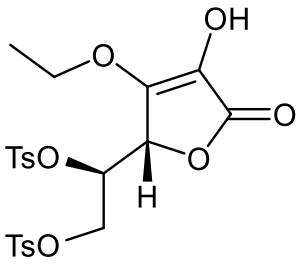

7.17 (9.90 g, 20.4 mmol) was dissolved in DMSO (30 mL) before addition of sodium hydrogen carbonate (2.60 g, 20.4 mmol). Solution was stirred for 30 minutes before iodoethane (2.63 mL, 20.4 mmol) was added in one portion and allowed to stir for 16 hours at 50 °C. Solution was neutralised with HCl (1M) and diluted with brine (50 mL) then extracted with ethyl acetate (3 x 100 mL). Organic layers were combined and washed several times with brine then dried over sodium sulfate. After filtration, solvent was removed under reduced pressure and residue purified by column chromatography using ethyl acetate:hexane as eluent (1:2) to give a yellow viscous oil (3.31 g, 6.46 mmol, 31.6%). ^{1}H NMR (400 MHz, $CDCl_3$) δ ppm 1.40 (t, *J* = 7.1 Hz, 3H, CH_3), 2.44 (s, 3H, $ArCH_3$), 2.45 (s, 3H, $ArCH_3$), 4.07 – 4.17 (m, 1H, CH), 4.20 – 4.24 (m, 2H, CH_2), 4.61 (q, *J* = 7.0 Hz, 2H, CH_2), 4.74 (d, *J* = 1.8 Hz, 1H, CH), 7.34 – 7.37 (m, 4H, ArCH), 7.79 (d, *J* = 8.4 Hz, ArCH), 7.90 (d, *J* = 8.3 Hz, ArCH); ^{13}C NMR (100 MHz, $CDCl_3$) δ ppm 14.9 (CH_3), 21.7 ($ArCH_3$), 21.8 ($ArCH_3$), 67.4 (CH_2), 68.9 (CH), 69.8 (CH_2), 75.2 (CH), 112.9 (C_{quat}), 128.0 (ArCH), 128.9 (ArCH), 129.9 (ArCH), 130.1 (ArCH), 132.2 (ArC), 145.4 (ArC), 146.3 (ArC), 163.0 (C_{quat}), 166.8 (C_{quat}); HRMS (ESI) required for $C_{22}H_{25}O_{10}S_2$ 513.0811 observed $C_{22}H_{25}O_{10}S_2$ 513.0884

7.19 2-*O*-Phenyl-3-*O*-*e*thyl-L-ascorbic acid (25) [188]

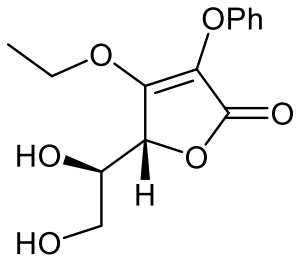

5 mL of 2N HCl was added to a suspension of **7.5** (3.00 g, 9.37 mmol) in MeOH (10 mL) and THF (10 mL). The mixture was stirred overnight at room temperature before solvent removed under reduced pressure to give the product as a yellow oil with no need for further purification. (1.72 g, 6.14 mmol, 65.5%). ^{1}H NMR (400 MHz, $CDCl_3$) δ ppm 1.33 (t, 3 H, *J* = 8 Hz, CH_3), 3.95 (m, 1 H, CH), 4.15 (m, 2 H, CH_2), 4.54 (q, 2 H, *J* = 8 Hz, CH_2-CH_3), 4.68 (d, 1H, *J* = 4 Hz, CH), 7.06 (m, 3H, ArCH), 7.34 (m, 2H, ArCH); ^{13}C NMR (100 MHz, $CDCl_3$) δ ppm 15.2 (CH_3), 63.4 (CH_2), 68.2 (CH_2), 70.0 (CH), 76.0 (CH), 115.1 (ArCH), 117.1 (C_{quat}), 121.4 (ArCH), 129.9 (ArCH), 145.5 (C_{quat}), 157.0 (ArC), 168.4 (C_{quat}); HRMS (ESI) required for $C_{14}H_{17}O_6$ 281.1020 observed $C_{14}H_{17}O_6$ 281.1020

7.20 2-*O*-Phenyl-3-*O*-*e*thyl-5,6-*O*-tosyl-L-ascorbic acid (23) [176]

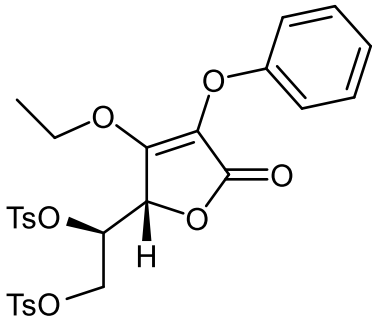

To a solution of **7.19** (2.09 g, 7.46 mmol) in dry pyridine (10 mL) at 0 °C was added tosyl chloride (3.00 g, 15.7 mmol) in portions and the mixture stirred under inert atmosphere for 36 hours at room temperature. Solution was diluted with DCM (100 mL) and washed with 3M aq HCl (3 x 100 mL) followed by brine (100 mL) and dried over sodium sulfate. Evaporation of solvent unveiled the crude material as a dark brown oil which was purified by column chromatography using ethyl acetate:hexane as eluent (1:3) to give a yellow oil. (900 mg, 1.49 mmol, 20%). ^{1}H NMR (400 MHz, $CDCl_3$) δ ppm 1.44 (m, 3H, CH_3), 2.49 (s, 6H, $ArCH_3$), 5.32 (s, 1H, CH), 7.04 (m, 3H, ArCH), 7.28 (m, 6H, ArCH), 7.83 (m, 2H, ArCH), 7.95 (m, 2H, ArCH); HRMS (ESI) required for $C_{28}H_{32}O_{10}S_2$ 606.1462 observed $C_{28}H_{32}NO_{10}S_2$ 606.1485

7.21 2-*O*-Phenyl-3-*O*-*e*thyl-5,6-*O*-mesyl-L-ascorbic acid (27) [176]

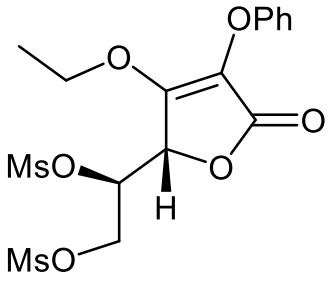

To a solution of **7.19** (1.09 g, 3.89 mmol) in dry pyridine (7 mL) at 0 °C was added mesyl chloride (0.6 mL, 7.79 mmol) in portions and the mixture stirred under inert atmosphere for 36 hours at room temperature. Solution was diluted with DCM (70 mL) and washed with 3M aq HCl (3 x 100 mL) followed by brine (100 mL) and dried over sodium sulfate. Evaporation of solvent unveiled the crude material as a dark brown oil which was purified by column chromatography using ethyl acetate:hexane as eluent (1:3) to give a yellow oil. (380 mg, 0.87 mmol, 22.4%). ^{1}H NMR (400 MHz, $CDCl_3$) δ ppm 1.39 (t, 3H, *J* = 7 Hz, CH_3), 3.14 (s, 3H, CH_3), 3.19 (s, 3H, CH_3), 4.55 (m, 4H, 2 x CH_2), 4.99 (d, 1H, *J* = 4 Hz, CH), 5.29 (m, 1H, CH), 7.08 (m, 3H, ArCH), 7.35 (m, 2H, ArCH); ^{13}C NMR (100 MHz, $CDCl_3$) δ ppm 15.0 (CH_3), 37.9 (CH_3), 39.2 (CH_3), 66.8 (CH_2), 69.5 (CH_2), 73.4 (CH), 74.0 (CH), 115.2 (ArCH), 118.0 (C_{quat}), 123.4 (ArCH), 130.0 (ArCH), 156.6 (C_{quat}), 158.2 (ArC_{quat}), 166.9 (C_{quat}); HRMS (ESI) required for $C_{16}H_{21}O_{10}S_2$ 437.0571 observed $C_{16}H_{21}O_{10}S_2$ 437.0572

7.22 (Z)-2-(3-Ethoxy-5-oxo-4-phenoxyfuran-2(5H)-ylidene)-N,N,N-triethylethan-1-aminium (31) [169]

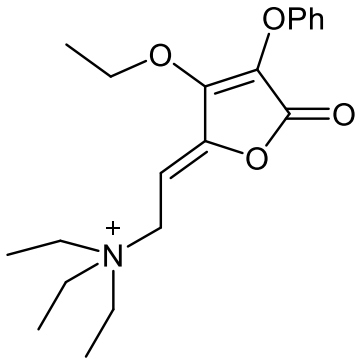

7.21 (270 mg, 0.619 mmol) was dissolved in dry THF (3 mL) under inert atmosphere before triethylamine (0.1 mL, 1 eq) was added in one portion and the resulting solution stirred at room temperature overnight. Analysis indicated reaction was incomplete so reaction was heated at reflux for a further 16 hours. Solvent was evaporated under reduced pressure and the resulting oil dissolved in ethyl acetate (10 mL) before being washed with water (3 x 10 mL), dried, and solvent evaporated to give the crude material as a dark yellow oil (108 mg, 0.313 mmol). This was taken forward without further purification. ^{1}H NMR (400 MHz, $CDCl_3$) δ ppm 1.40 (m, 12H, CH_3), 3.16 (q, 6H, *J* = 8 Hz, NCH_2), 4.22 (d, 2H, *J* = 8 Hz, CH_2), 4.51 (q, 2H, *J* = 4 Hz, CH_2), 5.59 (t, 1H, *J* = 8 Hz, CH), 7.02 (d, 2H, *J* = 8 Hz, ArCH), 7.13 (t, 1H, *J* = 8 Hz, ArCH), 7.37 (t, 2H, *J* = 8 Hz, ArCh); ^{13}C NMR (100 MHz, $CDCl_3$) δ ppm 8.6 (CH_3), 15.1 (CH_3), 46.2 (CH_2), 53.6 (CH_2), 69.2 (CH_2), 94.0 (CH_{alkene}), 115.5 (ArCH), 119.8 (C_{quat}), 123.9 (C_{quat}), 130.1 (ArCH), 149.0 (C_{alkene}), 151.3 (C_{quat}), 156.3 (ArCH), 162.0 (C_{quat}); HRMS (ESI) required for $C_{20}H_{28}O_4N$ 346.2018 observed $C_{20}H_{28}O_4N$ 346.2032

7.23 (Z)-5-(2-(Cyclopropylmethoxy)ethylidene)-4-ethoxy-3-phenoxyfuran-2(5H)-one (21) [176]

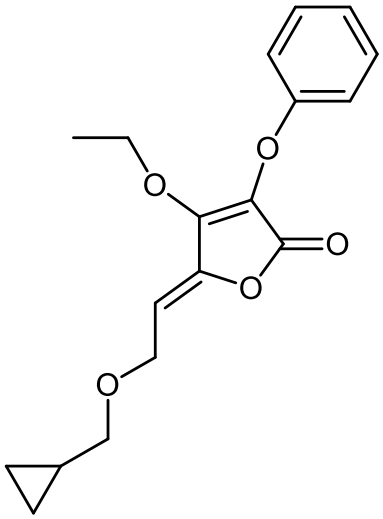

Cyclopropylmethanol (0.04 mL, 2 eq, 0.625 mmol) was dissolved in THF (2 mL) and NaH (60% in mineral oil) (24 mg, 0.625 mmol) added dropwise. The solution was stirred for 30 mins before being added dropwise to a solution of **7.22** (108 mg, 0.313 mmol) dissolved in THF (2 mL) (colour change from yellow to deep red). This was allowed to stir at room temperature for 16 hours (colour change to dark red) after which a further equivalent of cyclopropylmethanol/NaH/THF solution was added dropwise. After stirring for 72 hours solvent was removed under reduced pressure to give crude product. This was purified by silica gel column chromatography using hexane:ethyl acetate as eluent (3:1) to give the title compound as a clear oil (24.0 mg, 0.076 mmol, 24.2 %). ^{1}H NMR (400 MHz, $CDCl_3$) δ ppm 0.19 – 0.29 (m, 2H, CH_2), 0.54 – 0.63 (m, 2H, CH_2), 1.04 – 1.17 (m, 1H, CH), 1.34 – 1.40 (m, 3H, CH_3), 3.33 – 3.38 (m, 2H, CH_2), 4.34 (d, *J* = 7 Hz, 2H, CH_2), 4.41 – 4.48 (m, 2H, CH_2), 5.69 (t, *J* = 7 Hz, Alkene CH), 6.91 – 7.03 (m, 2H, ArCH), 7.04 – 7.18 (m, 1H, ArCH), 7.30 – 7.40 (m, 2H, ArCH); ^{13}C NMR (100 MHz, $CDCl_3$) δ ppm 3.0 (CH_2), 10.5 (CH), 15.2 (CH_3), 63.6 (CH_2), 68.3 (CH_2), 75.7 (CH_2), 105.3 (AlkCH), 115.2 (ArCH), 123.2 (ArCH), 129.9 (ArCH), 132.5 (C_{quat}), 142.4 (C_{quat}), 152.2 (C_{quat}), 156.8 (ArC), 163.7 (C_{quat}); MS (ESI) required for $C_{18}H_{20}O_5Na$ 339.1208 observed $C_{18}H_{20}O_5Na$ 339.1204

7.24 2-O-Benzyl-L-ascorbic acid (37) [188]

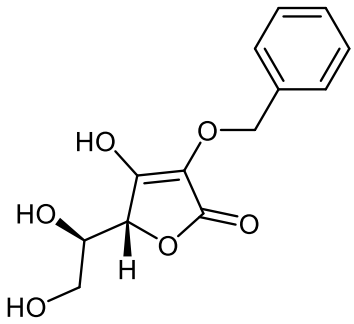

7.32 (1.00 g, 2.38 mmol) was dissolved in THF (5 mL) before addition of MeOH (5 mL) and 1M HCl (5 mL). This clear solution was stirred at room temperature overnight. Evaporation of the solvent afforded a clear oil which was used without any further purification. (390 mg, 1.46 mmol, 61.9%). $[\alpha]_D$ + 46.35 (*c* 1.00 in MeOH) (lit + 46.6 *c* 1 MeOH)[189]; ^{1}H NMR (400 MHz, DMSO) δ ppm 3.37 – 3.47 (m, 2H, CH_2), 3.69 (ddd, 1H*, J* = 7.75, 6.03, 1.42 Hz, CH), 4.80 (d, 1H*, J* = 1.40 Hz, CH), 5.34 – 5.53 (m, 2H, CH_2), 7.27 – 7.48 (m, 5H, ArCH); ^{13}C NMR (100 MHz, DMSO) δ ppm 62.1 (CH_2), 68.9 (CH), 72.4 (CH_2), 75.1 (CH), 120.0 (C_{quat}), 128.2, (ArCH), 128.7 (ArCH), 128.9 (ArCH), 137.0 (ArC), 150.9 (C_{quat}), 170.8 (C_{quat}); MS (ESI) required for $C_{13}H_{15}O_6^+$ 267.0863 observed $C_{13}H_{15}O_6^+$ 267.0870

7.25 2,3-O-Bis(2-cyclohexylethoxy)-5,6-isopropylidene-L-ascorbic acid (47) [179]

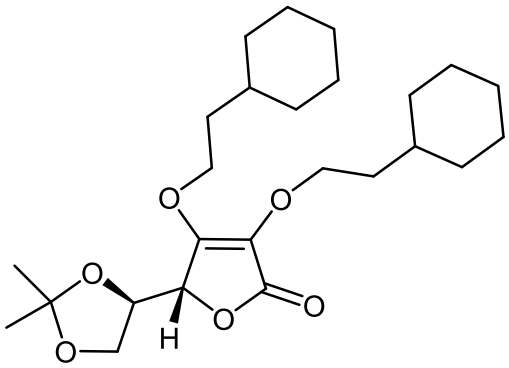

A solution of 2 equiv of potassium tert-butoxide (^{t}BuOK) (104 mg, 0.926 mmol) in dry DMSO/THF (3:2) (1.00 mL) was added dropwise to a solution of 5,6-O-Isopropylidene-L-ascorbic acid (100 mg, 0.463 mmol) in the same solvent (1.00 mL) at -10 °C under nitrogen to produce a bright yellow solution with an orange tint. The stirring of the mixture was continued for about 2 min after which 1.1 equiv of bromoethylcyclohexane (96.7 mg, 0.509 mmol) in the same solvent (1.00 mL) was added dropwise over a period of 3 min with stirring continued for an additional 5 min at -10 °C. The cooling bath was removed, and the reddish orange reaction solution was stirred for 3 h at room temperature. The reaction mixture was quenched with a cold solution of 0.25 M HCl (2.00 mL) and extracted with ethyl acetate (3 x 10 mL). The organic layer was dried over Na_2SO_4, and the solvents were removed under reduced pressure. The product was purified by silica gel column chromatography using hexane:ethyl acetate (3:1) to give the pure product as a clear oil (50.5 mg, 25%, 0.116 mmol). ^{1}H NMR (400 MHz, $CDCl_3$) δ ppm 0.87 – 1.04 (m, 6H, CH + CH_2), 1.13 – 1.33 (m, 8H, CH_2), 1.38 (s, 3H, CH_3), 1.42 (s, 3H, CH_3), 1.59 – 1.67 (m, 4H, CH_2), 1.69 – 1.79 (m, 8H, CH_2), 4.00 – 4.22 (m, 4H, CH_2), 4.25 – 4.29 (td, 1H, *J* = 6.7, 2.8 Hz, CH), 4.47 – 4.49 (m, 2H, CH_2), 4.40 – 4.41 (d, *J* = 4 Hz, CH); ^{13}C NMR (100 MHz, $CDCl_3$) δ ppm 25.6 (CH_3), 25.9 (CH_3), 26.2 (CH_2), 26.3 (CH_2), 26.4 (CH_2), 26.5 (CH_2), 33.1 (CH_2), 33.2 (CH_2), 33.3 (CH_2), 33.3 (CH_2), 34.3 (CH), 34.4 (CH), 36.8 (CH_2), 37.2 (CH_2), 65.3 (CH_2), 70.4 (CH_2), 70.5 (CH_2), 74.2 (CH), 74.6 (CH), 110.2 (C_{quat}), 121.9

(C_{quat}), 155.9 (C_{quat}), 169.3 (C_{quat}); MS (ESI) required for $C_{25}H_{41}O_6^+$ 437.2898 observed $C_{25}H_{41}O_6^+$ 437.2916

7.26 2,3-O-Bis(*para*-iodobenzyl)-5,6-isopropylidene-L-ascorbic acid (48) [179]

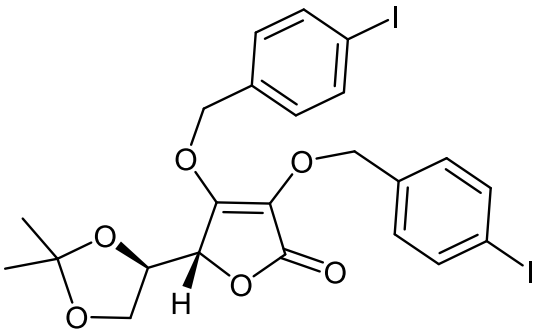

A solution of 2 equiv of potassium tert-butoxide (^{t}BuOK) (104 mg, 0.926 mmol) in dry DMSO/THF (3:2) (1.00 mL) was added dropwise to a solution of 5,6-O-Isopropylidene-L-ascorbic acid (100 mg, 0.463 mmol) in the same solvent (1.00 mL) at -10 °C under nitrogen to produce a bright yellow solution with an orange tint. The stirring of the mixture was continued for about 2 min after which 1.1 equiv of 1-(bromomethyl)-4-iodobenzene (150.7 mg, 0.509 mmol) in the same solvent (1.00 mL) was added dropwise over a period of 3 min with stirring continued for an additional 5 min at -10 °C. The cooling bath was removed, and the reddish orange reaction solution was stirred for 3 h at room temperature. The reaction mixture was quenched with a cold solution of 0.25 M HCl (2.00 mL) and extracted with ethyl acetate (3 x 10 mL). The organic layer was dried over Na_2SO_4, and the solvents were removed under reduced pressure. The product was purified by silica gel column chromatography using hexane:ethyl acetate (3:1) to give the pure product as a clear oil (72.5 mg, 22%, 0.112 mmol). ^{1}H NMR (400 MHz, $CDCl_3$) 1.39 (s, 3H, CH_3), 1.41 (s, 3H CH_3), 4.03 – 4.17 (m, 2H, CH_2), 4.29 (td, 1H, *J* = 6.8, 2.7 Hz, CH), 4.56 (d, 1H, *J* = 2.7 Hz, CH), 4.99 – 5.08 (m, 2H, CH_2), 5.11 – 5.19 (m, 2H, CH_2), 6.97 (d, 2H, *J* = 8.3 Hz, ArCH), 7.12 (d, 2H, *J* = 6.8 Hz, ArCH), 7.70 – 7.73 (m, 4H, ArCH); ^{13}C

NMR (100 MHz, $CDCl_3$) δ ppm 25.7 (CH_3), 25.9 (CH_3), 65.3 (CH_2), 77.8 (CH_2), 77.9 (CH_2), 73.6 (CH), 75.5 (CH), 94.5 (ArCH), 94.5 (ArCH), 110.4 (C_{quat}), 121.2 (Ar_{quat}), 129.4 (ArCH), 130.8 (ArCH), 134.9 (ArC), 135.6 (ArC), 137.8 (ArCH), 137.8 (ArCH), 156.1 (ArC_{quat}), 168.8 (ArC_{quat})

7.27 2,3-O-Bis(*para*-isopropylbenzyl)-5,6-isopropylidene-L-ascorbic acid (49) [179]

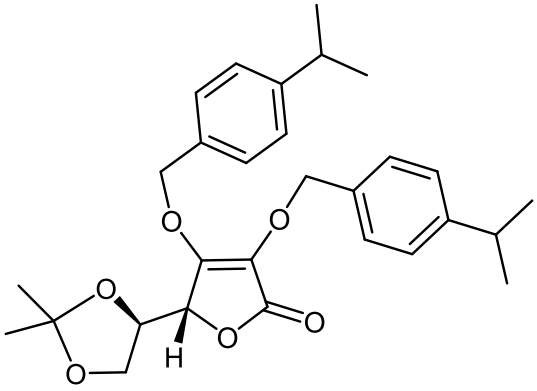

A solution of 2 equiv of potassium tert-butoxide (^tBuOK) (104 mg, 0.926 mmol) in dry DMSO/THF (3:2) (1.00 mL) was added dropwise to a solution of 5,6-O-Isopropylidene-L-ascorbic acid (100 mg, 0.463 mmol) in the same solvent (1.00 mL) at -10 °C under nitrogen to produce a bright yellow solution with an orange tint. The stirring of the mixture was continued for about 2 min after which 1.1 equiv of 1-(bromomethyl)-4-isopropylbenzene (107.8 mg, 0.509 mmol) in the same solvent (1.00 mL) was added dropwise over a period of 3 min with stirring continued for an additional 5 min at -10 °C. The cooling bath was removed, and the reddish orange reaction solution was stirred for 3 h at room temperature. The reaction mixture was quenched with a cold solution of 0.25 M HCl (2.00 mL) and extracted with ethyl acetate (3 x 10 mL). The organic layer was dried over Na_2SO_4, and the solvents were removed under reduced pressure. The product was purified by silica gel column chromatography using hexane:ethyl acetate (3:1) to give the pure product as a clear oil (73.3 mg, 30%, 0.153 mmol). ^1H NMR (400 MHz, $CDCl_3$) 1.25

– 1.29 (m, 12H, CH_3), 1.39 (s, 3H, CH_3), 1.43 (s, 3H, CH_3), 2.83 – 3.02 (m, 2H, CH), 3.95 – 4.14 (m, 2H, CH_2), 4.25 (td, 1H, *J* = 6.8, 3.3 Hz, CH), 4.54 (d, 1H, *J* = 3.3 Hz, CH), 4.96 – 5.29 (m, 4H, CH_2), 7.09 – 7.38 (m, 8H, ArCH); ^{13}C NMR (100 MHz, $CDCl_3$) δ ppm 23.9 (CH_3), 24.0 (CH_3), 25.7 (CH_3), 26.0 (CH_3), 33.9 (CH), 65.3 (CH_2), 73.6 (CH_2), 73.8 (CH_2), 74.1 (CH), 74.7 (CH), 110.3 (C_{quat}), 121.2 (C_{quat}), 126.7 (ArCH), 128.2 (ArCH), 129.4 (ArCH), 132.8 (ArC), 133.4 (ArC), 149.5 (ArC), 149.7 (ArC), 156.8 (C_{quat}), 169.2 (C_{quat}); HRMS (ESI) required for $C_{29}H_{37}O_6^+$ 481.2585 observed $C_{29}H_{37}O_6^+$ 481.2585

7.28 3–*O*-TBDMS, 2-*O*-ethylcyclohexyl, 5,6-*O*-isopropylidene-L-ascorbic acid (50) [178]

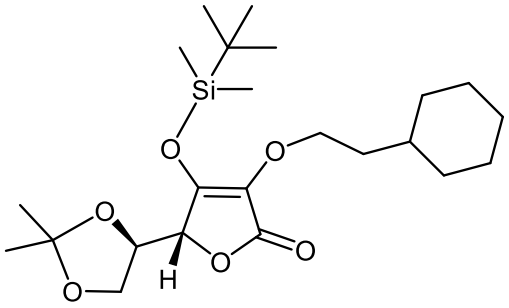

7.11 (182.5 mg, 553.0 μM) was dissolved in DCM (5 mL) before addition of triethylamine (0.6 mL) in one portion. The solution was allowed to stir at room temperature for 30 minutes before addition of a solution of (2-bromoethyl)cyclohexane (105.6 mg, 553.0 μM) in DCM (4 mL) in one portion. This was allowed to stir at room temperature for 16 hours before solvent was removed under reduced pressure. The resulting yellow oil was re-dissolved in ethyl acetate (5 mL) and then washed with brine (3 x 5 mL). The organic layer was drier over sodium sulfate before being filtered, the filtrate was removed under reduced pressure. The resulting oil was purified by silica gel column chromatography using hexane:ethyl acetate (3:1) to give the pure product as a yellow oil (73 mg, 165.9 μM, 30 %). ^{1}H NMR (400 MHz, $CDCl_3$) δ ppm 0.29 (s, 3H, $SiCH_3$), 0.30 (s, 3H, $SiCH_3$), 0.97 (s, 9H, ^{t}Bu-Si), 1.38 (s, 3H, CH_3), 1.41 (s, 3H, CH_3), 1.45 – 1.81 (m, 13H, CH/CH_2), 4.00 – 4.09 (m, 2H, CH_2), 4.20 – 4.30 (td, *J* = 6.8, 3.5 Hz, 1H, CH), 4.44 – 4.55 (m, 3H, CH/CH_2);

^{13}C NMR (100 MHz, $CDCl_3$) δ ppm 25.7 (CH_3), 25.8 (^{t}BuSi), 25.9 (CH_2), 26.2 (CH_2), 26.4 (C_{quat}), 33.1 (CH_2), 33.2 (CH_2), 34.3 (CH), 37.0 (CH_2), 65.4 (CH_2), 70.0 (CH_2), 74.4 (CH), 74.7 (CH), 110.2 (C_{quat}), 119.4 (C_{quat}), 152.5 (C_{quat}), 169.8 (C_{quat}); HRMS (ESI) required for $C_{23}H_{41}O_6Si^+$ 441.2667 observed $C_{23}H_{41}O_6Si^+$ 441.2659

7.29 3–*O*-TBDMS, 2-*O*-ethylbenzyl, 5,6-*O*-isopropylidene-L-ascorbic acid (51) [178]

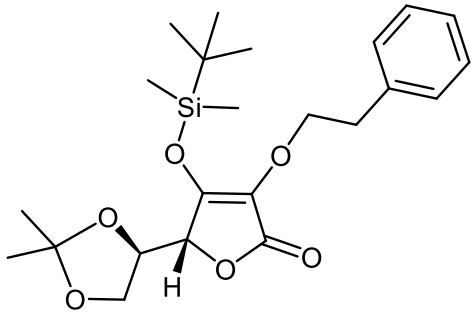

7.11 (76.4 mg, 231 μM) was dissolved in DCM (1.5 mL) before addition of triethylamine (0.2 mL) in one portion. The solution was allowed to stir at room temperature for 30 minutes before addition of a solution of (2-bromoethyl)benzene (42.5 mg, 231 μM) in DCM (1.5 mL) in one portion. This was allowed to stir at room temperature for 16 hours before solvent was removed under reduced pressure. The resulting yellow oil was re-dissolved in ethyl acetate (2 mL) and then washed with brine (3 x 2 mL). The organic layer was drier over sodium sulfate before being filtered, the filtrate was removed under reduced pressure. The resulting oil was purified by silica gel column chromatography using hexane:ethyl acetate (3:1) to give the pure product as a yellow oil (27.1 mg, 62.5 μM, 27%). ^{1}H NMR (400 MHz, $CDCl_3$) δ ppm 0.29 (s, 3H, $SiCH_3$), 0.29 (s, 3H, $SiCH_3$), 0.94 (s, 9H, ^{t}Bu-Si), 1.37 (s, 3H, CH_3), 1.40 (s, 3H, CH_3), 3.04 (t, *J* = 6.8 Hz, 2H, CH_2), 3.94 – 4.06 (m, 2H, CH_2), 4.17 (td, *J* = 6.7, 3.6 Hz, 1H, CH), 4.44 (d, *J* = 3.6 Hz, 1H, CH), 4.70 (t, *J* = 6.8 Hz, 2H, CH_2), 7.14 – 7.42 (m, 5H, ArCH); ^{13}C NMR (100 MHz, $CDCl_3$) δ ppm -4.1 ($SiCH_3$), -4.0 ($SiCH_3$), 25.7 (CH_3), 25.8 (^{t}BuSi), 25.9 (CH_3), 29.7 (C_{quat}), 36.1 (CH_2),

65.3 (CH_2), 71.9 (CH_2), 74.3 (CH), 74.7 (CH), 110.2 (C_{quat}), 119.8 (C_{quat}), 126.8 (ArCH), 128.6 (ArCH), 128.8 (ArCH), 137.2 (ArC), 152.0 (C_{quat}), 169.6 (C_{quat}); HRMS (ESI) required for $C_{23}H_{35}O_6Si^+$ 435.2197 observed $C_{23}H_{35}O_6Si^+$ 435.2191

7.30 3–*O*-TBDMS, 2-*O*-benzoxymethyl ether, 5,6-*O*-isopropylidene-L-ascorbic acid (52) [178]

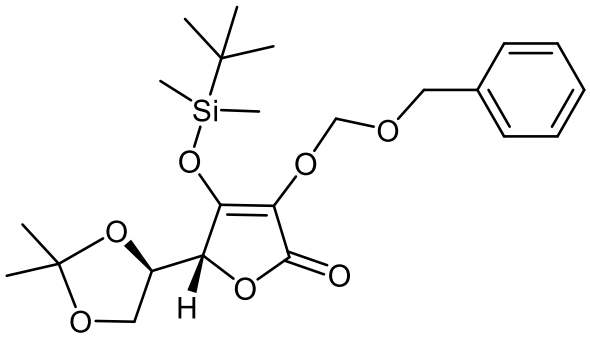

7.11 (30.1 mg, 91.0 μM) was dissolved in DCM (1 mL) before addition of triethylamine (0.01 mL) in one portion. The solution was allowed to stir at room temperature for 30 minutes before addition of a solution of ((chloromethoxy)methyl)benzene (14.2 mg, 91.0 μM) in DCM (1 mL) in one portion. This was allowed to stir at room temperature for 16 hours before solvent was removed under reduced pressure. The resulting yellow oil was re-dissolved in ethyl acetate (2 mL) and then washed with brine (3 x 2 mL). The organic layer was drier over sodium sulfate before being filtered, the filtrate was removed under reduced pressure. The resulting oil was purified by silica gel column chromatography using hexane:ethyl acetate (3:1) to give the pure product as a yellow oil (4.10 mg, 9.10 μM, 10%). ^{1}H NMR (400 MHz, $CDCl_3$) δ ppm 0.27 (s, 3H, $SiCH_3$), 0.30 (s, 3H, $SiCH_3$), 0.95 (s, 9H, ^{t}BuSi), 1.36 (s, 3H, CH_3), 1.40 (s, 3H, CH_3), 4.01 – 4.17 (m, 2H, CH_2), 4.28 (td, *J* = 6.8, 3.1 Hz, CH), 4.43 (d, *J* = 3.0 Hz, 1H, CH), 4.69 – 4.83 (m, 2H, CH_2), 5.51 – 5.62 (m, 2H, CH_2), 7.29 – 7.43 (m, 5H, ArCH); ^{13}C NMR (100 MHz, $CDCl_3$) δ ppm -4.15 ($SiCH_3$), -3.96 ($SiCH_3$), 18.3 (C_{quat}), 25.6 (CH_3), 25.8 (^{t}BuSi), 25.9 (CH_3), 65.3 (CH_2), 71.5 (CH_2), 73.9 (CH), 74.5 (CH), 94.1 (CH_2), 110.3 (C_{quat}), 121.1 (C_{quat}), 127.9 (ArCH), 128.1 (ArCH),

128.5 (ArCH), 136.8 (ArC), 150.1 (C_{quat}), 169.3 (C_{quat}); HRMS (ESI) required for $C_{23}H_{35}O_7Si^+$ 451.2147 observed $C_{23}H_{35}O_7Si^+$ 451.2145

7.31 2-*O*-Benzoxymethyl ether, 5,6-*O*-isopropylidene-L-ascorbic acid (53) [178]

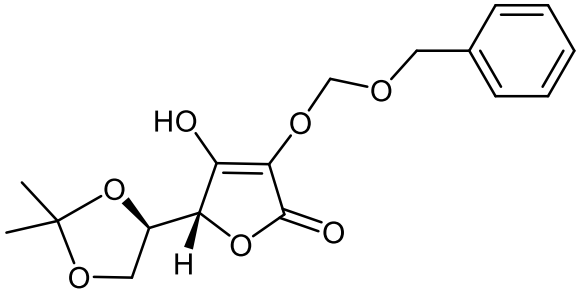

7.30 (4.02 mg, 8.92 μM) was dissolved in THF (1 mL) and cooled to 0 °C before dropwise addition of TBAF (1M in THF) (0.01 mL). The yellow solution was allowed to warm to room temperature and stirred for 16 hours, over which a darker yellow colour emerged. After this time, solvent was removed under reduced pressure and the resulting yellow oil was re-dissolved in ethyl acetate (1 mL) then washed with brine (3 x 1 mL). The organic layer was dried over sodium sulfate and filtered. The filtrate was removed under reduced pressure. The resulting oil was purified by preparative TLC using hexane:ethyl acetate (3:1) as eluent to give the pure product as a yellow oil (1.8 mg, 5.36 μM, 60 %). ^{1}H NMR (400 MHz, $CDCl_3$) δ ppm 1.37 (s, 3H, CH_3), 1.41 (s, 3H, CH_3), 4.00 – 4.20 (m, 2H, CH_2), 4.26 – 4.33 (m, 1H, CH), 4.55 (d, *J* = 3.1 Hz, 1H, CH), 4.75 – 4.90 (m, 2H, CH_2), 5.45 (s, 2H, CH_2), 7.34 – 7.44 (m, 5H, ArCH); ^{13}C NMR (100 MHz, $CDCl_3$) δ ppm 25.7 (CH_3), 25.9 (CH_3), 65.2 (CH_2), 71.7 (CH_2), 73.8 (CH), 74.6 (CH), 93.8 (CH_2), 110.3 (C_{quat}), 128.4 (ArCH), 128.7 (ArCH), 128.8 (ArCH), 145.6 (C_{quat}); HRMS (ESI) required for $C_{17}H_{20}O_7Na^+$ 359.1107 observed $C_{17}H_{20}O_7Na^+$ 359.1129

7.32 3–*O*-TBDMS, 2-*O*-benzyl, 5,6-*O*-isopropylidene-L-ascorbic acid (14)

178

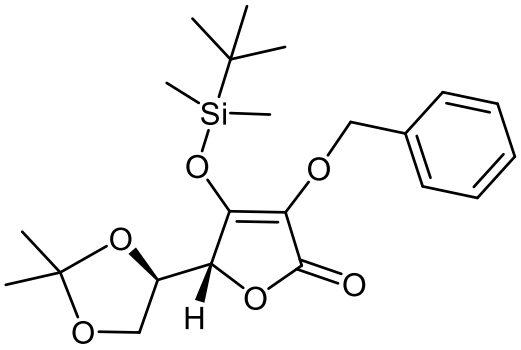

7.11 (261 mg, 791 μM) was dissolved in DCM (6 mL) before addition of triethylamine (0.6 mL) in one portion. The solution was allowed to stir at room temperature for 30 minutes before addition of a solution of benzyl bromide (133 mg, 791 μM) in DCM (3 mL) in one portion. This was allowed to stir at room temperature for 16 hours before solvent was removed under reduced pressure. The resulting yellow oil was re-dissolved in ethyl acetate (5 mL) and then washed with brine (3 x 5 mL). The organic layer was drier over sodium sulfate before being filtered, the filtrate was removed under reduced pressure. The resulting oil was purified by silica gel column chromatography using hexane:ethyl acetate (3:1) to give the pure product as a yellow oil (113 mg, 269 μM, 34%). ^{1}H NMR (400 MHz, $CDCl_3$) δ ppm 0.34 (s, 3H, $SiCH_3$), 0.35 (s, 3H, $SiCH_3$), 1.00 (s, 9H, ^{t}BuSi), 1.37 (s, 3H, CH_3), 1.41 (s, 3H, CH_3), 3.99 – 4.12 (m, 2H, CH_2), 4.27 (td, *J* = 6.7, 3.4 Hz, 1H, CH), 4.52 (d, *J* = 3.4 Hz, CH), 5.45 – 5.55 (m, 2H, CH_2), 7.11 – 7.17 (m, 1H, ArCH), 7.31 (dd, *J* = 5.0, 1.9 Hz, 2H, ArCH), 7.37 – 7.47 (m, 2H, ArCH); ^{13}C NMR (100 MHz, $CDCl_3$) δ ppm -4.08 ($SiCH_3$), -3.90 ($SiCH_3$), 18.4 (C_{quat}), 25.5 (CH_3), 25.7 (CH_3), 25.8 (^{t}BuSi), 65.3 (CH_2), 73.2 (CH_2), 74.2 (CH), 74.8 (CH), 110.2 (C_{quat}), 120.3 (C_{quat}), 128.0 (ArCH), 128.7 (ArCH), 135.7 (ArC), 130.1 (ArCH), 152.2 (C_{quat}), 169.6 (C_{quat}); HRMS (ESI) required for $C_{22}H_{33}O_6Si^+$ 421.2041 observed $C_{22}H_{33}O_6Si^+$ 421.2022

7.33 2-*O*-Benzyl, 5,6-*O*-isopropylidene-L-ascorbic acid (54) [178]

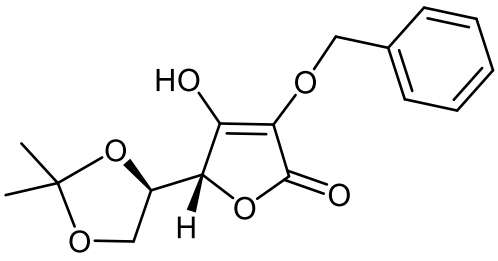

7.32 (113 mg, 269 μM) was dissolved in THF (3 mL) and cooled to 0 °C before dropwise addition of TBAF (1M in THF) (0.03 mL). The yellow solution was allowed to warm to room temperature and stirred for 16 hours, over which a darker yellow colour emerged. After this time, solvent was removed under reduced pressure and the resulting yellow oil was re-dissolved in ethyl acetate (3 mL) then washed with brine (3 x 3 mL). The organic layer was dried over sodium sulfate and filtered. The filtrate was removed under reduced pressure. The resulting oil was purified by silica gel column chromatography using hexane:ethyl acetate (3:1) to give the pure product as a yellow oil (70.0 mg, 228 μM, 85%). $[\alpha]_D$ + 36.10 (*c* 1.00 in MeOH)(lit + 36.40 *c* 1 in MeOH)[168]; ^{1}H NMR (400 MHz, $CDCl_3$) δ ppm 1.38 (s, 3H, CH_3), 1.41 (s, 3H, CH_3), 3.99 – 4.17 (m, 2H, CH_2), 4.29 (td, *J* = 6.7, 3.7 Hz, 1H, CH), 4.59 (d, *J* = 3.7 Hz, 1H, CH), 5.52 (s, 2H, CH_2), 7.34 – 7.46 (m, 5H, ArCH); ^{13}C NMR (100 MHz, $CDCl_3$) δ ppm 25.6 (CH_3), 25.9 (CH_3), 65.4 (CH_2), 73.6 (CH_2), 74.2 (CH), 75.7 (CH), 110.3 (C_{quat}), 119.3 (C_{quat}), 128.1 (ArCH), 128.7 (ArCH), 128.8 (ArCH), 135.7 (ArC), 148.0 (C_{quat}), 170.8 (C_{quat}); HRMS (ESI) required for $C_{16}H_{19}O_6^+$ 307.1176 observed $C_{16}H_{19}O_6^+$ 307.1191

7.34 3–*O*-TBDMS, 2-*O*-PMB, 5,6-*O*-isopropylidene-L-ascorbic acid (55) [178]

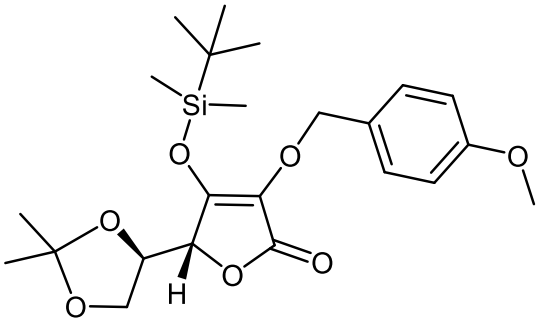

7.11 (308 mg, 932 μM) was dissolved in DCM (5 mL) before addition of triethylamine (0.9 mL) in one portion. The solution was allowed to stir at room temperature for 30 minutes before addition of a solution of (bromomethyl)-4-methoxybenzene (187 mg, 932 μM) in DCM (2 mL) in one portion. This was allowed to stir at room temperature for 16 hours before solvent was removed under reduced pressure. The resulting yellow oil was re-dissolved in ethyl acetate (5 mL) and then washed with brine (3 x 5 mL). The organic layer was drier over sodium sulfate before being filtered, the filtrate was removed under reduced pressure. The resulting oil was purified by silica gel column chromatography using hexane:ethyl acetate (3:1) to give the pure product as a yellow oil (118 mg, 261 μM, 28%). ^{1}H NMR (400 MHz, $CDCl_3$) δ ppm 0.34 (s, 3H, $SiCH_3$), 0.35 (s, 3H, $SiCH_3$), 1.00 (s, 9H, ^{t}BuSi), 1.37 (s, 3H, CH_3), 1.40 (s, 3H, CH_3), 3.85 (s, 3H, CH_3), 3.95 – 4.10 (m, 2H, CH_2), 4.23 (td, *J* = 6.8, 3.5 Hz, 1H, CH), 4.48 (d, *J* = 3.5 Hz, 1H, CH), 5.42 (m, 2H, CH_2), 6.93 (d, *J* = 8.6 Hz, 2H, ArCH), 7.32 (d, *J* = 8.6 Hz, 2H, ArCH); ^{13}C NMR (100 MHz, $CDCl_3$) δ ppm -4.1 ($SiCH_3$), -3.9 ($SiCH_3$), 18.4 (C_{quat}), 25.5 (CH_3), 25.7 (CH_3), 25.8 (^{t}BuSi), 53.3 (OCH_3), 65.3 (CH_2), 73.0 (CH_2), 74.2 (CH), 74.9 (CH), 110.2 (C_{quat}), 114.1 (ArCH), 122.9 (C_{quat}), 127.8 (ArC), 130.0 (ArCH), 152.3 (C_{quat}), 160.1 (ArC), 169.7 (C_{quat}); HRMS (ESI) required for $C_{23}H_{34}O_7SiNa^+$ 473.1971 observed $C_{23}H_{34}O_7SiNa^+$ 473.1950

7.35 3–*O*-TBDMS, 2-*O*-*p*-iodobenzene, 5,6-*O*-isopropylidene-L-ascorbic acid (56) [178]

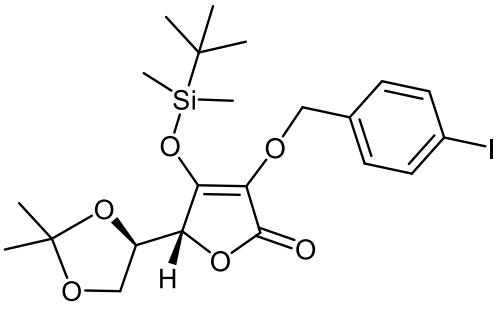

7.11 (53.7 mg, 163 μM) was dissolved in DCM (1.5 mL) before addition of triethylamine (0.1 mL) in one portion. The solution was allowed to stir at room temperature for 30 minutes before addition of a solution of (chloromethyl)-4-iodobenzene (40.9 mg, 163 μM) in DCM (2 mL) in one portion. This was allowed to stir at room temperature for 16 hours before solvent was removed under reduced pressure. The resulting yellow oil was re-dissolved in ethyl acetate (3 mL) and then washed with brine (3 x 3 mL). The organic layer was drier over sodium sulfate before being filtered, the filtrate was removed under reduced pressure. The resulting oil was purified by silica gel column chromatography using hexane:ethyl acetate (3:1) to give the pure product as a yellow oil (16.0 mg, 29.3 μM, 18%). ^{1}H NMR (400 MHz, $CDCl_3$) δ ppm 0.33 (s, 3H, $SiCH_3$), 0.34 (s, 3H, $SiCH_3$), 0.99 (s, 9H, ^{t}BuSi), 1.37 (s, 3H, CH_3), 1.40 (s, 3H, CH_3), 4.00 – 4.18 (m, 2H, CH_2), 4.27 (td, *J* = 6.8, 3.1 Hz, 1H, CH), 4.52 (d, *J* = 3.1 Hz, 1H, CH), 5.44 (s, 2H, CH_2), 7.13 (d, *J* = 8.3 Hz, 2H, ArCH), 7.75 (d, *J* = 8.3 Hz, 2H, ArCH); ^{13}C NMR (100 MHz, $CDCl_3$) δ ppm -4.1 ($SiCH_3$), -3.9 ($SiCH_3$), 18.4 (C_{quat}), 25.8 (^{t}BuSi), 25.9 (CH_3), 65.3 (CH_2), 72.4 (CH_2), 74.0 (CH), 74.6 (CH), 94.5 (ArCI), 110.3 (C_{quat}), 129.7 (ArCH), 135.3 (ArC), 137.9 (ArCH); HRMS (ESI) required for $C_{22}H_{32}O_6SiI^+$ 547.1007 observed $C_{22}H_{32}O_6SiI^+$ 547.1010

7.36 2-*O*-PMB, 5,6-*O*-isopropylidene-L-ascorbic acid (57) [178]

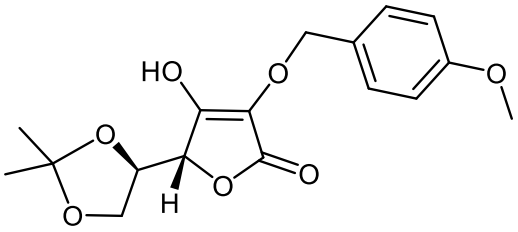

7.34 (118 mg, 261 μM) was dissolved in THF (2 mL) and cooled to 0 °C before dropwise addition of TBAF (1M in THF) (0.02 mL). The yellow solution was allowed to warm to room temperature and stirred for 16 hours, over which a darker yellow colour emerged. After this time, solvent was removed under reduced pressure and the resulting yellow oil was re-dissolved in ethyl acetate (2 mL) then washed with brine (3 x 2 mL). The organic layer was dried over sodium sulfate and filtered. The filtrate was removed under reduced pressure. The resulting oil was purified by silica gel column chromatography using hexane:ethyl acetate (3:1) to give the pure product as a clear oil (70.2 mg, 209 μM, 80%). ^{1}H NMR (400 MHz, $CDCl_3$) δ ppm 1.37 (s, 3H, CH_3), 1.40 (s, 3H, CH_3), 3.85 (s, 3H, OCH_3), 3.98 – 4.15 (m, 2H, CH_2), 4.25 (td, *J* = 6.7, 3.7 Hz, 1H, CH), 4.55 (d, *J* = 3.7 Hz, 1H, CH), 5.38 – 5.50 (m, 2H, CH_2), 6.93 (d, *J* = 8.6 Hz, 2H, ArCH), 7.37 (d, *J* = 8.6 Hz, 2H, ArCH); ^{13}C NMR (100 MHz, $CDCl_3$) δ ppm 25.6 (CH_3), 25.9 (CH_3), 55.3 (OCH_3), 65.4 (CH_2), 73.4 (CH_2), 74.2 (CH), 75.7 (CH), 110.3 (C_{quat}), 114.1 (ArCH), 119.0 (C_{quat}), 127.7 (ArC), 130.1 (ArCH), 147.7 (C_{quat}), 160.1 (ArC), 170.6 (C_{quat}); HRMS (ESI) required for $C_{17}H_{21}O_7^+$ 337.1282 observed $C_{17}H_{21}O_7^+$ 337.1296

7.37 2-*O*-*p*-Iodobenzene, 5,6-*O*-isopropylidene-L-ascorbic acid (58) [178]

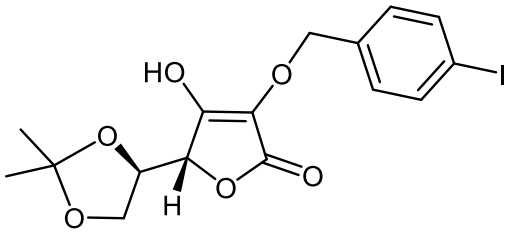

7.35 (15.6 mg, 28.5 μM) was dissolved in THF (1 mL) and cooled to 0 °C before dropwise addition of TBAF (1M in THF) (0.01 mL). The yellow solution was allowed to warm to room temperature and stirred for 16 hours, over which a darker yellow colour emerged. After this time, solvent was removed under reduced pressure and the resulting yellow oil was re-dissolved in ethyl acetate (2 mL) then washed with brine (3 x 2 mL). The organic layer was dried over sodium sulfate and filtered. The filtrate was removed under reduced pressure. The resulting oil was purified by preparative TLC using hexane:ethyl acetate (3:1) as eluent to give the pure product as a yellow oil (10.3 mg, 23.1 μM, 81%). ^{1}H NMR (400 MHz, $CDCl_3$) δ ppm 1.37 (s, 3H, CH_3), 1.40 (s, 3H, CH_3), 4.02 – 4.15 (m, 2H, CH_2), 4.28 (td, *J* = 6.8, 3.5 Hz, 1H, CH), 4.58 (d, *J* = 3.4 Hz, 1H, CH), 5.45 (s, 2H, CH_2), 7.17 (d, *J* = 8.0 Hz, 2H, ArCH), 7.74 (d, *J* = 8.0 Hz, 2H, ArCH); ^{13}C NMR (100 MHz, $CDCl_3$) δ ppm 25.6 (CH_3), 25.9 (CH_3), 65.3 (CH_2), 72.7 (CH_2), 74.0 (CH), 75.4 (CH), 94.6 (ArC), 110.3 (C_{quat}), 119.5 (C_{quat}), 129.8 (ArCH), 135.4 (ArC), 137.8 (ArCH), 147.4 (C_{quat}), 170.5 (C_{quat}); HRMS (ESI) required for $C_{16}H_{18}O_6I^+$ 433.0143 observed $C_{16}H_{18}O_6I^+$ 433.0157

7.38 3–*O*-TBDMS, 2-*O*-*p*-nitrobenzene, 5,6-*O*-isopropylidene-L-ascorbic acid (59) [178]

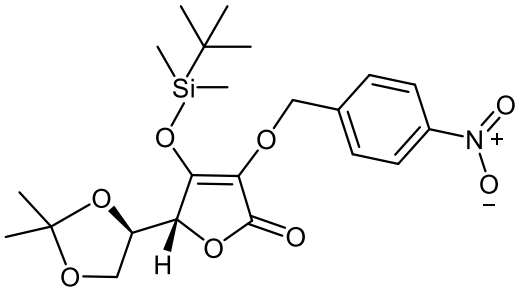

7.11 (189 mg, 573.2 μM) was dissolved in DCM (5 mL) before addition of triethylamine (0.05 mL) in one portion. The solution was allowed to stir at room temperature for 30 minutes before addition of a solution of (bromomethyl)-4-nitrobenzene (123.8 mg, 573.2 μM) in DCM (3 mL) in one portion. This was allowed to stir at room temperature for 16 hours before solvent was removed under reduced pressure. The resulting yellow oil was re-dissolved in ethyl acetate (5 mL) and then washed with brine (3 x 5 mL). The organic layer was drier over sodium sulfate before being filtered, the filtrate was removed under reduced pressure. The resulting oil was purified by silica gel column chromatography using hexane:ethyl acetate (3:1) to give the pure product as a dark yellow oil (61.3 mg, 131.8 μM, 23%). ^{1}H NMR (400 MHz, $CDCl_3$) δ ppm 0.32 (s, 3H, $SiCH_3$), 0.34 (s, 3H, $SiCH_3$), 0.97 (s, 9H, ^{t}BuSi), 1.38 (s, 3H, CH_3), 1.41 (s, 3H, CH_3), 4.04 – 4.20 (m, 2H, CH_2), 4.34 (td, *J* = 6.7, 2.8 Hz, 1H, CH), 4.59 (d, *J* = 2.7 Hz, 1H, CH), 5.56 – 5.68 (m, 2H, CH_2), 7.56 (d, *J* = 8.7 Hz, 2H, ArCH), 8.28 (d, *J* = 8.7 Hz, 2H, ArCH); ^{13}C NMR (100 MHz, $CDCl_3$) δ ppm -4.1 ($SiCH_3$), -3.9 ($SiCH_3$), 18.4 (C_{quat}), 25.5 (CH_3), 25.6 (CH_3), 25.8 (^{t}BuSi), 65.3 (CH_2), 71.4 (CH_2), 73.7 (CH), 74.5 (CH), 110.4 (C_{quat}), 120.6 (C_{quat}), 123.9 (ArCH), 127.9 (ArCH), 131.4 (ArC), 142.9 (ArCH), 151.3 (C_{quat}), 169.2 (C_{quat}); HRMS (ESI) required for $C_{22}H_{31}O_8SiNNa^+$ 488.1717 observed $C_{22}H_{31}O_8SiNNa^+$ 488.1701

7.39 3–*O*-TBDMS, 2-*O*-*p*-methylbenzene, 5,6-*O*-isopropylidene-L-ascorbic acid (60) [178]

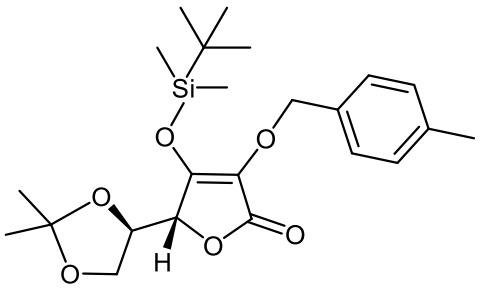

7.11 (38.5 mg, 0.117 mmol) was dissolved in DCM (1.5 mL) before addition of triethylamine (0.01 mL, 1.1 eq) in one portion. The solution was allowed to stir at room temperature for 30 minutes before addition of a solution of 1-(bromomethyl)-4-methylbenzene (21.4 mg, 0.117 mmol) in DCM (1 mL) in one portion. This was allowed to stir at room temperature for 16 hours before solvent was removed under reduced pressure. The resulting yellow oil was re-dissolved in ethyl acetate (1 mL) and then washed with brine (3 x 1 mL). The organic layer was drier over sodium sulfate before being filtered, the filtrate was removed under reduced pressure. The resulting oil was purified by silica gel column chromatography using hexane:ethyl acetate (3:1) to give the pure product as a yellow oil (16.9 mg, 39.1 μM, 25 %). ^{1}H NMR (400 MHz, $CDCl_3$) δ ppm 0.34 (s, 3H, $SiCH_3$), 0.35 (s, 3H, $SiCH_3$), 1.00 (s, 9H, ^{t}BuSi), 1.37 (s, 3H, CH_3), 1.40 (s, 3H, CH_3), 2.39 (s, 3H, $ArCH_3$), 3.98 – 4.14 (m, 2H, CH_2), 4.25 (td, *J* = 6.7, 3.5 Hz, 1H, CH), 4.50 (d, *J* = 3.4 Hz, 1H, CH), 5.45 (q, *J* = 11.3, 2H, CH_2), 7.03 (d, *J* = 7.9 Hz, 2H, ArCH), 7.11 (d, *J* = 7.8 Hz, 2H, ArCH); ^{13}C NMR (100 MHz, $CDCl_3$) δ ppm -4.1 ($SiCH_3$), -3.9 ($SiCH_3$), 18.3 (C_{quat}), 21.3 ($ArCH_3$), 25.5 (CH_3), 25.8 (^{t}BuSi), 65.4 (CH_2), 74.3 (CH), 74.9 (CH), 110.2 (C_{quat}), 128.2 (ArCH), 129.4 (ArCH), 129.6 (ArC), 130.0 (ArC); HRMS (ESI) required for $C_{23}H_{35}O_6Si^+$ 435.2197 observed $C_{23}H_{35}O_6Si^+$ 435.2200

7.40 2-*O*-*p*-Methylbenzene, 5,6-*O*-isopropylidene-L-ascorbic acid (61) [178]

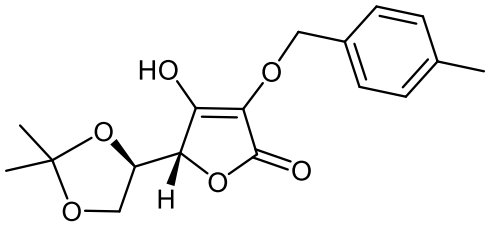

7.39 (16.9 mg, 39.1 μM) was dissolved in THF (1 mL) and cooled to 0 °C before dropwise addition of TBAF (1M in THF) (0.1 mL). The yellow solution was allowed to warm to room temperature and stirred for 16 hours, over which a darker yellow colour emerged. After this time, solvent was removed under reduced pressure and the resulting yellow oil was re-dissolved in ethyl acetate (1 mL) then washed with brine (3 x 1 mL). The organic layer was dried over sodium sulfate and filtered. The filtrate was removed under reduced pressure. The resulting oil was purified by preparative TLC using hexane:ethyl acetate (3:1) as eluent to give the pure product as a yellow oil (10.0 mg, 31.3 μM, 81%). ^{1}H NMR (400 MHz, $CDCl_3$) δ ppm 1.38 (s, 3H, CH_3), 1.41 (s, 3H, CH_3), 2.39 (s, 3H, $ArCH_3$), 4.07 (ddd, *J* = 33.3, 8.6, 6.7 Hz, 2H, CH_2), 4.27 (td, *J* = 6.7, 3.7 Hz, 1H, CH), 4.57 (d, *J* = 3.7 Hz, 1H, CH), 5.41 – 5.53 (m, 2H, CH_2), 7.22 (d, *J* = 7.8 Hz, 2H, ArCH), 7.32 (d, *J* = 7.8 Hz, 2H, ArCH); ^{13}C NMR (100 MHz, $CDCl_3$) δ ppm 21.3 ($ArCH_3$), 25.6 (CH_3), 25.9 (CH_3), 65.4 (CH_2), 73.6 (CH_2), 74.2 (CH), 75.7 (CH), 110.3 (C_{quat}), 119.1 (C_{quat}), 128.3 (ArCH), 129.4 (ArCH), 132.7 (ArC), 138.8 (ArC), 148.0 (C_{quat}), 170.7 (C_{quat}); HRMS (ESI) required for $C_{17}H_{21}O_6^+$ 321.1333 observed $C_{17}H_{21}O_6^+$ 321.1335

7.41 2-*O*-Ethylbenzene, 5,6-*O*-isopropylidene-L-ascorbic acid (62) [178]

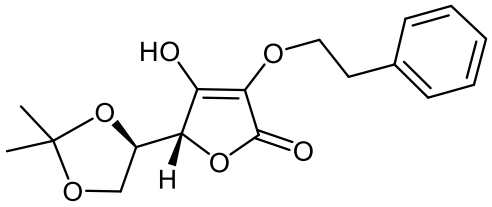

7.29 (27.1 mg, 62.5 μM) was dissolved in THF (1 mL) and cooled to 0 °C before dropwise addition of TBAF (1M in THF) (0.01 mL). The yellow solution was allowed to warm to room temperature and stirred for 16 hours, over which a darker yellow colour emerged. After this time, solvent was removed under reduced pressure and the resulting yellow oil was re-dissolved in ethyl acetate (1 mL) then washed with brine (3 x 1 mL). The organic layer was dried over sodium sulfate and filtered. The filtrate was removed under reduced pressure. The resulting oil was purified by silica gel column chromatography using hexane:ethyl acetate (3:1) to give the pure product as a yellow oil (15.2 mg, 46.9 μM, 75 %). ^{1}H NMR (400 MHz, $CDCl_3$) δ ppm 1.38 (s, 3H, CH_3), 1.41 (s, 3H, CH_3), 3.08 (t, *J* = 6.9 Hz, CH_2), 3.97 – 4.08 (m, 2H, CH_2), 4.20 (td, *J* = 6.8, 4.0 Hz, 1H, CH), 4.53 (d, *J* = 3.8 Hz, 1H, CH), 4.59 – 4.78 (m, 2H, CH_2), 7.25 – 7.42 (m, 5H, ArCH); ^{13}C NMR (100 MHz, $CDCl_3$) δ ppm 25.6 (CH_3), 25.9 (CH_3), 36.1 (CH_2), 65.3 (CH_2), 72.4 (CH_2), 74.3 (CH), 75.5 (CH), 110.3 (C_{quat}), 118.7 (C_{quat}), 125.9 (ArCH), 128.6 (ArCH), 129.0 (ArCH), 137.1 (ArC), 147.7 (C_{quat}), 170.6 (C_{quat}); HRMS (ESI) required for $C_{17}H_{21}O_6^+$ 321.1333 observed $C_{17}H_{21}O_6^+$ 321.1330

7.42 3–*O*-TBDMS, 2-*O*-*3,5*-dimethylbenzene, 5,6-*O*-isopropylidene-L-ascorbic acid (63) [178]

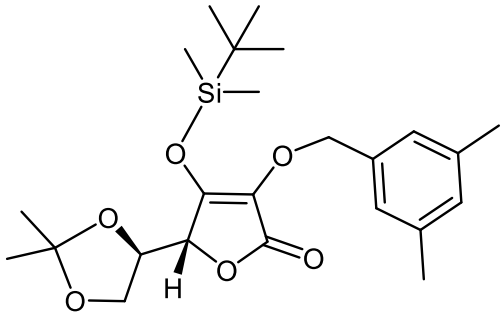

7.11 (134.7 mg, 408.2 μM) was dissolved in DCM (5 mL) before addition of triethylamine (0.5 mL) in one portion. The solution was allowed to stir at room temperature for 30 minutes before addition of a solution of (bromomethyl)-3,5-dimethylbenzene (80.8 mg, 408.2 μM) in DCM (4 mL) in one portion. This was allowed to stir at room temperature for 16 hours before solvent was removed under reduced pressure. The resulting yellow oil was re-dissolved in ethyl acetate (5 mL) and then washed with brine (3 x 5 mL). The organic layer was drier over sodium sulfate before being filtered, the filtrate was removed under reduced pressure. The resulting oil was purified by silica gel column chromatography using hexane:ethyl acetate (3:1) to give the pure product as a yellow oil (51.2 mg, 114.3 μM, 28 %). ^{1}H NMR (400 MHz, $CDCl_3$) δ ppm 0.33 (s, 3H, $SiCH_3$), 0.35 (s, 3H, $SiCH_3$), 1.00 (s, 9H, ^{t}BuSi), 1.38 (s, 3H, CH_3), 1.41 (s, 3H, CH_3), 2.35 (s, 6H, $ArCH_3$), 3.97 – 4.11 (m, 2H, CH_2), 4.28 (td, *J* = 6.8, 3.4 Hz, 1H, CH), 4.52 (d, *J* = 3.3 Hz, 1H, CH), 5.42 (q, *J* = 11.3 Hz, 2H, CH_2), 6.75 (s, 1H, ArCH), 7.00 (s, 2H, ArCH); ^{13}C NMR (100 MHz, $CDCl_3$) δ ppm -4.1 ($SiCH_3$), -3.9 ($SiCH_3$), 18.4 (C_{quat}), 25.5 (CH_3), 25.7 (CH_3), 25.8 (^{t}BuSi), 65.4 (CH_2), 73.4 (CH_2), 74.2 (CH), 74.8 (CH), 110.2 (C_{quat}), 120.1 (C_{quat}), 125.9 (ArCH), 127.9 (ArCH), 135.5 (ArC), 138.4 (ArC), 152.4 (C_{quat}), 169.7 (C_{quat});

7.43 2-*O*-*3,5*-Dimethylbenzene, 5,6-*O*-isopropylidene-L-ascorbic acid (64) [178]

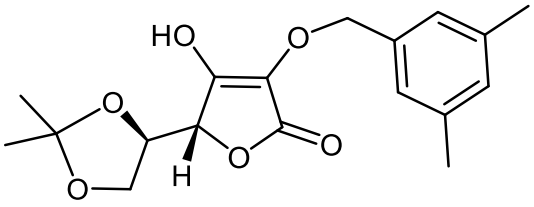

7.42 (49.7 mg, 110.9 μM) was dissolved in THF (2 mL) and cooled to 0 °C before dropwise addition of TBAF (1M in THF) (0.02 mL). The yellow solution was allowed to warm to room temperature and stirred for 16 hours, over which a darker yellow colour emerged. After this time, solvent was removed under reduced pressure and the resulting yellow oil was re-dissolved in ethyl acetate (5 mL) then washed with brine (3 x 5 mL). The organic layer was dried over sodium sulfate and filtered. The filtrate was removed under reduced pressure. The resulting oil was purified by silica gel column chromatography using hexane:ethyl acetate (3:1) to give the pure product as a yellow oil (30.0 mg, 89.8 μM, 81%). ^{1}H NMR (400 MHz, $CDCl_3$) δ ppm 1.39 (s, 3H, CH_3), 1.41 (s, 3H, CH_3), 2.35 (s, 6H, $ArCH_3$), 3.95 – 4.19 (m, 2H, CH_2), 4.30 (td, *J* = 6.7, 3.6 Hz, 1H, CH), 4.58 (d, *J* = 3.6 Hz, 1H, CH), 5.32 – 5.54 (m, 2H, CH_2), 7.03 (m, 3H, ArCH); ^{13}C NMR (100 MHz, $CDCl_3$) δ ppm 21.3 (CH_3), 25.7 (CH_3), 65.4 (CH_2), 73.7 (CH_2), 74.2 (CH), 75.6 (CH), 110.3 (C_{quat}), 119.0 (C_{quat}), 125.8 (ArCH), 130.4 (ArCH), 138.3 (ArC), 147.8 (C_{quat}); HRMS (ESI) required for $C_{18}H_{23}O_6^+$ 335.1489 observed $C_{18}H_{23}O_6^+$ 335.1490

7.44 2-*O*-Methylnapthalene, 5,6-*O*-isopropylidene-L-ascorbic acid (65) [178]

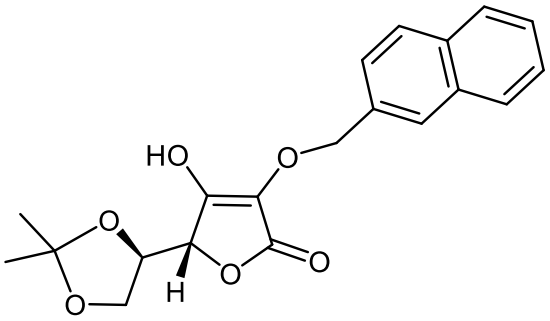

3-*O*-TBDMS, 2-*O*-methylnapthalene, 5,6-*O*-isopropylidene-L-ascorbic acid (27.5 mg, 58.5 μM) was dissolved in THF (1 mL) and cooled to 0 °C before dropwise addition of TBAF (1M in THF) (0.01 mL). The yellow solution was allowed to warm to room temperature and stirred for 16 hours, over which a darker yellow colour emerged. After this time, solvent was removed under reduced pressure and the resulting yellow oil was re-dissolved in ethyl acetate (2 mL) then washed with brine (3 x 2 mL). The organic layer was dried over sodium sulfate and filtered. The filtrate was removed under reduced pressure. The resulting oil was purified by silica gel column chromatography using hexane:ethyl acetate (3:1) to give the pure product as a yellow oil (15 mg, 42.1 μM, 72%). ^{1}H NMR (400 MHz, $CDCl_3$) δ ppm 1.35 (s, 3H, CH_3), 1.39 (s, 3H, CH_3), 4.00 – 4.17 (m, 2H, CH_2), 4.30 (td, *J* = 6.8, 3.6 Hz, 1H, CH), 4.60 (d, *J* = 3.6 Hz, 1H, CH), 5.67 (s, 2H, CH_2), 7.35 – 7.46 (m, 1H, ArCH), 7.49 – 7.55 (m, 3H, ArCH), 7.84 – 7.90 (m, 3H, ArCH); ^{13}C NMR (100 MHz, $CDCl_3$) δ ppm 25.6 (CH_3), 25.9 (CH_3), 65.4 (CH_2), 73.6 (CH_2), 74.1 (CH), 75.7 (CH), 110.4 (C_{quat}), 119.4 (C_{quat}), 125.5 (ArCH), 126.5 (ArCH), 126.6 (ArCH), 127.4 (ArCH), 127.8 (ArCH), 128.1 (ArCH), 128.6 (ArCH), 133.0 (ArC), 133.1 (ArC), 133.4 (ArC), 148.0 (C_{quat}), 170.8 (C_{quat}); HRMS (ESI) required for $C_{20}H_{20}O_6Na^+$ 379.1158 observed $C_{20}H_{20}O_6Na^+$ 379.1162

7.45 Methyl (R)-2-((S)-2,2-dimethyl-1,3-dioxolan-4-yl)-2-hydroxyacetate (D1) [166]

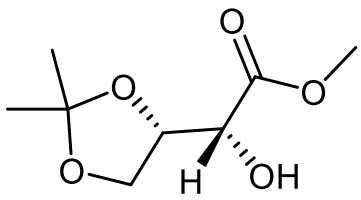

5,6-O-isopropylidene-L-ascorbic acid (10.0 g, 46.2 mmol) and distilled water (45.0 mL). To this suspended solution was added aqueous 30% NaOH (3.41 mL) and the reaction mixture was stirred to become a clear solution. To the clear solution was added $NaHCO_3$ (9.78 g, 117.0 mmol), and then 35% hydrogen peroxide (9.09 mL, 93.1 mmol) was added dropwise and the reaction mixture was stirred for further 1 h at room temperature. After sodium sulfite (704.5 mg, 5.57 mmol) and $NaHCO_3$ (5.88 g, 69.9 mmol) were added to the reaction mixture at room temperature, the resulting solution was warmed to 40 °C and dimethylsulfate (17.4 mL, 186 mmol) was added dropwise at 40 °C. After being stirred for 4 h at 40 °C, the reaction mixture was cooled to room temperature, extracted with DCM (3 x 50 mL). The combined organic layers were dried over $MgSO_4$, filtered, and concentrated under reduced pressure to give the pure product as a colorless oil (3.00 g, 15.8 mmol, 33.7 %). ^{1}H NMR (400 MHz, $CDCl_3$) δ ppm 1.24 (s, 3H, CH_3), 1.31 (s, 3H, CH_3), 3.71 (s, 3H, OCH_3), 3.78 – 4.02 (m, 2H, CH_2), 4.03 – 4.07 (m, 1H, CH), 4.29 (td, *J* = 6.8, 3.0 Hz, 1H, CH); ^{13}C NMR (100 MHz, $CDCl_3$) δ ppm 25.2 (CH_3), 26.0 (CH_3), 52.5 (CH_3), 65.4 (CH_2), 70.3 (CH), 76.3 (CH), 109.8 (C_{quat}), 172.5 (C_{quat}); HRMS (ESI) required for $C_8H_{14}O_5^+$ 191.0914 observed $C_8H_{14}O_5^+$ 191.0929

7.46 Methyl (R)-2-acetoxy-2-((S)-2,2-dimethyl-1,3-dioxolan-4-yl)acetate (D2) [166]

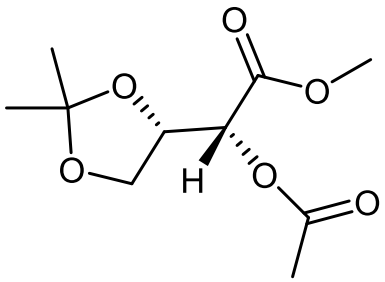

To a solution of methyl 3,4-O-isopropylidene-L-threonate (3.00 g, 15.8 mmol) in dry CH_2Cl_2 (35 mL) and pyridine (20 mL) was added dropwise acetyl chloride (1.60 mL, 24.5 mmol) with stirring at 0 °C. A white solid formed over the course of the reaction. After 2 h, water (15 mL) was added. The separated aqueous layer was extracted with CH_2Cl_2 (20 mL). The combined organic layers were washed with H_2O (3 x 30 mL) and brine (3 x 30 mL) and were dried over sodium sulfate. Removal of the solvent gave a clear liquid that was purified by silica gel column chromatography using EtOAc:Hex (3:1) to produce the pure compound as a colorless liquid (2.00 g, 8.62 mmol, 55%). $[\alpha]_D$ + 37.10 (*c* 0.50 in MeOH)(lit + 37.40 *c* 0.50 in MeOH)[182]; ^{1}H NMR (400 MHz, $CDCl_3$) δ ppm 1.30 (CH_3), 1.38 (CH_3), 2.13 (s, 3H, CH_3), 3.72 (s, 3H, OCH_3), 3.81 – 4.15 (m, 2H, CH_2), 4.39 - 4.52 (m, 1H, CH), 5.03 (d, *J* = 5.0 Hz, 1H, CH); ^{13}C NMR (100 MHz, $CDCl_3$) δ ppm 20.5 (CH_3), 25.2 (CH_3), 26.0 (CH_3), 52.5 (OCH_3), 65.5 (CH_2), 72.3 (CH), 74.3 (CH), 110.2 (C_{quat}), 168.0 (C_{quat}), 170.2 (C_{quat}); HRMS (ESI) required for $C_{10}H_{16}O_6Na^+$ 255.0845 observed $C_{10}H_{16}O_6Na^+$ 255.0847

7.47 Methyl (2R,3S)-2-acetoxy-3,4-dihydroxybutanoate (D3) [188]

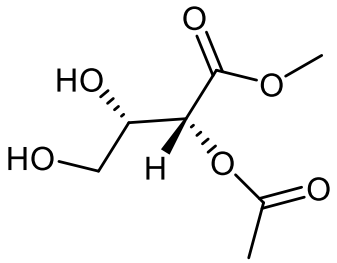

A solution of compound **7.46** (1.85 g, 7.97 mmol) in HCl (1M)(10 mL):MeOH (10 mL):THF (10 mL) was stirred at room temperature for 18 h. Evaporation of the solvent below 30 °C gave a colorless oil. This was dissolved in EtOAc (15 mL), and the solution was carefully washed with 5% $NaHCO_3$ until neutral (pH 6-7). The organic layer was separated, washed successively with H_2O (20 mL) and brine (20 mL), before being dried over sodium sulfate. After filtration, solvent was removed to give a colorless oil that was taken forward without any further purification (1.27 g, 6.61 mmol, 83.3%). HRMS (ESI) required for $C_7H_{13}O_6^+$ 193.0707 observed $C_7H_{13}O_6^+$ 193.0701

7.48 Methyl (2R,3S)-2-acetoxy-3-hydroxy-4-(trityloxy)butanoate (D4) 166

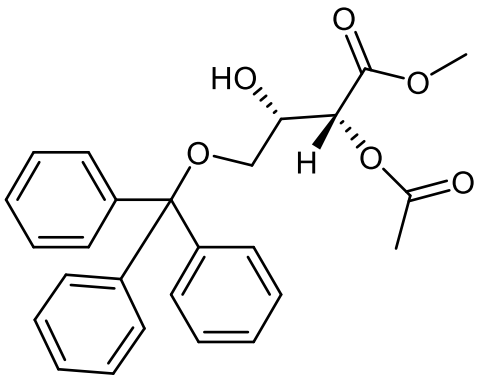

7.48 (1.02 g, 5.31 mmol) was dissolved in THF (10 mL) before addition of NaH (60% in mineral oil) (212 mg, 5.31 mmol). This solution initially emitted gas and was allowed to stir for 30 minutes at room temperature. A solution of trityl chloride (1.53 g, 5.31 mmol) in THF (10 mL) was added in one portion. The solution was stirred at room temperature for 16 h, after which time mass spec analysis indicated minimal reaction procedure. The mixture was heated to reflux and stirred for an additional 8 h before being poured into ice cold water. The organic layer was removed under reduced pressure, and the resulting aqueous layer partitioned with ethyl acetate (10 mL). The aqueous phase was extracted into ethyl acetate (3 x 20 mL). The combined organic layers were thoroughly washed with water (15 mL × 4) and dried over sodium sulfate. Removal of the solvent gave a thick oily residue which was purified by silica gel column chromatography using hexane:ethyl acetate (3:1) to give the title compound as a colourless oil (680 mg, 1.38 mmol, 26.0%). ^{1}H NMR (400 MHz, $CDCl_3$) δ ppm 2.22 (s, 3H, CH_3), 3.81 (s, 3H, OCH_3), 3.94 – 4.13 (m, 2H, CH_2), 4.55 (dt, *J* = 6.5, 5.4 Hz, 1H, CH), 5.12 (d, *J* = 5.0 Hz, 1H, CH), 7.26 – 7.49 (m, 15H, ArCH); ^{13}C NMR (100 MHz, $CDCl_3$) δ ppm 20.6 (CH_3), 52.6 (CH_3), 65.6 (CH_2), 72.4 (CH), 74.4 (CH), 82.0 (C_{quat}), 127.3 (ArCH), 127.9 (ArCH), 128.0 (ArCH), 147.0 (ArC), 168.1 (C_{quat}), 170.4 (C_{quat}); MS (ESI) required for $C_{26}H_{26}O_6Na^+$ 457.1622 observed $C_{26}H_{26}O_6Na^+$ 457.1627

7.49 5,6-*O*-Tosyl-3-*O*-tertbutyldimethylsilyl-L-ascorbic acid (39) [178]

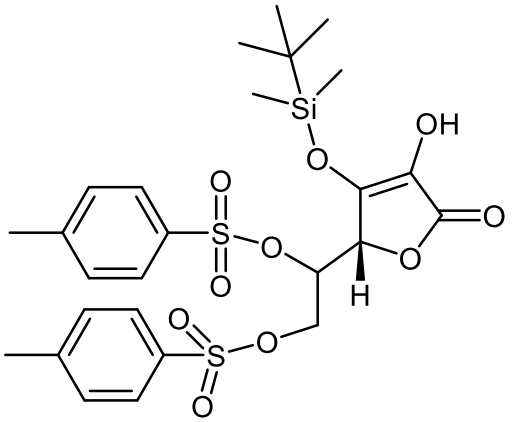

7.17 (7.00 g, 14.5 mmol) was dissolved in DCM (25 mL) before addition of NEt_3 (1.9 mL, 1 eq). This solution was allowed to stir for 30 minutes at room temperature before a solution of TBDMSCl (50% w/w Tol) (4.8 mL, 1 eq) was added in one portion at 0 °C. This was allowed to stir at room temperature for four hours after which TLC analysis indicated minimal reaction progression. The reaction was then heated at reflux for 16 hours after which solvent was removed under reduced pressure. The resulting oil was redissolved in EtOAc (40 mL) and washed with brine (3 x 40 mL). Organic layer was dried over sodium sulfate and filtered before solvent removed under reduced pressure. The crude material was purified by column chromatography using EtOAc:Hex (3:1 – 1:1) to give the pure product as a clear oil (1.80 g, 3.01 mmol, 20.8 %). ^{1}H NMR (400 MHz, $CDCl_3$) δ ppm 0.05 (s, 6H, $SiCH_3$), 0.79 (s, 9H, ^{t}Bu-Si), 2.41 (s, 6H, $ArCH_3$), 3.98 – 4.08 (m, 2H, CH_2), 4.34 (m, 1H, CH), 4.74 (m, 1H, CH), 7.37 – 7.91 (m, 8H, ArCH); ^{13}C NMR (100 MHz, $CDCl_3$) δ ppm -5.3 ($SiCH_3$), -4.8 ($SiCH_3$), 17.8 (C_{quat}), 21.7 ($ArCH_3$), 25.4 (^{t}Bu-Si), 67.7 (CH_2), 68.5 (CH), 74.9 (CH), 128.0 (ArCH), 128.9 (ArCH), 130.0 (ArCH), 130.1 (ArCH), 130.1 (ArC_{quat}), 130.2 (ArCH), 131.9 (ArC_{quat}), 145.5 (C_{quat}); HRMS (ESI) required for $C_{26}H_{35}O_{10}S_2Si^+$ 599.1435 observed $C_{26}H_{35}O_{10}S_2Si^+$ 599.1415

7.50 3–*O*-TBDMS, 2-*O*-p-^{I}Pr-benzyl, 5,6-*O*-isopropylidene-L-ascorbic acid (66) [178]

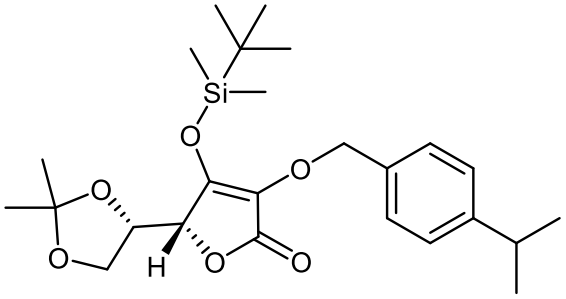

7.11 (211.7 mg, 641 μM) was dissolved in DCM (5 mL) before addition of triethylamine (0.6 mL) in one portion. The solution was allowed to stir at room temperature for 30 minutes before addition of a solution of (bromomethyl)-4-isopropylbenzene (136 mg) in DCM (3 mL) in one portion. This was allowed to stir at room temperature for 16 hours before solvent was removed under reduced pressure. The resulting yellow oil was re-dissolved in ethyl acetate (5 mL) and then washed with brine (3 x 5 mL). The organic layer was drier over sodium sulfate before being filtered, the filtrate was removed under reduced pressure. The resulting oil was purified by silica gel column chromatography using hexane:ethyl acetate (3:1) to give the pure product as a yellow oil (83.0 mg, 179.7 μM, 28%). ^{1}H NMR (400 MHz, $CDCl_3$) δ ppm 0.34 (s, 3H, $SiCH_3$), 0.35 (s, 3H, $SiCH_3$), 1.00 (s, 9H, ^{t}BuSi), 1.27 (s, 3H, CH_3), 1.29 (s, 3H, CH_3), 1.37 (s, 3H, CH_3), 1.40 (s, 3H, CH_3), 2.85 – 3.00 (m, 1H, CH), 3.97 – 4.18 (m, 2H, CH_2), 4.26 (td, *J* = 6.7, 3.4 Hz, 1H, CH), 4.50 (d, *J* = 3.4 Hz, 1H, CH), 5.38 – 5.52 (m, 2H, CH_2), 7.26 (m, 2H, ArCH), 7.32 (d, *J* = 8.2 Hz, 2H, ArCH); ^{13}C NMR (100 MHz, $CDCl_3$) δ ppm – 3.6 ($SiCH_3$), 23.9 (CH_3), 25.7 (^{t}BuSi), 25.8 (CH_3), 33.9 (CH), 65.4 (CH_2), 73.3 (CH_2), 74.2 (CH), 74.9 (CH), 110.2 (C_{quat}), 120.2 (C_{quat}), 126.8 (ArCH), 128.3 (ArCH), 133.0 (ArC), 149.8 (ArC), 152.3 (C_{quat}), 169.7 (C_{quat});

7.51 2-*O*-*p*-^{I}Pr-benzyl, 5,6-*O*-isopropylidene-L-ascorbic acid (67) [178]

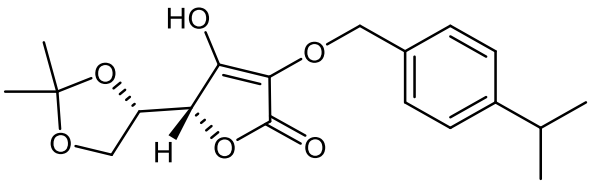

7.50 (82.4 mg, 178.4 μM) was dissolved in THF (2 mL) and cooled to 0 °C before dropwise addition of TBAF (1M in THF) (0.02 mL). The yellow solution was allowed to warm to room temperature and stirred for 16 hours, over which a darker yellow colour emerged. After this time, solvent was removed under reduced pressure and the resulting yellow oil was re-dissolved in ethyl acetate (2 mL) then washed with brine (3 x 2 mL). The organic layer was dried over sodium sulfate and filtered. The filtrate was removed under reduced pressure. The resulting oil was purified by silica gel column chromatography using hexane:ethyl acetate (3:1) as eluent to give the pure product as a yellow oil (50.3 mg, 144.5 μM, 81%). ^{1}H NMR (400 MHz, $CDCl_3$) δ ppm 1.28 (d, *J* = 6.9 Hz, 6H, CH_3), 1.38 (s, 3H, CH_3), 1.41 (s, 3H, CH_3), 2.95 (hept, *J* = 6.8 Hz, 1H, CH), 4.02 – 4.14 (m, 2H, CH_2), 4.28 (td, *J* = 6.8, 3.7 Hz, 1H, CH), 4.57 (d, *J* = 3.7 Hz, 1H), 5.41 – 5.53 (m, 2H, CH_2), 7.27 (d, *J* = 8.2 Hz, ArCH), 7.35 (d, *J* = 8.1 Hz, ArCH); ^{13}C NMR (100 MHz, $CDCl_3$) δ ppm; 23.9 (CH_3), 25.6 (CH_3), 25.9 (CH_3), 33.9 (CH), 65.4 (CH_2), 73.6 (CH_2), 74.2 (CH), 75.6 (CH), 110.3 (C_{quat}), 119.0 (C_{quat}), 126.8 (ArCH), 128.3 (ArCH), 133.0 (ArC), 147.8 (ArC), 149.7 (C_{quat}), 170.6 (C_{quat}); HRMS (ESI) required for $C_{19}H_{25}O_6^+$ 349.1646 observed $C_{19}H_{25}O_6^+$ 349.1660

8.0 References

1. E. Uberoi, Bovine TB statistics: Great Britain, House of Commons Library, 2019.
2. M. Temming, A new way to make bacteria glow could simplify TB screening, https://www.sciencenews.org/article/new-way-make-bacteria-glow-could-simplify-tb-screening, (accessed 28/02/2018).
3. W. H. Organization, *Global Tuberculosis Report 2016*, Report 924156539X, 2016.
4. W. H. Organization, *Global Tuberculosis Report 2017*, 2018.
5. J. L. Flynn and J. Chan, *Infection and immunity*, 2001, **69**, 4195-4201.
6. N. Haddad, M. Masselot and B. Durand, *Res. Vet. Sci.*, 2004, **76**, 1-18.
7. J. K. Kuria, in *Bacterial Cattle Diseases*, IntechOpen, 2019.
8. J. M. Gray and D. L. Cohn, 2013.
9. T. J. Sullivan, J. J. Truglio, M. E. Boyne, P. Novichenok, X. Zhang, C. F. Stratton, H.-J. Li, T. Kaur, A. Amin and F. Johnson, *ACS Chem. Biol.*, 2006, **1**, 43-53.
10. S. E. Dorman and R. E. Chaisson, *Nat. Med.*, 2007, **13**, 295-298.
11. C. A. Peloquin, *Antimicrob. Agents Chemother.*, 2012, **56**, 1666-1666.
12. A. Zumla, E. Petersen, T. Nyirenda and J. Chakaya, *Int. J. Infect. Dis.*, 2015, **32**, 46-49.
13. W. H. Organisation, *Global tuberculosis report 2019*, 2019.
14. P. Olliaro and P. Smith, *J. HIV Ther.*, 2004, **9**, 53-56.
15. J. E. Bennett, R. Dolin and M. J. Blaser, *Mandell, Douglas, and Bennett's principles and practice of infectious diseases*, Elsevier Health Sciences, 2014.
16. K. E. Dooley, T. Tang, J. E. Golub, S. E. Dorman and W. Cronin, *Am. J. Trop. Med*, 2009, **80**, 634-639.
17. D. Menzies, H. Al Jahdali and B. Al Otaibi, *Ind. J. Med. Res*, 2011, **133**, 257.
18. L. M. O'Reilly and C. Daborn, *Tuber. Lung. Dis*, 1995, **76**, 1-46.
19. H. Huitema, *Sel. Pap. Roy. Neth. Tub. Assoc.*, 1969, **12**, 62-67.
20. C. Allix-Béguec, M. Fauville-Dufaux, K. Stoffels, D. Ommeslag, K. Walravens, C. Saegerman and P. Supply, *Eur. Respir. J.*, 2010, **35**, 692-694.

21. S. Fitzgerald and J. Kaneene, *Vet. Pathol.*, 2013, **50**, 488-499.

22. F. Vayr, G. Martin-Blondel, F. Savall, J.-M. Soulat, G. Deffontaines and F. Herin, *PLoS Neglected Trop. Dis.*, 2018, **12**, e0006208.

23. J. A. Davidson, M. G. Loutet, C. O'Connor, C. Kearns, R. M. Smith, M. K. Lalor, H. L. Thomas, I. Abubakar and D. Zenner, *Emerging Infect. Dis.*, 2017, **23**, 377.

24. F. Olea-Popelka, A. Muwonge, A. Perera, A. S. Dean, E. Mumford, E. Erlacher-Vindel, S. Forcella, B. J. Silk, L. Ditiu and A. El Idrissi, *Lancet Infect Dis*2017, **17**, e21-e25.

25. J. Kean, N. Barlow and G. Hickling, *N. Z. J. Agric. Res.*, 1999, **42**, 101-106.

26. A. I. Ward, G. C. Smith, T. R. Etherington and R. J. Delahay, *J. Wildl. Dis.*, 2009, **45**, 1104-1120.

27. P. Lambert, *J. Appl. Microbiol.*, 2002, **92**, 35S - 45S.

28. C. E. Barry, R. E. Lee, K. Mdluli, A. E. Sampson, B. G. Schroeder, R. A. Slayden and Y. Yuan, *Prog. Lipid Res.*, 1998, **37**, 143-179.

29. K. Takayama, C. Wang and G. S. Besra, *Clin. Microbiol. Rev.*, 2005, **18**, 81-101.

30. R. Van der Geize, K. Yam, T. Heuser, M. H. Wilbrink, H. Hara, M. C. Anderton, E. Sim, L. Dijkhuizen, J. E. Davies and W. W. Mohn, *Proc. Natl. Acad. Sci.*, 2007, **104**, 1947-1952.

31. E. C. Hett and E. J. Rubin, *Microbiol. Mol. Biol. Rev.*, 2008, **72**, 126-156.

32. J. S. Blanchard, *Annu. Rev. Biochem.*, 1996, **65**, 215-239.

33. D. Chatterjee, *Curr. Opin. Chem. Biol.*, 1997, **1**, 579-588.

34. V. Jarlier and H. Nikaido, *J. Bacteriol.*, 1990, **172**, 1418-1423.

35. P. J. Brennan and H. Nikaido, *Annu. Rev. Biochem.*, 1995, **64**, 29-63.

36. D. M. Yajko, C. A. Sanders, P. S. Nassos and W. K. Hadley, *Antimicrob. Agents Chemother.*, 1990, **34**, 2442-2444.

37. J. P. Sarathy, V. Dartois and E. J. D. Lee, *Pharmaceuticals*, 2012, **5**, 1210-1235.

38. J. Trias, V. Jarlier and R. Benz, *Science*, 1992, **258**, 1479-1479.

39. S. T. Thomas, B. C. VanderVen, D. R. Sherman, D. G. Russell and N. S. Sampson, *J. Biol. Chem.*, 2011, **286**, 43668-43678.

40. P. J. Brennan, *Tuberculosis*, 2003, **83**, 91-97.

41. E. N. Houben, L. Nguyen and J. Pieters, *Curr. Opin. Microbiol.*, 2006, **9**, 76-85.

42. H. A. Chart, Progression Of Pulmonary Tuberculosis, https://humananatomychart.us/diagrams-about-tuberculosis/diagrams-about-tuberculosis-0914-progression-of-pulmonary-tuberculosis-medical-images-for-powerpoint-slide01/).

43. R. Niemi, An Overview of the Pathogenesis of tuberculosis, http://www.intellectualventureslab.com/invent/overview-of-tuberculosis-pathogenesis).

44. J. Grosset, *Antimicrob. Agents Chemother.*, 2003, **47**, 833-836.

45. J. Y. Lee, *Tuberc. Respir. Dis.*, 2015, **78**, 47-55.

46. J. M. Vyas, Tuberculosis, advanced - chest x-rays, https://medlineplus.gov/ency/imagepages/1607.htm).

47. NHS, Tuberculosis (TB) Diagnosis, https://www.nhs.uk/conditions/tuberculosis-tb/diagnosis/).

48. D. Menzies, *Am. J. Respir. Crit. Care Med.*, 1999, **159**, 15-21.

49. J. Dinnes, J. Deeks, H. Kunst, A. Gibson, E. Cummins, N. Waugh, F. Drobniewski and A. Lalvani, in *NIHR Health Technology Assessment programme: Executive Summaries*, NIHR Journals Library, 2007.

50. G. Ferrara, M. Losi, R. D'Amico, P. Roversi, R. Piro, M. Meacci, B. Meccugni, I. M. Dori, A. Andreani and B. M. Bergamini, *J.-Lancet*, 2006, **367**, 1328-1334.

51. N. H. Smith, S. V. Gordon, R. de la Rua-Domenech, R. S. Clifton-Hadley and R. G. Hewinson, *Nat. Rev. Microbiol.*, 2006, **4**, 670.

52. P. Livingstone, N. Hancox, G. Nugent and G. de Lisle, *N. Z. Vet. J.*, 2015, **63**, 4-18.

53. E. Rodríguez-Hernández, O. E. Pizano-Martínez, G. Canto-Alarcón, S. Flores-Villalva, L. I. Quintas-Granados and F. Milián-Suazo, *Rev. Med. Microbiol.*, 2016, **27**, 20-24.

54. C. A. Donnelly and R. Woodroffe, *Nature*, 2015, **526**, 640.

55. W. H. Organization, *Global tuberculosis report 2015*, World Health Organization, 2015.

56. W. H. Organization, *Bull. W. H. O.*, 2007, **85**, 325-420.

57. X.-Z. Li and H. Nikaido, *Drugs*, 2009, **69**, 1555-1623.

58. K. Styblo and J. Meijer, *Tubercle*, 1976, **57**, 17-43.

59. L. C. Rodrigues, V. K. Diwan and J. G. Wheeler, *Int. J. Epidemiol.*, 1993, **22**, 1154-1158.

60. A. Roy, M. Eisenhut, R. Harris, L. Rodrigues, S. Sridhar, S. Habermann, L. Snell, P. Mangtani, I. Adetifa and A. Lalvani, *BMJ*, 2014, **349**, g4643.

61. G. F. Black, R. E. Weir, S. Floyd, L. Bliss, D. K. Warndorff, A. C. Crampin, B. Ngwira, L. Sichali, B. Nazareth and J. M. Blackwell, *Lancet*, 2002, **359**, 1393-1401.

62. Z. F. Udwadia, R. A. Amale, K. K. Ajbani and C. Rodrigues, *Clin. Infect. Dis.*, 2012, **54**, 579-581.

63. A. A. Velayati, M. R. Masjedi, P. Farnia, P. Tabarsi, J. Ghanavi, A. H. ZiaZarifi and S. E. Hoffner, *Chest Journal*, 2009, **136**, 420-425.

64. A. A. Velayati, P. Farnia and A. M. Farahbod, *Int. J. Mycobact.*, 2016, **5**, S161.

65. A. Saxena, R. Kumari, U. Mukherjee, P. Singh and R. Lal, *Genome Announc.*, 2014, **2**, e00662-00614.

66. C. Calvori, L. Frontali, L. Leoni and G. Tecce, *Nature*, 1965, **207**, 417.

67. E. A. Campbell, N. Korzheva, A. Mustaev, K. Murakami, S. Nair, A. Goldfarb and S. A. Darst, *Cell*, 2001, **104**, 901-912.

68. A. Feklistov, V. Mekler, Q. Jiang, L. F. Westblade, H. Irschik, R. Jansen, A. Mustaev, S. A. Darst and R. H. Ebright, *Proc. Natl. Acad. Sci.*, 2008, **105**, 14820-14825.

69. J. Baysarowich, K. Koteva, D. W. Hughes, L. Ejim, E. Griffiths, K. Zhang, M. Junop and G. D. Wright, *Proc. Natl. Acad. Sci.*, 2008, **105**, 4886-4891.

70. N. Dookie, S. Rambaran, N. Padayatchi, S. Mahomed and K. Naidoo, *J. Antimicrob. Chemother.*, 2018, **73**, 1138-1151.

71. D. Sharma, A. R. Cukras, E. J. Rogers, D. R. Southworth and R. Green, *J. Mol. Biol.*, 2007, **374**, 1065-1076.

72. B. Springer, Y. G. Kidan, T. Prammananan, K. Ellrott, E. C. Böttger and P. Sander, *Antimicrob. Agents Chemother.*, 2001, **45**, 2877-2884.

73. A. Prayle, A. Watson, H. Fortnum and A. Smyth, *Thorax*, 2010, **65**, 654-658.

74. H. M. Blumberg, W. J. Burman, R. E. Chaisson and C. L. Daley, *Am. J. Respir. Crit. Care Med.*, 2003, **167**, 603.

75. R. Goude, A. Amin, D. Chatterjee and T. Parish, *Antimicrob. Agents Chemother.*, 2009, **53**, 4138-4146.

76. V. E. Escuyer, M.-A. Lety, J. B. Torrelles, K.-H. Khoo, J.-B. Tang, C. D. Rithner, C. Frehel, M. R. McNeil, P. J. Brennan and D. Chatterjee, *J. Bio. Chem*, 2001, **276**, 48854-48862.

77. C. Plinke, K. Walter, S. Aly, S. Ehlers and S. Niemann, *Antimicrob. Agents Chemother.*, 2011, **55**, 2891-2896.

78. L.-l. Zhao, Q. Sun, H.-c. Liu, X.-c. Wu, T.-y. Xiao, X.-q. Zhao, G.-l. Li, Y. Jiang, C.-y. Zeng and K.-l. Wan, *Antimicrob. Agents Chemother.*, 2015, **59**, 2045-2050.

79. L. Malone, A. Schurr, H. Lindh, D. McKenzie, J. Kiser and J. Williams, *Am. Rev Tb*, 1952, **65**, 511-518.

80. M. Njire, Y. Tan, J. Mugweru, C. Wang, J. Guo, W. Yew, S. Tan and T. Zhang, *Adv. Med. Sci.*, 2016, **61**, 63-71.

81. Y. Zhang, A. Scorpio, H. Nikaido and Z. Sun, *J. Bacteriol*, 1999, **181**, 2044-2049.

82. Y. Zhang, W. Shi, W. Zhang and D. Mitchison, *Microbiol. Spectrum*, 2013, **2**, 1.

83. S. Zhang, J. Chen, W. Shi, W. Liu, W. Zhang and Y. Zhang, *Emerging Microbes Infect.*, 2013, **2**, e34.

84. U. H. Manjunatha, S. P. Rao, R. R. Kondreddi, C. G. Noble, L. R. Camacho, B. H. Tan, S. H. Ng, P. S. Ng, N. L. Ma and S. B. Lakshminarayana, *Sci. Transl. Med.*, 2015, **7**, 269ra263-269ra263.

85. P. Pan and P. J Tonge, *Curr. Top. Med. Chem.* , 2012, **12**, 672-693.

86. A. Banerjee, E. Dubnau, A. Quemard, V. Balasubramanian, K. S. Um, T. Wilson, D. Collins, G. De Lisle and W. R. Jacobs Jr, *Science*, 1994, **263**, 227-229.

87. A. Dessen, A. Quemard, J. S. Blanchard, W. R. Jacobs Jr and J. C. Sacchettin, *Science*, 1995, **267**, 1638.

88. J. Suarez, K. Ranguelova, A. A. Jarzecki, J. Manzerova, V. Krymov, X. Zhao, S. Yu, L. Metlitsky, G. J. Gerfen and R. S. Magliozzo, *J. Biol. Chem.*, 2009, **284**, 7017-7029.

89. C. Vilchèze and J. Jacobs, William R, *Annu. Rev. Microbiol.*, 2007, **61**, 35-50.

90. R. Rawat, A. Whitty and P. J. Tonge, *Proc. Natl. Acad. Sci.*, 2003, **100**, 13881-13886.

91. C. Vilchèze, F. Wang, M. Arai, M. H. Hazbón, R. Colangeli, L. Kremer, T. R. Weisbrod, D. Alland, J. C. Sacchettini and W. R. Jacobs, *Nat. Med.*, 2006, **12**, 1027-1029.

92. A. N. Unissa, S. Subbian, L. E. Hanna and N. Selvakumar, *Infect., Genet. Evol.*, 2016, **45**, 474-492.

93. G. S. Timmins and V. Deretic, *Mol. Microbiol.*, 2006, **62**, 1220-1227.

94. G. Storz and L. A. Tartaglia, *J. Nutr.*, 1992, **122**, 627.

95. C. Vilchèze, H. R. Morbidoni, T. R. Weisbrod, H. Iwamoto, M. Kuo, J. C. Sacchettini and W. R. Jacobs, *J. Bacteriol*, 2000, **182**, 4059-4067.

96. Y. Zhang, B. Heym, B. Allen, D. Young and S. Cole, *Nature*, 1992, **358**, 591-593.

97. J. M. Musser, V. Kapur, D. L. Williams, B. N. Kreiswirth, D. Van Soolingen and J. D. Van Embden, *J. Infect. Dis.*, 1996, **173**, 196-202.

98. C. E. Cade, A. C. Dlouhy, K. F. Medzihradszky, S. P. Salas-Castillo and R. A. Ghiladi, *Protein Sci.*, 2010, **19**, 458-474.

99. J. Isakova, N. Sovkhozova, D. Vinnikov, Z. Goncharova, E. Talaibekova, N. Aldasheva and A. Aldashev, *BMC Microbiol.*, 2018, **18**, 22.

100. L. Liu, F. Jiang, L. Chen, B. Zhao, J. Dong, L. Sun, Y. Zhu, B. Liu, Y. Zhou and J. Yang, *Emerging Microbes Infect.*, 2018, **7**, 1-10.

101. J. S. Blanchard, *Biochemistry*, 1995, **34**, 8235-8241.

102. P. Lempens, C. J. Meehan, K. Vandelannoote, K. Fissette, P. de Rijk, A. Van Deun, L. Rigouts and B. C. de Jong, *Sci. Rep.*, 2018, **8**, 3246.

103. J. F. Murray and J. A. Nadel, *Murray & Nadel's Textbook of respiratory medicine*, Elsevier Saunders, 2016.

104. C. E. Maus, B. B. Plikaytis and T. M. Shinnick, *Antimicrob. Agents Chemother.*, 2005, **49**, 3192-3197.

105. A. Rahman, S. S. Srivastava, A. Sneh, N. Ahmed and M. V. Krishnasastry, *BMC Biochem.*, 2010, **11**, 35.

106. D. M. Campoli-Richards, J. P. Monk, A. Price, P. Benfield, P. A. Todd and A. Ward, *Drugs*, 1988, **35**, 373-447.

107. G. A. Jacoby, *Clin. Infect. Dis.*, 2005, **41**, S120-S126.

108. S. Norrby, *Eur. J. Clin. Microbiol. Infect. Dis.*, 1991, **10**, 378-383.

109. L. Galatti, S. E. Giustini, A. Sessa, G. Polimeni, F. Salvo, E. Spina and A. P. Caputi, *Pharmacol. Res.*, 2005, **51**, 211-216.

110. P. R. Donald and A. H. Diacon, *Lancet Infect. Dis.*, 2015, **15**, 1091-1099.

111. G. K. McEvoy, *AHFS drug information, 2000*, American society of health-system pharmacists, 2000.

112. V. Mathys, R. Wintjens, P. Lefevre, J. Bertout, A. Singhal, M. Kiass, N. Kurepina, X.-M. Wang, B. Mathema and A. Baulard, *Antimicrob. Agents Chemother.*, 2009, **53**, 2100-2109.

113. C. Vilchèze and W. R. Jacobs, in *Molecular Genetics of Mycobacteria, Second Edition*, American Society of Microbiology, 2014, pp. 431-453.

114. J. E. Bennett, R. Dolin and M. J. Blaser, *Mandell, Douglas, and Bennett's Principles and Practice of Infectious Diseases: 2-Volume Set*, Elsevier Health Sciences, Philadelphia, 2014.

115. E. B. Chahine, L. R. Karaoui and H. Mansour, *Ann. Pharmacother.*, 2014, **48**, 107-115.

116. E. Cox and K. Laessig, *N. Engl. J. Med.*, 2014, **371**, 689-691.

117. S. K. Field, *Therapeutic advances in chronic disease*, 2015, **6**, 170-184.

118. J. Fischer, C. Klein and W. E. Childers, *Successful Drug Discovery*, John Wiley & Sons, 2018.

119. J. M. Lewis and D. J. Sloan, *Ther. Clin. Risk Manage.*, 2015, **11**, 779.

120. C. Roger, J. A. Roberts and L. Muller, *Clin. Pharmacokinet.*, 2018, **57**, 559-575.

121. G. French, *J. Antimicrob. Chemother.*, 2003, **51**, ii45-ii53.

122. G. Maartens and C. A. Benson, *EBioMedicine*, 2015, **2**, 1568-1569.

123. W. H. Organization, *WHO treatment guidelines for drug-resistant tuberculosis*, World Health Organization, 2016.

124. J. L. Arbiser and S. L. Moschella, *J. Am. Acad. Dermatol.*, 1995, **32**, 241-247.

125. R. Baptista, D. M. Fazakerley, M. Beckmann, L. Baillie and L. A. Mur, *Sci. Rep.*, 2018, **8**, 5084.

126. FDA, FDA approves new drug for treatment-resistant forms of tuberculosis that affects the lungs, https://www.fda.gov/news-events/press-announcements/fda-approves-new-drug-treatment-resistant-forms-tuberculosis-affects-lungs, (accessed 22-Aug, 2019).

127. J. Vinsova, A. Imramovsky, J. Jampilek, J. F. Monreal and M. Dolezal, *Anti-Infect. Agents Med. Chem.*, 2008, **7**, 12-31.

128. V. Judge, B. Narasimhan and M. Ahuja, *Med. Chem. Res.*, 2012, **21**, 3940-3957.

129. Z. Rychtarčíková, M. Krátký, M. Gazvoda, M. Komlóová, S. Polanc, M. Kočevar, J. Stolaříková and J. Vinšová, *Molecules*, 2014, **19**, 3851-3868.

130. L. Kremer, J. D. Douglas, A. R. Baulard, C. Morehouse, M. R. Guy, D. Alland, L. G. Dover, J. H. Lakey, W. R. Jacobs and P. J. Brennan, *J. Biol. Chem.*, 2000, **275**, 16857-16864.

131. E. Sieniawska, *Chem. Biol. (Oxford, U. K.)*, 2015, **22**, 1288-1300.

132. A. Thompson, P. Griffin, R. Stuetz and E. Cartmell, *Water. Environ. Res.*, 2005, **77**, 63-67.

133. S. L. Parikh, G. Xiao and P. J. Tonge, *Biochemistry*, 2000, **39**, 7645-7650.

134. M. J. Stewart, S. Parikh, G. Xiao, P. J. Tonge and C. Kisker, *J. Mol. Biol.*, 1999, **290**, 859-865.

135. L.-Q. Wang, C. N. Falany and M. O. James, *Drug Metab. Dispos.*, 2004, **32**, 1162-1169.

136. J. Stec, C. Vilchèze, S. Lun, A. L. Perryman, X. Wang, J. S. Freundlich, W. Bishai, W. R. Jacobs and A. P. Kozikowski, *ChemMedChem*, 2014, **9**, 2528-2537.

137. H. Kanetaka, Y. Koseki, J. Taira, T. Umei, H. Komatsu, H. Sakamoto, G. Gulten, J. C. Sacchettini, M. Kitamura and S. Aoki, *Eur. J. Med. Chem.*, 2015, **94**, 378-385.

138. T. Kinjo, Y. Koseki, M. Kobayashi, A. Yamada, K. Morita, K. Yamaguchi, R. Tsurusawa, G. Gulten, H. Komatsu and H. Sakamoto, *J Chem Inf Model.*, 2013, **53**, 1200-1212.

139. P. Kamsri, A. Punkvang, P. Saparpakorn, S. Hannongbua, S. Irle and P. Pungpo, *J. Mol. Model.*, 2014, **20**, 1-12.

140. J. D. Bhatt, C. J. Chudasama and K. D. Patel, *Bioorg. Med. Chem.*, 2015, **23**, 7711-7716.

141. D. Castagnolo, F. Manetti, M. Radi, B. Bechi, M. Pagano, A. De Logu, R. Meleddu, M. Saddi and M. Botta, *Bioorg. Med. Chem.*, 2009, **17**, 5716-5721.

142. R. J. Heath, Y.-T. Yu, M. A. Shapiro, E. Olson and C. O. Rock, *J. Biol. Chem.*, 1998, **273**, 30316-30320.

143. W. W. Mohn, R. Van Der Geize, G. R. Stewart, S. Okamoto, J. Liu, L. Dijkhuizen and L. D. Eltis, *J. Biol. Chem.*, 2008, **283**, 35368-35374.

144. G. S. Pedgaonkar, J. P. Sridevi, V. U. Jeankumar, S. Saxena, P. B. Devi, J. Renuka, P. Yogeeswari and D. Sriram, *Bioorg. Med. Chem.*, 2014, **22**, 6134-6145.

145. G. S. Pedgaonkar, J. P. Sridevi, V. U. Jeankumar, S. Saxena, P. B. Devi, J. Renuka, P. Yogeeswari and D. Sriram, *Eur. J. Med. Chem.*, 2014, **86**, 613-627.

146. J. B. Baell and G. A. Holloway, *J. Med. Chem.*, 2010, **53**, 2719-2740.

147. P. J. Tonge, C. Kisker and R. A. Slayden, *Curr. Top. Med. Chem.* , 2007, **7**, 489-498.

148. U. H. Manjunatha, H. Boshoff, C. S. Dowd, L. Zhang, T. J. Albert, J. E. Norton, L. Daniels, T. Dick, S. S. Pang and C. E. Barry, *Proc. Natl. Acad. Sci.*, 2006, **103**, 431-436.

149. T. Matviiuk, F. Rodriguez, N. Saffon, S. Mallet-Ladeira, M. Gorichko, A. L. d. J. L. Ribeiro, M. R. Pasca, C. Lherbet, Z. Voitenko and M. Baltas, *Eur. J. Med. Chem.*, 2013, **70**, 37-48.

150. A. Chollet, G. Mori, C. Menendez, F. Rodriguez, I. Fabing, M. R. Pasca, J. Madacki, J. Korduláková, P. Constant and A. Quémard, *Eur. J. Med. Chem.*, 2015, **101**, 218-235.

151. A. R. Bhat, A. Azam, I. Choi and F. Athar, *Eur. J. Med. Chem.*, 2011, **46**, 3158-3166.

152. A. Foroumadi, Z. Kargar, A. Sakhteman, Z. Sharifzadeh, R. Feyzmohammadi, M. Kazemi and A. Shafiee, *Bioorg. Med. Chem. Lett.*, 2006, **16**, 1164-1167.

153. A. Foroumadi, S. Pournourmohammadi, F. Soltani, M. Asgharian-Rezaee, S. Dabiri, A. Kharazmi and A. Shafiee, *Bioorg. Med. Chem. Lett.*, 2005, **15**, 1983-1985.

154. S. D. Joshi, U. A. More, K. Pansuriya, T. M. Aminabhavi and A. K. Gadad, *J. Saudi Chem. Soc.*, 2013.

155. U. A. More, S. D. Joshi, T. M. Aminabhavi, A. K. Gadad, M. N. Nadagouda and V. H. Kulkarni, *Eur. J. Med. Chem.*, 2014, **71**, 199-218.

156. N. Desai, H. Somani, A. Trivedi, K. Bhatt, L. Nawale, V. M. Khedkar, P. C. Jha and D. Sarkar, *Bioorg. Med. Chem. Lett.*, 2016, **26**, 1776-1783.

157. D. J. Denhart, J. A. Deskus, J. L. Ditta, Q. Gao, H. D. King, E. S. Kozlowski, Z. Meng, M. A. LaPaglia, G. K. Mattson and T. F. Molski, *Bioorg. Med. Chem. Lett.*, 2009, **19**, 4031-4033.

158. P. Singh, *Eur. J. Med. Chem.*, 2014, **74**, 440-450.

159. S. K. Sharma, P. Kumar, B. Narasimhan, K. Ramasamy, V. Mani, R. K. Mishra and A. B. A. Majeed, *Eur. J. Med. Chem.*, 2012, **48**, 16-25.

160. L. P. Liew, J. M. Fleming, A. Longeon, E. Mouray, I. Florent, M.-L. Bourguet-Kondracki and B. R. Copp, *Tetrahedron*, 2014, **70**, 4910-4920.

161. C. R. W. Guimarães, D. L. Boger and W. L. Jorgensen, *J. Am. Chem Soc*, 2005, **127**, 17377-17384.

162. R. A. Friesner, J. L. Banks, R. B. Murphy, T. A. Halgren, J. J. Klicic, D. T. Mainz, M. P. Repasky, E. H. Knoll, M. Shelley and J. K. Perry, *J. Med. Chem.*, 2004, **47**, 1739-1749.

163. A. Guardia, G. Gulten, R. Fernandez, J. Gómez, F. Wang, M. Convery, D. Blanco, M. Martínez, E. Pérez-Herrán and M. Alonso, *ChemMedChem*, 2016, **11**, 687-701.

164. M. M. Ghorab, M. S. El-Gaby, A. M. Soliman, M. S. Alsaid, M. M. Abdel-Aziz and M. M. Elaasser, *Chem. Cent. J.*, 2017, **11**, 42.

165. S. B. University of California, Table of Acids with Ka and pKa Values, http://clas.sa.ucsb.edu/staff/Resource%20folder/Chem109ABC/Acid,%20Base%20Strength/Table%20of%20Acids%20w%20Kas%20and%20pKas.pdf).

166. B. H. Cho, J. H. Kim, H. B. Jeon and K. S. Kim, *Tetrahedron*, 2005, **61**, 4341-4346.

167. R. P. Tripathi, B. Singh, S. S. Bisht and J. Pandey, *ChemInform*, 2010, **41**.

168. M. G. Kulkarni and S. R. Thopate, *Tet.*, 1996, **52**, 1293-1302.

169. R. Tripathi, N. Dwivedi, N. Singh and M. Misra, *Med Chem Res*, 2008, **17**, 53-61.

170. Y. Nihro, S. Sogawa, A. Izumi, A. Sasamori, T. Sudo, T. Miki, H. Matsumoto and T. Satoh, *J Med Chem*, 1992, **35**, 1618-1623.

171. E. Stridfelt, Doctor of Philosophy in Organic Chemistry, Stockholm University, 2017.

172. R. A. Altman, A. Shafir, A. Choi, P. A. Lichtor and S. L. Buchwald, *J Org Chem*, 2008, **73**, 284-286.

173. M. Bielawski, M. Zhu and B. Olofsson, *Adv. Synth. Catal.*, 2007, **349**, 2610-2618.

174. E. Lindstedt, R. Ghosh and B. Olofsson, *Org. Lett*, 2013, **15**, 6070-6073.

175. K. Wimalasena and M. P. Mahindaratne, *J. Org. Chem*, 1994, **59**, 3427-3432.

176. M. A. Khan and H. Adams, *Synthesis*, 1995, **1995**, 687-692.

177. T. W. Green and P. G. Wuts, *Protective groups in organic synthesis*, Wiley, New York, 1999.

178. S. R. Thopate, R. A. Dengale and M. G. Kulkarni, *Synlett*, 2013, **24**, 1555-1557.

179. A. O. Olabisi and K. Wimalasena, *J. Org. Chem*, 2004, **69**, 7026-7032.

180. S. J. Blanksby and G. B. Ellison, *Acc. Chem. Res.*, 2003, **36**, 255-263.

181. P. Ge and K. L. Kirk, *J. Org. Chem*, 1997, **62**, 3340-3343.

182. P. Ge and K. L. Kirk, *J. Org. Chem*, 1996, **61**, 8671-8673.

183. A. Ahmed, University of Nottingham, 2015.

184. L. Encinas, H. O'Keefe, M. Neu, M. J. Remuiñán, A. M. Patel, A. Guardia, C. P. Davie, N. Perez-Macias, H. Yang and M. A. Convery, *J. Med. Chem.*, 2014, **57**, 1276-1288.

185. M. R. Kuo, H. R. Morbidoni, D. Alland, S. F. Sneddon, B. B. Gourlie, M. M. Staveski, M. Leonard, J. S. Gregory, A. D. Janjigian and C. Yee, *J. Biol. Chem.*, 2003, **278**, 20851-20859.

186. ChemBK, Diphenyliodonium triflate, https://www.chembk.com/en/chem/%20Diphenyliodonium%20triflate, (accessed 15 Aug, 2019).

187. M. G. Kulkarni and S. D. Kate, *Synth. Commun.*, 2004, **34**, 2365-2370.

188. K. Tanino, K. Onuki, K. Asano, M. Miyashita, T. Nakamura, Y. Takahashi and I. Kuwajima, *J. Am. Chem Soc* 2003, **125**, 1498-1500.

189. K. Kato, S. Terao, N. Shimamoto and M. Hirata, *J. Med. Chem.*, 1988, **31**, 793-798.